Carbohydrate conjugated porphyrins targeting Photodynamic Therapy (PDT): potent inducers of cancer cell death both by necrosis and apoptosis; solution-phase combinatorial libraries with whole cell selection method

by

Xin Chen

A dissertation submitted to the Graduate Faculty in Biochemistry in partial fulfillment of the requirements for the degree of Doctor of Philosophy, The City University of New York

2005

UMI Number: 3187388

ProQuest Information and Learning Company
300 North Zeeb Road
P.O. Box 1346
Ann Arbor, MI 48106-1346

This manuscript has been read and accepted for the Graduate Faculty in Biochemistry in satisfaction of the dissertation requirement for the degree of Doctor of the Philosophy.

11-23-04 — Date
Charles Michael Drain — Chair of Examining Committee

06/16/05 — Date
Lesley Davenport — Executive Officer

Professor Richard Franck

Professor Manfred Philipp

Professor Wilma Suffran

Professor Maria Tomasz

Supervisory Committee

THE CITY UNIVERSITY OF NEW YORK

Abstract

Carbohydrate conjugated porphyrins targeting Photodynamic Therapy (PDT): potent inducers of cancer cell death both by necrosis and apoptosis; solution-phase combinatorial libraries with whole cell selection method

by

Xin Chen

Advisor: Professor Charles M. Drain

Carbohydrate conjugated porphyrins are of great interests in the application of Photodynamic Therapy (PDT) for cancer treatment, as they have good solubility and bear cell recognition groups. A thorough review on this topic is presented. A tetra-glucose derivative (P-Glu_4) of $TPPF_{20}$ is a more potent drug over the tetra-galactose derivative (P-Gal_4) in affinity, cell death and apoptotic induction in human breast cancer cells. They also have good selectivity toward cancer cells over normal cells. The latter effects were investigated using rat fibroblasts where the selectivity for the transformed cells is found to be over 3 times that of the normal cells. Synthesis of solution-phase combinatorial porphyrin libraries is accomplished and a whole-cell selection methodology is presented.

This work is dedicated to

my parents for their tremendous support and encouragement

Acknowledgments

I'd like to take the opportunity to express my gratefulness to my mentor Prof. Charles Michael Drain for his guidance, encouragement and support. Without him, this thesis could never be written and presented. I also like to thank my committee members Prof. Richard Franck, Prof. Manfred Philipp, Prof. Wilma Suffran and Prof. Maria Tomasz for their suggestions.

My thank also goes to our lab alumni Dr. Xianchang Gong, Dr. Fotis Nifiatis, Dr. Xinxu Shi, Dr. Tatjana Milic, Dr. Isabelle Sylvain and Dr. Kaifan Cheng for help and discussion, undergraduates Margareta Sorenson and Tatyana Groysman who have worked with me, as well as current lab members Diana Samaroo, Gabriela Smeureanu and Giorgio Bazzan.

Prof. David A. Foster and his lab members from the Department of Biological Sciences are highly appreciated for a fruitful collaboration and a pleasant experience.

I thank Dr. Clifford E. Soll and Dr. Michael Blumenstein for their support on mass and NMR spectrometry, respectively.

I also want to express my appreciation to my husband Guoliang Qian for his encouragement, support and love.

At last, but not the least, I am truly grateful to my dear mom and dad for their forever caring, tremendous encouragement and unconditional love.

Table of Contents

Chapter 3

S-Glucosylated Porphyrin as a Potent Apoptosis Inducer in Human Breast Cancer Cells Targeting Photodynamic Therapy

Chapter 4

Synthesis of solution-phase combinatorial porphyrin library and selection from human breast cancer cells targeting Photodynamic Therapy

References

List of Tables

List of Figures

Chapter 1

Chapter 2

List of Appendices

Chapter 4

List of Schemes

Abbreviations

ANS	1-anilino naphthalene-8-sulfonate
$\Delta\Psi$	voltage gradient
Apaf	apoptotic protease activating factor
BER	base excision repair
caspases	cysteine aspartate-specific proteases
DAPI	4',6-diamidino-2-phenylindole
DCC	dynamic combinatorial chemistry
DISCs	death-inducing signaling complexes
DME	ethylene glycol dimethyl ether
DMEM	Dulbecco's Modified Eagle Medium
DMPC	dimyristoylphosphatidyl choline
DMPG	dimyristoylphosphatidylglycerol
DPH	1,6-diphenyl-1,3,5-hexatriene
ECM	extracellular matrix
ESI-MS	Electron Spray Ionization Mass Spectroscopy
HDL	high density lipoprotein
HpD	hematoporphyrin derivatives
LDL	low density lipoprotein
MALDI	matrix-assisted laser desorption/ionization
MDR	multidrug resistance
MS	mass spectrometry
MTT	3-(4,5-dimethylthiazol-2-yl)-2,5-diphenyltetrazolium bromide

PARP	poly-(ADP ribose) polymerase
PDT	Photodynamic Therapy
PE	phosphatidylethanolamine
P-Gal_4	5,10,15,20-tetrakis (4,1'-thio-galactose-2,3,5,6-tetrafluorophenyl)porphyrin
P-Glu_4	5,10,15,20-tetrakis (4,1'-thio-glucose-2,3,5,6-tetrafluorophenyl)porphyrin
PI	propidium iodide
PT	permeability transition
RGD	arginine-glycine-asparatate
ROS	reactive oxygen species
SER	sequestration enabling reagent
TPP	tetraphenylporphyrin
$TPPF_{20}$	5,10,15,20-tetrakis(pentafluorophenyl)porphyrin
TUNEL	terminal deoxynucleotidyl transferase (TdT)-mediated dUTP-biotin nick end labeling
UV-VIS	ultraviolet-visible
VCLs	virtual combinatorial libraries
VLDL	very low density lipoprotein

Chapter 1

Review: Photodynamic Therapy Using Carbohydrate Conjugated Porphyrins

Abstract:

There has been a long interest and history in using porphyrins for applications in Photodynamic Therapy (PDT) for cancer treatment. These applications arise from their photosensitizing and phototoxic properties. PDT combines a photosensitizer and light to produce highly toxic singlet oxygen and therefore destroy any unwanted cells or tissues. The therapeutic properties of porphyrins and their interactions with different cell organelles and components are dependent on their chemical structures. Research on porphyrins with sugar moieties has been of great interest in the last decade. Glycosylated porphyrins can have greater water solubility than most naturally occurring and synthetic, *meso* substituted, porphyrins. This property can not only increase the efficacy of drug delivery but also assist the drug elimination from the organism after treatment. The proper lipophilicity of neutral saccharide conjugated porphyrins enable them to permeate better in both lipophilic and hydrophilic biological structures. Furthermore, they can have specific interactions with proteins on cell membranes and thus exhibit specific targeting of cancer cells. Therefore, porphyrins with carbohydrate moieties are very promising candidates for PDT in cancer treatment, and for other therapeutics.

Introduction:

Photodynamic Therapy

Porphyrins are tetrapyrrole macrocycles that are ubiquitous in nature [1, 2]. They play fundamental roles in a variety of biological processes, such as oxygen transport in hemoglobin and myoglobin [3], cytochrome P-450 enzyme catalyzed oxidations [4], electrical conduits or shuttles in cytochromes C, bacterial and plant photosynthesis [5], and as reducing agents in methyl-coenzyme-M reductase [6]. It is not surprising, then, that the chemistry, structure, and function of porphyrins continue to be of interest even after over 150 years of research [1, 7].

In recent decades, research efforts focusing on porphyrins has increased rapidly, due to their wide range of applications, including self-assembled molecular electronics and photonics [8-11], nanoparticles for catalysis [12], molecular sieves [13, 14], sensors [14, 15], chiral catalysis, carriers for selective transport of biomolecules [16], DNA binders [17-19], anticancer [20-26] and antiviral [27, 28] therapeutics, etc.

One major focus from the above areas is the use of porphyrins in Photodynamic Therapy (PDT) [26, 29-31]. PDT is a methodology in which: (1) photosensitizers (e.g. porphyrins) are introduced into body; (2) they accumulate preferentially in tumor tissues [30, 32]; (3) upon visible light irradiation at a specific wavelength (often from laser) or by white light, they are activated to their triplet states; (4) the triplet photosensitizers then interact with molecular oxygen to result in the photosensitizer ground states and highly reactive singlet oxygen; (5) singlet oxygen reacts with various cellular components; (6) cell or tissue death is caused by necrosis and/or apoptosis [33-35].

The advantages of PDT [36, 37] include:

(1) PDT allows selective treatment of localized cancer. The selectivity of PDT is modulated both by preferential uptake and retention of the photosensitizers in tumor tissues over normal tissues, and the selective irradiation of light. The tissue is rapidly destroyed only precisely where the light has been directed.

(2) PDT avoids systemic treatment. The treatment occurs only where the light is delivered, thus the patients do not go through the needless systemic treatment for localized disease. Therefore, side effects can be dramatically reduced, from losing hair or suffering nausea to more serious complications.

(3) PDT is applicable when surgery is not possible. PDT fulfills a need for minimally invasive approach toward localized tissue removal. For example, when the site is a vital structure and cannot be removed surgically; or when the site is deep inside the body and surgery would constitute a major trauma.

(4) PDT is low cost.

(5) PDT is repeatable. It offers a means of long-term management of cancer even if complete cure is not attainable.

There is only one potentially adverse effect – the drug may cause skin photosensitivity, which means that the patients need to stay out of bright light for a period of time after treatment. One current limitation of PDT is that this treatment is mainly used for tumors on or just under the skin or on the lining of internal organs, because the laser light in use often cannot pass through more than about 3 cm of tissue.

Though an old concept with many clear advantages, there are only a couple of PDT agents (over $3 billion in world-wide sales) that are FDA approved and a couple in the pipeline [26]. Though PDT is still an on-going experimental therapy and currently

only applicable to a small range of patients, it is now clear that there are some indications where PDT is at least as good as and possibly better than alternative treatments.

Carbohydrate Conjugated Porphyrins

PDT has been used against bladder cancers, brain cancers, breast metastases, skin cancers, lung cancers, esophageal cancers, gynecological malignancies, colorectal cancer, thoracic malignancies, and oral head and neck cancers [23, 26, 36, 38, 39]. Examples of photosensitizers in various phases of clinical trials are: *meta*-tetrahydroxyphenyl chlorin (*m*-THPC), tradenamed Foscan®, against esophageal, lung laryngeal, thoracic, and skin cancers; benzoporphyrin derivatives verteporfin (tradename Visudyne®) in treating skin cancer, basal cell carcinoma, metastatic skin lesions and FDA approved for wet form of age-related macular degeneration; and lutetium texaphyrin, tradenamed Lutex®, for treatment of malignant melanoma, breast metastases, Kaposi's sarcoma, invasive basal cell carcinoma and squamous cell carcinoma (Appendix I). The first and only FDA approved drug for PDT in cancer treatment is called Photofrin®. Photofrin® is derived from hematoporphyrin through hematoporphyrin derivatives (HpD) and Photofrin II® by different treatments and purification methods (Appendix II). It is widely used for the treatment of advanced stage esophageal, early- and late-stage lung cancer, and prophylactic treatment of papillary bladder tumor [25, 26, 40]. Despite of its efficacy and effectiveness, Photofrin® has some drawbacks: (1) it is not a well-defined structure as it is a mixture of porphyrin dimers and/or oligomers with ester and ether linkages; (2) poor solubility in water; (3) nonspecific recognition by tumor cells, therefore low selectivity in tumor over normal tissues; (4) long elimination time from patients, so the patients must

remain without exposure to sunlight for at least 6 weeks after treatment [29]. Therefore,

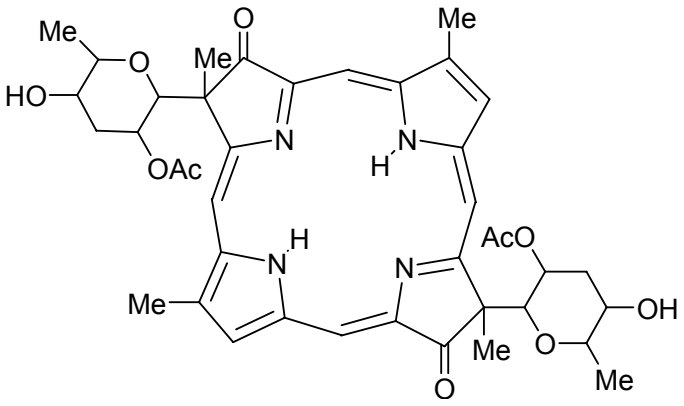

Figure 1. Tolyporphin, a lipophilic extract of blue-green alga *Tolypothrix nodosa* as a multidrug resistance reversing agent [41].

research and development on the next generation PDT agent has been of great interest among industrial and academic labs. One promising route is to synthesize carbohydrate conjugated porphyrins and to evaluate their properties in biological systems. Actually, a C-glyco-conjugated porphyrin, tolyporphin [Fig. (**1**)], naturally occurrs in blue-green alga *Tolypothrix nodosa* and has been extracted [41]. Tolyporphin is found to be able to reverse multidrug resistance (MDR) in a vinblastine-resistant subline (SK-VLB) of a human ovarian adenocarcinoma cell line (SK-OV-3).

The advantages of saccharide appended porphyrins are:

(1) Their good solubility in aqueous solution can increase the efficacy of drug delivery and the efficiency of drug elimination from organism after treatment.

(2) They can accumulate preferably in tumor tissues due to a slightly more acidic environment in abnormal tissues;

(3) Since one of their functions in biology is cell recognition, sugars can facilitate specific recognition of a drug via receptors on cells, so the drug can be actively taken up by a cell;

(4) The amphiphilic character of the neutral saccharide-porphyrin conjugates facilitates the incorporation of the drug into the membrane. The nature and number of carbohydrate residues, and hydrophobic substituents linked to the porphyrin macrocycle allow a large variability in the hydrophilic or lipophilic characters. A proper lipophilic property can assist the drug to bind cell membranes and possibly increase diffusion and cellular uptake.

Binding / Uptake (Lipophilicity & Amphiphilicity)

The uptake of exogenous molecules such as drugs into cells arises from a variety of mechanisms that can be broadly classified as mediated and nonmediated transport. The former occurs through the action of specific carrier proteins. The latter occurs through simple diffusion.

For simple diffusion, there is a general agreement that drugs (e.g. porphyrins) can partition into the head group region, the polar ester/ether region, or the hydrocarbon region of a membrane depending on their hydrophilic/lipophilic properties [42]. In general, non-polar lipophilic porphyrins will tend to partition into the hydrocarbon region, whereas highly polar porphyrin will partition into the head group or water-bilayer interface. Polar porphyrins then, partition into the polar ester/ether regions of the bilayer. Of course, partition does not indicate all of the compound is in only one region as there may be a distribution (e.g. between the polar ester/ether region and the hydrocarbon core).

Lipophilic porphyrins can cross the bilayer with a much lower energetic barrier than hydrophilic derivatives. As such there are reports that correlate lipophilicity with PDT effectiveness [37]. However, there are also reports on the effectiveness of polar

compounds [43]. Amphiphilic compounds (such as some porphyrins) have been described as having both polar part(s) and non-polar part(s) and interact with the head group and tail regions of a bilayer, respectively [44]. Since there are many methods using different lipids, bilayers, and cell lines to determine the extent that porphyrins partition into membranes, the comparison of many of these results on passive uptake is difficult.

The specific cell membrane structure varies from one cell type to another. The presence of proteins, saccharides, and other molecules such as cholesterol, not to mention lipid composition, result in the drugs partition into cell membranes in a much more complex way. Correlation of cell membrane binding to lipophilic / hydrophilic / amphiphilic properties is at best heuristic. The purpose of this review is not to reiterate the extensive literature [44, 45] on passive binding/uptake, but to infer some correlations between molecular properties and cell uptake / therapeutic response. Few labs use the same methods, or indeed report quantitative partition or binding on uptake data. So, only general inferences are made. The amphiphilicity can vary significantly, for a given drug, with different cell or bilayer systems. Since there is no describable scale for amphiphilicity, we only use 'high-low' to represent amphiphilicity. Thus, for example, a series of porphyrin derivatives with 0, 1, 2, 3, 4 saccharides is increasingly hydrophilic, but the amphiphilicity may reach a maximum with 2 or 3 substituents.

The large (~1 nm^2) porphyrin core is somewhat polarizable due to the extensive π system and the local dipole from the pyrrole N and NH (or the metal ion), but it is non-polar. A common carbohydrate-tetraphenylporphyrin (TPP) conjugate is about 2 nm in diameter and the thickness of a typical bilayer is about 8 nm (the cell membrane may be a bit thicker.). Given the above facts, if a porphyrin binds into a membrane, it must reside

in a region ranging from the water/bilayer interface, head group and the core. Plus, cell membrane is constantly under dynamic motion, thus the location of porphyrin may vary ± ~1 nm [42, 46].

Increasing amphiphilicity can assist a better binding of the porphyrins to cell membrane, but it probably will slow down the internalization of the drug because of the increasing difficulties in crossing the low dielectric core. On the other hand, a porphyrin binding into the cell membrane, but not crossing them, may be enough for a sufficient PDT effect.

This Review

In this review, we will focus on the synthesis of glycosylated porphyrins and their biological evaluations. Those sugar porphyrins with promising PDT effects will be emphasized. The materials where carbohydrate appended to other multichromophoric systems, such as porphyrazine and phthalocyanine (Appendix III), are beyond the scope of this review, but the applications and conclusions hold true for these systems. Intense studies related to PDT have also been devoted to delivery of photosensitizers [47], biodistribution and pharmacokinetics of photosensitizers [48], behaviors of photosensitizers in membranes and photomodification of biological & model membranes [42, 46, 49-51], but unfortunately these topics will not be discussed in this review.

Research on carbohydrate-porphyrin conjugates is still at an early stage of basic investigation. Because of the set-up of individual research labs, many different methods and many different biological systems (such as liposomes, proteins, cell lines, etc.) have

been used for studies on PDT activities, it makes it virtually impossible to compare the PDT potentialities of different molecules coming from different sources.

In this review, the saccharide conjugated porphyrins are categorized by the linkage between the porphyrin macrocycle and the sugar: I. ether linkage; II. carbon-carbon linkage; III. thioether linkage; IV. other linkages. The structures of carbohydrates appearing in this review can be found in Appendix IV, unless otherwise specified.

I. Ether Linkage:

Following nature's lead, most research efforts on glycoporphyrins have been focused on ether linkages between the carbohydrate moieties and the porphyrin macrocycles. Tetraphenylporphyrins (TPPs) are most often used, due to their relatively easy synthesis and greater quantum yield of singlet oxygen than Photofrin®. All the glyco-substitution is at the anomeric position, unless otherwise stated.

i. A Series of Porphyrins with Different Saccharides and Substituents

A. Synthesis

Meso-tetrakis(*ortho*-tetraacetylglucosylphenyl)porphyrin and *meso*-tetrakis(*ortho*-heptaacetylglucosylphenyl)porphyrin [52] were made by the Lindsey method [53, 54], starting from 2-(tetraacetyl-β-D-glucosyl)benzaldehyde and 2-(heptaacetyl-β-D-maltosyl)benzaldehyde with pyrrole, a Lewis acid catalyst ($BF_3{\cdot}Et_2O$) and an oxidizing agent (DDQ or p-chloranil). The tetraglucose derivative was found to have 3 atropoisomers, as αβαβ, ααββ and αααβ [Fig. (**2A**)], while the tetramaltose derivative has only one atropoisomer. Difficulties in preparation of the zinc complex of these

porphyrins and low affinity constants for ligand binding indicated a very strong steric

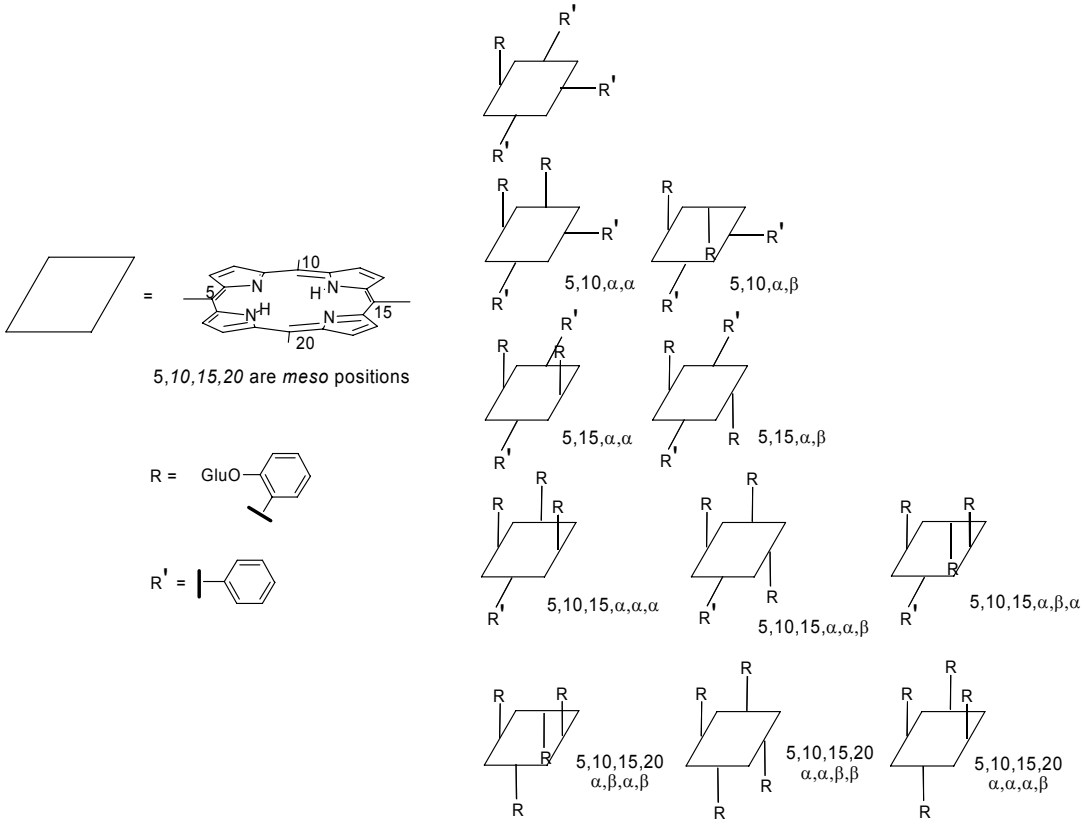

Figure 2A. Different atropoisomers of *ortho* glyco-substituted phenylporphyrins [52].

hindrance to both faces of the porphyrin macrocycle due to the *ortho* substitution of the glycosylated groups on the *meso*-phenyl groups. Mono-, bis- tris[(*ortho*-tetraacetylglucosyl)phenyl]porphyrins where the remaining *meso*-substituents are phenyl groups were synthesized by using a mixture of pyrrole, benzaldehyde and 2-(tetraacetyl-β-D-glucosyl)benzaldehyde at 4:2:2 ratio to minimize the formation of tetraphenylporphyrin and *meso*-tetrakis(*ortho*-tetraacetylglucosylphenyl)porphyrin. The isolated products had 8 out of 10 possible porphyrins (including atropoisomers) shown in Fig. (**2A**).

In a second phase of this research [55], four series of flat glycosylated porphyrins [Fig. (**2B**)] were synthesized: (1) four different *meso*-tetrakis(*para*-

glycosylphenyl)porphyrins each with one type of sugar, such as glucose (**2Aa**), galactose (**2Ab**), maltose (**2Ac**) and N-acetyl glucosamine (**2Ad**) at the *meso*- *para*-phenyl position; (2) *meso*-(*para*-glucosylphenyl)$_i$(phenyl)$_{4-i}$ porphyrins (for i=1,2,3) (**2Ba-2Bd**) and *meso*-(*para*-galactosylphenyl)$_i$(phenyl)$_{4-i}$ porphyrins (for i=1,2,3) (**2Ca-2Cd**); (3) *meso*-(*para*-glucosylphenyl)$_i$(n-butyl)$_{4-i}$ porphyrins (for i=1,2,3) (**2Da-2Dd**); *meso*-(*para*-glucosylphenyl)$_i$(n-undecyl)$_{4-i}$ porphyrins (for i=1,2,3) (**2Ea-2Ed**); and *meso*-(*para*-maltosylphenyl)$_i$(n-undecyl)$_{4-i}$ porphyrins (for i=1,2,3) (**2Fa-2Fd**); (4) *meso*-(*para*-glucosylphenyl)$_i$(pentafluorophenyl)$_{4-i}$ porphyrins (for i=1,2,3) (**2Ga-2Gd**). These mixed flat *meso*-(glycosylaryl)arylporphyrins and *meso*-(glycosylaryl)alkylporphyrins provided a wide range of amphiphilic characters by changing the number & nature of carbohydrates and the number & nature of aryl or alkyl substituents on the remaining *meso* positions. The presence of phenyl, n-butyl, n-undecyl and pentafluorophenyl groups increased the lipophilicity of these porphyrins and may contribute to increasing nonspecific incorporation into the cell membranes. The carbohydrate substituents could be responsible for specific cell recognition. These porphyrins could serve as a pool of scaling lipophilic, amphiphilic and hydrophilic character to systematically study the correlation between porphyrin polarity and binding to cell membrane or PDT activity.

B. Photocytotoxicity

In order to investigate the structure-activity relationship in glycosylated porphyrins, selected compounds from Fig. (**2A**) and (**2B**) were used to test their photocytotoxicity in KB cells, a cell line derived from human carcinoma of the nasopharynx [43]. a. In order to study the effects of the linking position of saccharide on

meso-TPPs, the photocytotoxicity of three glucosylated phenylporphyrins was compared.

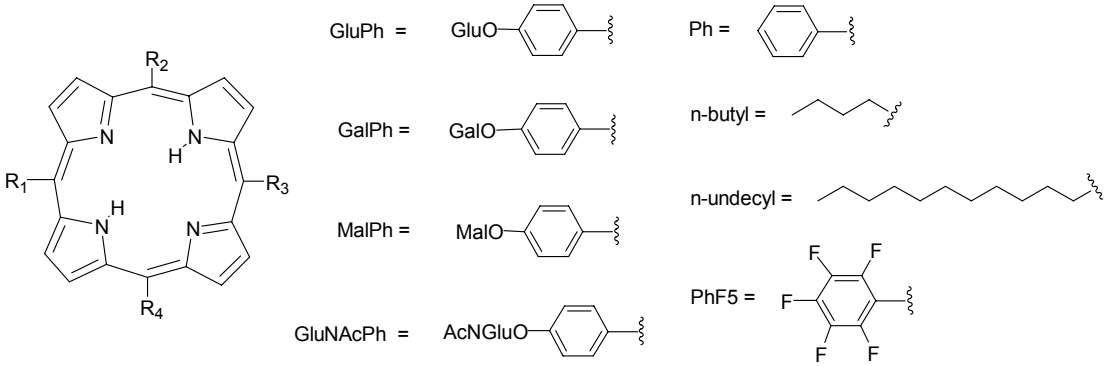

	R_1	R_2	R_3	R_4
2Aa	GluPh	GluPh	GluPh	GluPh
2Ab	GalPh	GalPh	GalPh	GalPh
2Ac	MalPh	MalPh	MalPh	MalPh
2Ad	GluNAcPh	GluNAcPh	GluNAcPh	GluNAcPh
2Ba	GluPh	Ph	Ph	Ph
2Bb	GluPh	GluPh	Ph	Ph
2Bc	GluPh	Ph	GluPh	Ph
2Bd	GluPh	GluPh	GluPh	Ph
2Ca	GalPh	Ph	Ph	Ph
2Cb	GalPh	GalPh	Ph	Ph
2Cc	GalPh	Ph	GalPh	Ph
2Cd	GalPh	GalPh	GalPh	Ph
2Da	GluPh	n-butyl	n-butyl	n-butyl
2Db	GluPh	GluPh	n-butyl	n-butyl
2Dc	GluPh	n-butyl	GluPh	n-butyl
2Dd	GluPh	GluPh	GluPh	n-butyl
2Ea	GluPh	n-undecyl	n-undecyl	n-undecyl
2Eb	GluPh	GluPh	n-undecyl	n-undecyl
2Ec	GluPh	n-undecyl	GluPh	n-undecyl
2Ed	GluPh	GluPh	GluPh	n-undecyl
2Fa	MalPh	n-undecyl	n-undecyl	n-undecyl
2Fb	MalPh	MalPh	n-undecyl	n-undecyl
2Fc	MalPh	n-undecyl	MalPh	n-undecyl
2Fd	MalPh	MalPh	MalPh	n-undecyl
2Ga	GluPh	PhF5	PhF5	PhF5
2Gb	GluPh	GluPh	PhF5	PhF5
2Gc	GluPh	PhF5	GluPh	PhF5
2Gd	GluPh	GluPh	GluPh	PhF5

Figure 2B. Flat glycosylated porphyrins [43, 55-57].

The results are: spherical shaped *meso*-tetrakis(*ortho*-glucosylphenyl)porphyrin ($\alpha\beta\alpha\beta$) in Fig. (**2A**) had no photocytotoxicity at all concentrations tested; planar *meso*-tetrakis(*para*-glucosylphenyl)porphyrin (**2Aa**) in Fig. (**2B**) was very phototoxic; and

meso-tetrakis(*meta*-glucosylphenyl)porphyrin, which has a structure between a globular and a flat geometry, displayed an intermediate activity. All three compounds have the same level of hydrophilicity, and the photocytotoxicities largely depend on their geometry. The flat one showed a better penetrating ability toward the KB cell membranes. b. The effects of the nature of saccharide were studied by four *meso*-tetrakis(*para*-glycosylphenyl)porphyrins bearing different sugar moieties. The compounds are: tetraglucose (**2Aa**), tetragalactose (**2Ab**), tetramaltose (**2Ac**) and tetra-N-acetyl glucosamine (**2Ad**) derivatives. The tetraglucose appended porphyrin (**2Aa**) was the most effective photosensitiz

er in this series, which was five times more active than the tetragalactose derivative (**2Ab**). The two more hydrophilic compounds tetramaltosyl (**2Ac**) and tetra-N-acetylglucosamino (**2Ad**) porphyrins were totally inactive even at high concentrations. c. The number and position of saccharide substituents largely influenced their ability of inducing cell death, due to different binding/uptake properties. The *meso*-tris(*para*-glucosylphenyl)monophenylporphyrin (**2Bd**) displayed a slightly higher photocytotoxicity than *meso*-5,10-bis(*para*-glucosylphenyl)15,20-diphenyl porphyrin (**2Bb**). The 5, 10- substituted glucosyl porphyrin (*cis*-isomer) (**2Bb**) exhibited far better photo activity than its 5, 15- substituted *trans*-isomer (**2Bc**). d. Not surprisingly, the nature of lipophilic substituents plays an important role in the overall lipophilicity of porphyrins, which may in turn affect the photo activity. Four *meso*-tris(*para*-glucosylphenyl)porphyrins bearing different mono-hydrophobic groups were studied. They are: mono(n-undecyl) (**2Ed**), mono(n-butyl) (**2Dd**), monophenyl (**2Bd**) and mono(pentafluorophenyl) (**2Gd**) derivatives. As a consequence of the decreasing

lipophilic character of the four substituents, there is an increasing hydrophilic property of the overall porphyrin molecule in the order of **2Ed**, **2Dd**, **2Bd** and **2Gd**. An increase in the photocytotoxicity among the four porphyrins in KB cells correlated with the increasing hydrophilicity. *Meso*-tris(*para*-glucosylphenyl)mono(pentafluorophenyl)porphyrin (**2Gd**) is the most active photodamaging agent among the 16 tested glycosylated porphyrins. Similarly, the lipophilic compound *meso*-5,10-bis(*para*-glucosylphenyl)15,20-di(n-undecyl)porphyrin (**2Eb**) was not active at all, but when the glucosyl groups were replaced by more hydrophilic maltosyl groups, compound (**2Fb**), a moderate photo activity was restored. Likewise, when the n-undecyl substituents in compound (**2Eb**) were changed to more hydrophilic n-butyl groups (**2Db**), the restored photocytotoxicity was even greater than HpD. This comprehensive investigation of carbohydrate conjugated porphyrins provided an overview of the effects of different substituents. The results indicated that both planar structure and proper lipophilic character of glycoporphyrins are essential for effective photodynamic activities.

C. Binding Properties Based on Liposomes

Furthermore, four glycosylated porphyrins with different photocytotoxicities were chosen to study [56]: (1) photophysical properties by light absorption and fluorescence spectrometries; (2) aggregation; (3) localization within liposomes as a simple model of the lipid region of cell membranes using fluorescent markers. The tested porphyrins are: symmetric derivatives with 4 polar sugar groups on the porphyrin macrocycle (i) *meso*-tetrakis(*ortho*-glucosylphenyl)porphyrin ($\alpha\beta\alpha\beta$ in Fig. (**2A**)) in a spherical geometry, and

(ii) *meso*-tetrakis(*para*-glucosylphenyl)porphyrin (**2Aa**) in a planar geometry; and asymmetrically substituted derivatives (iii) *meso*-tris(*para*-glucosylphenyl)monophenylporphyrin (**2Bd**), and (iv) *meso*-tris(*para*-galactosylphenyl)mono(pentafluorophenyl)porphyrin. The fluorescence lifetime thus fluorescence intensity were markedly increased by the two asymmetrically substituted moleclules --- triglucosyl (**2Bd**) and trigalactosyl derivatives --- in the presence of dimyristoylphosphatidyl choline (DMPC) liposomes. This increased fluorescence indicated binding interactions between the lipid membranes and the porphyrins. The symmetrically substituted porphyrin (*ortho*-tetraglucosyl αβαβ and *para*-tetraglucosyl derivatives) did not exhibit these effects. The fluorescence anisotropy changes of two fluorescent markers 1-anilino naphthalene-8-sulfonate (ANS) and 1,6-diphenyl-1,3,5-hexatriene (DPH) were investigated in liposomes containing these porphyrins. Amphiphilic ANS can localize in both the lipid & polar region of the liposome and DPH stays at the hydrophobic region of the lipid bilayer. The asymmetrically substituted porphyrins (triglucosyl and trigalactosyl derivatives) significantly increased the anisotropy of both DPH & ANS and shifted the phase transition to higher temperatures, while the symmetric derivatives (*ortho*-tetraglucosyl αβαβ and *para*-tetraglucosyl compounds) did not. It was assumed that the amphiphilic macrocycles with asymmetric substitutions (triglycoporphyrins) intercalated between hydrocarbon chains of DMPC liposomes and the symmetric porphyrins (tetra-sugar substituents) only interacted at the headgroup-water interface. In this research program, asymmetrically substituted amphiphilic molecules exhibited better penetration into the cell membrane models.

Symmetric porphyrins *meso*-tetrakis(*para*-glucosylphenyl)porphyrin (**2Aa**) & *meso*-tetrakis(*para*-xylosylphenyl)porphyrin and asymmetric porphyrins *meso*-tris(*para*-glucosylphenyl)monophenylporphyrin (**2Bd**) & *meso*-tris(*para*-galactosylphenyl)mono(pentafluorophenyl)porphyrin were synthesized in a similar manner [57]. Liposomes without net charge (DMPC) and with negative charge (DMPC/dimyristoylphosphatidylglycerol (DMPG)) were used as models to investigate the interaction between these macrocycles and cell membranes. In both types of liposomes, the order of association constants among the four porphyrins followed the order of their lipophilicity. A special case was that the tetraglucose derivative (**2Aa**) only bound to the liposomes with negatively charged surfaces. Kinetic studies on these liposomes supported a biphasic process, for the passive incorporation of porphyrins. This implies that these porphyrins may quickly bind to the surface of cytoplasmic membranes, followed by a slow migration to internal membrane areas. An understanding of the processes involved in porphyrins binding to membranes can help in the design of better and more potent photosensitizers for PDT.

D. Summary

In this collection of nearly 40 saccharide-porphyrin conjugates, the authors have provided an excellent opportunity to compare different photocytotoxicities that depend on the number & nature of saccharides and the number & nature of lipophilic alkyl/aryl substituents. The above results have indicated:

(1) In designing carbohydrate conjugated porphyrins, planar geometry, compare to globular structure, is essential both for photocytotoxicity and binding/intercalating to

liposomes or cell membrane. But note that different conclusions are reached for an octa-saccharides conjugated porphyrin (see below Section Iv iii).

(2) Mediated transport might be involved. Tetra-glucose porphyrin derivative (**2Aa**) has a 5-fold higher photocytotoxicity than the tetra-galactose derivative (**2Ab**) and the tetra-maltose (**2Ac**) & tetra-N-acetyl glucosamine (**2Ad**) compounds have no effect. These results may be somewhat related to mediated transport. Glucose uptake is known to be increased in cancer cells due to their elevated energy requirements. The 5-fold increase in PDT effectiveness of glucose over galactose substitution is probably due to the high metabolic rate of the KB cells. Thus, in designing sugar-appended porphyrins to target PDT, glucose derivatives might be on the top of the list.

(3) The result that *cis*-glucose isomer (**2Bb**) is much more potent PDT agent than the *trans*-glucose isomer (**2Bc**) indicates that they might have a different amphiphilicity. The *cis*-isomer has a structure that the two glucose groups are substituted at the adjacent *meso*-phenyl groups, while they are on the opposite positions in the *trans*-isomer. Thus, the *cis*-compound is more likely to distribute into both the polar head group and the non-polar tail of the cell membrane, due to its well-separated polar and non-polar groups. Though only differing in the positions of substitutions, they have very different partition coefficients ($OD_{2\text{-octanol}}/OD_{PBS\ buffer}$): 270 for the *cis* and 3.9 for the *trans*. The higher lipophilicity of the *cis*-molecule may allow the compound to intercalate better toward the lipophilic core of the cell membrane.

(4) These and other results indicate that there is a general trend that correlates increasing lipophilicity with increasing PDT effectiveness, and this does not take into account active uptake. More hydrophilic substituents are needed to join the compounds tested in order to

draw any conclusion. Nonetheless, proper lipophilicity is one of the decisive characteristics for designing efficient drugs.

(5) The liposome studies supported the speculation that those compounds with higher amphiphilicity show higher photocytotoxicity. Only the carbohydrate porphyrins with the substituents on the same side can reside in both the hydrophilic head and the lipophilic core of the liposome bilayer.

ii. Carbohydrates Anchored on TPP by a hydrocarbon spacer

With PDT in mind, 13 porphyrins bearing carbohydrate moieties separated from the phenyl porphyrin by a hydrocarbon spacer [Fig. (**3**)] were synthesized [58, 59] by direct glycosylation of the *ortho*- or *para*-hydroxypropyloxyphenylporphyrin, or by condensation of the glycosylated aldehyde with either pyrrole or *meso*-(*para*-

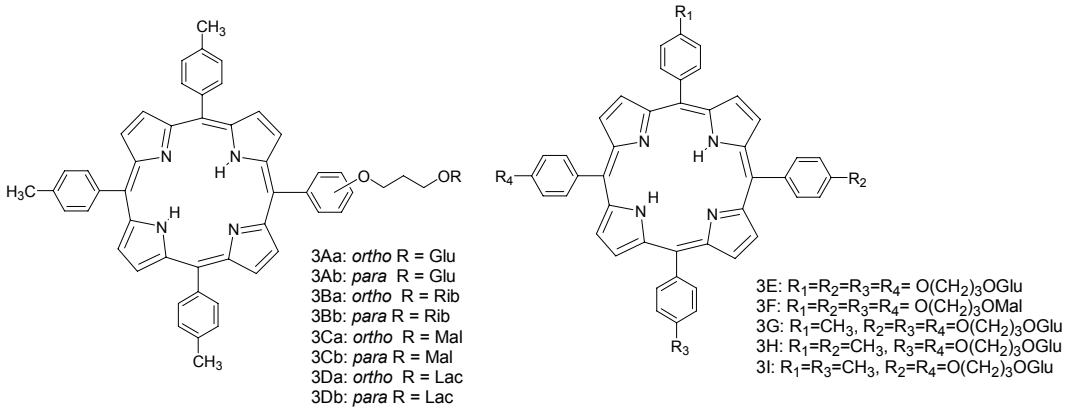

Figure 3. 13 Porphyrins where carbohydrate moieties are separated from the phenyl porphyrin by a hydrocarbon spacer [58-60].

tolyl)dipyrromethane. The photofungicidal properties of some porphyrins were investigated [60] against yeast *Saccharomyces cerevisiæ*. The studied compounds are *para* substituted *meso*-TPPs: monoglucosyl (**3Ab**), *cis*-diglucosyl (**3H**), *trans*-diglucosyl (**3I**), triglucosyl (**3G**), tetraglucosyl (**3E**) and tetramaltosyl (**3F**) porphyrins. In the

presence of these glycoporphyrins, fungal clonogenicity and cell membrane integrity measured by propidium iodide (PI) permeability were tested and compared with the effects of hematoporphyrin. The most active compounds were monoglucosyl (**3Ab**) and *cis*-diglucosyl (**3H**) porphyrins (which both were better than hematoporphyrin), indicated by loss of clonogenicity and high percentage of cell death with short irradiation time. Triglucosyl porphyrin (**3G**) was the least active. Terminal deoxynucleotidyl transferase (TdT)-mediated dUTP-biotin nick end labeling (TUNEL) assays detected extensive DNA fragmentation in *S. cerevisiæ* cells treated with the monoglucosyl derivative (**3Ab**), but not in those treated with triglucosyl (**3G**) porphyrin, suggesting the presence of photosensitizer inside the cells. Cell penetration of these porphyrins was investigated by microspectrofluorimetry. Consistent with the results in photoinduced loss of clonogenicity and cell death, mono-glucosyl (**3Ab**) and *cis*-diglucosyl (**3H**) derivatives had better penetration into the cells, while the fluorescence intensity of triglucosyl (**3G**), tetra-glucosyl (**3E**) and tetra-maltosyl (**3F**) derivatives was even lower than the cellular background, therefore could not be determined. The studies found a correlation between partition coefficients and activities --- porphyrins (**3Ab** & **3H**) with higher partition coefficients (higher lipophilicity) exhibited greater photobiological activity than derivatives with more hydrophilic characters. It's worth pointing out that the *cis*-diglucosyl (**3H**) & *trans*-diglucosyl (**3I**) porphyrins only differ in the position of sugar on the macrocycle and they have slightly difference in partition coefficients, yet *cis*-isomer displayed markedly higher antifungal activity than *trans*-isomer, most probably due to its well-separated hydrophobic and hydrophilic poles.

Yeast, as a branch of fungus, has a rigid cell wall with different components, compared to the soft plasma membrane in cancer cells. Thus, the structural properties related with photofungicidal effects can not be fully generalized to antitumor photo activity. Nonetheless, the results are still valuable:

(1) Only mono- and di-glucose derivatives exhibited photodynamic effects on fungus, but not the tri-, tetra-glucose and tetra-maltose derivatives. This indicates that one of the key factors for biological effect is proper lipophilicity, which can be reflected by partition coefficient. The partition coefficients for the active compounds are in the range of 20-90, while these numbers are much greater than the non-active ones (< 0.5).

(2) The *cis*-diglucose isomer has much higher antifungal activity than its *trans*-counterpart. This is consistent with above discussion in Section I i D (3). The separation of different lipophilic/hydrophilic groups is important for enhanced activity.

iii. Glycosylated Nitroaryl Porphyrins

With the aim of studying photoinhibition of Gram positive bacteria, nitroglycosylated *meso*-arylporphyrins [Fig, (**4**)] were synthesized and evaluated [61]. Two glyco-porphyrins (**4B** & **4C**) displayed significant antibacterial activities upon illumination with Gram positive bacteria *Staphylococcus aureus*, while none of the porphyrins exhibited any activity toward Gram negative bacteria *Escherichia coli*. The positive results came from mono(*para*-nitrophenyl)tris(*para*-glucosylphenyl)porphyrin (**4B**) and *cis*-bis(*para*-nitrophenyl)bis(*para*-glucosylphenyl)porphyrin (**4C**), and this indicated: (1) the presence of unprotected sugar is essential, since neither the porphyrins with acetyl protected sugar moieties nor unglycosylated derivative (**4H**) exhibited any

bacterial growth inhibition; (2) the presence of nitro group in *para* position is important, since there was no activity in *ortho*-nitro substituted porphyrin (**4A**) or unnitrated

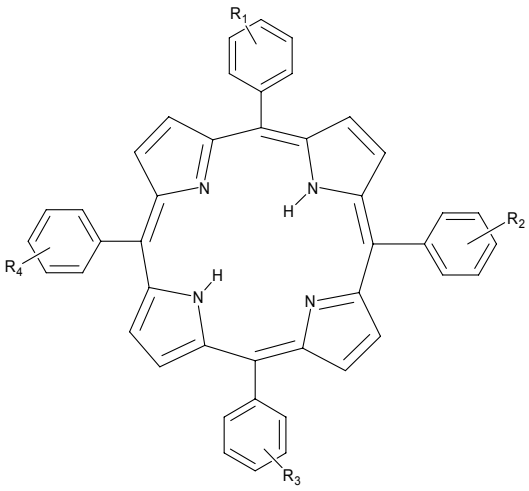

4A: R_1 = *ortho* NO_2, $R_2 = R_3 = R_4$ = *para* OGlu
4B: R_1 = *para* NO_2, $R_2 = R_3 = R_4$ = *para* OGlu
4C: $R_1 = R_2$ = *para* NO_2, $R_3 = R_4$ = *para* OGlu
4D: $R_1 = R_3$ = *para* NO_2, $R_2 = R_4$ = *para* OGlu
4E: R_1 = *ortho* OGlu, $R_2 = R_3 = R_4$ = *para* NO_2
4F: R_1 = *para* OGlu, $R_2 = R_3 = R_4$ = *para* NO_2
4G; R_1 = *para* OH, $R_2 = R_3 = R_4$ = *para* OGlu
4H: R_1 = *para* NO_2, $R_2 = R_3 = R_4$ = *para* CH_3

Figure 4. Nitroglycosylated *meso*-arylporphyrins [61].

porphyrin (**4G**); (3) *cis*-bis(*para*-nitrophenyl)bis(*para*-glucosylphenyl)porphyrin (**4C**) is much more potent photoantibacterial agent than its *trans*-isomer (**4D**); (4) the antimicrobial activity required at least two glucose units and one *para*-nitro group present.

Again, one should keep in mind that the bacterial cell wall is much different from cancer cell membrane. The cell wall of bacterial cells creates a physical and chemical barrier that may prevent sensitizer binding to bacterial membrane or proteins. Caution must be used when generalizing these results to cancer cells. The unique outer membrane of Gram negative bacteria may require a small peptide to stimulate the translocation of porphyrin through the outer membrane and to stimulate photosensitization [62]. Besides the requirements of unprotected sugar and nitro group, not surprisingly, *cis*-isomer is also more potent than its *trans*-isomer in photo antibacterial activity.

iv. Cationic Glyco-porphyrins

Because of the enhanced affinity of cationic porphyrins [19] toward DNA and their high solubility, porphyrins bearing three cationic substitution groups (N-methylpyridinium, N-isopropylpyridinium or N-n-octylpyridinium) and one glyco group (glucose, maltose or lactose) were prepared [63, 64], but no biological evaluation was

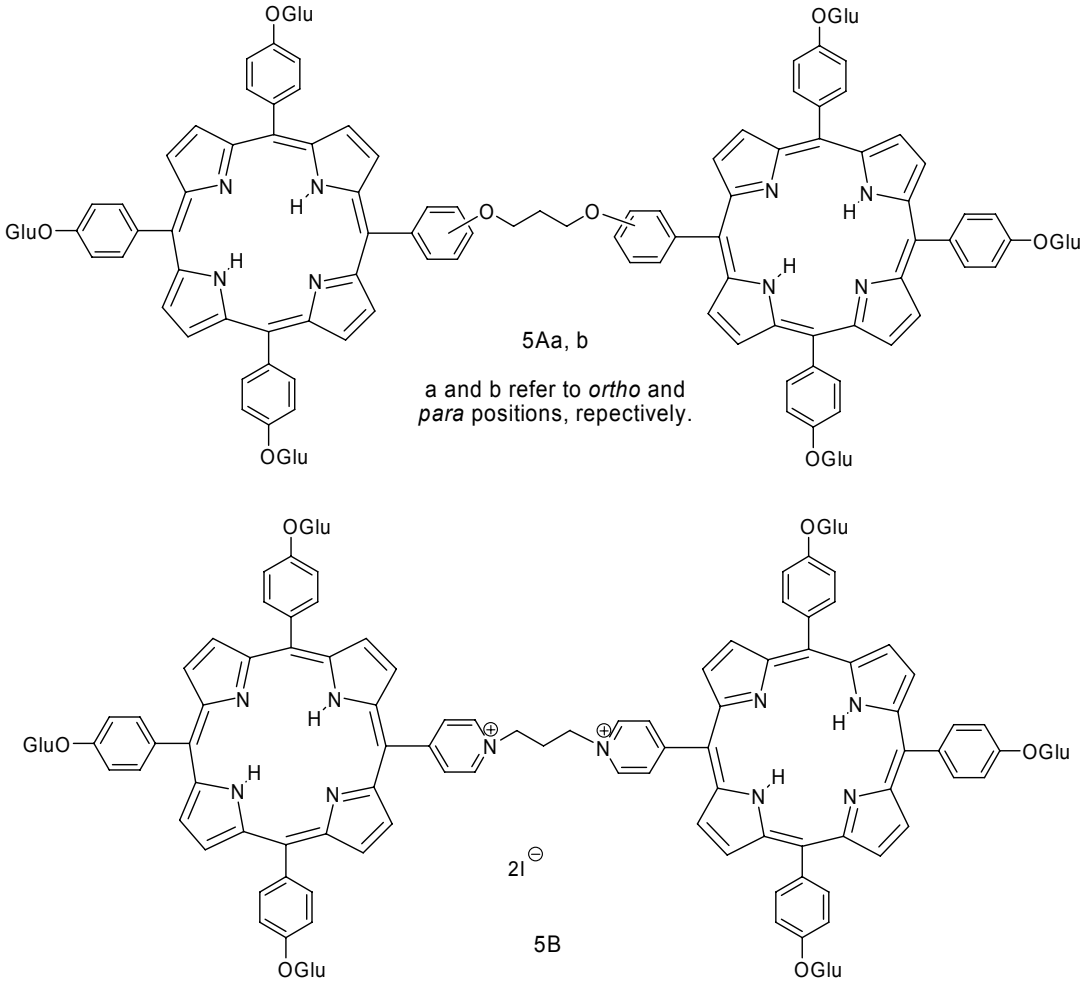

Figure 5. Glycosylated neutral and cationic porphyrin dimers [65].

presented. Recently, another synthesis was accomplished in making glycosylated neutral and cationic porphyrin dimers [Fig. (**5**)] [65]. These porphyrins lacked photocytotoxicity when tested against K562 human leukemia promyelocytary cells. This result suggested that the bulky structure of the neutral dimers (**5Aa** & **5Ab**) and high hydrophilicity of the

cationic glycosylated dimer (**5B**) may inhibit interaction with cell membranes and result in low cellular permeability.

Though no favorable photodynamic effects were observed with these cationic dimers, more studies are needed to rule out the effectiveness by putting positive charge(s) onto glyco-porphyrins. Indeed, preliminary results (Chen & Drain, data not published) have shown that those cationic porphyrins known to bind DNA [19] have high affinity toward cancer cells. We expect more investigations toward this aspect.

v. Functions of Unprotected Sugars on Porphyrins

In an effort to systematically understand the correlation between hydrophilic properties due to the sugar moieties and the phototherapeutic activities, four families of OH-protected and unprotected glycosylated TPPs were investigated [66]. The sugar moieties include tetra- glucose, galactose, N-acetyl glucosamine and octa- glucose. The octaglucosylated derivative was obtained from bis-(tetraacetylglucopyranosyloxy)benzaldehyde by a modified Lindsey method [67]. The photocytotoxicity of these compounds was evaluated by a 3-(4,5-dimethylthiazol-2-yl)-2,5-diphenyltetrazolium bromide (MTT) assay in HeLa cells. In all the porphyrins tested, acetyl protected sugar porphyrins were always more potent than their unprotected counterparts, where *meso*-tetrakis(tetraacetylglucosylphenyl)porphyrin was the strongest candidate. These results indicated that the lipophilic properties play an important role in cell uptake, where drugs that are too hydrophilic (unprotected sugar porphyrins, esp. the octaglucose derivative) cannot incorporate well into cell membranes, because of the

hydrophobic core of the membrane. Also, the globular structures (octaglucose derivatives) are less favorable for cell uptake than flat structures (*para*-tetraglycosylated derivatives), which is consistent with the results from studies using similar geometry of compounds described above.

Note that, contrary to the observations from the above research, in this study on HeLa cells, porphyrins are effective only when they bear protected sugars, but not the unprotected ones, which may depend on the specific environment of cell membranes and the hydrophobicities of the drugs. Only one single case as such is not sufficient to conclude the importance of unprotected sugars in photodynamic activities of porphyrins. Only the deprotected derivatives of similar octa-galactosyl porphyrin (**18A**) (Section IV iii) and tetra-glycosyl porphyrin (**14A**) (Section III) act against rat hepatoma cells and human breast cancer cells, respectively.

vi. Cholesteryl Glyco-Porphyrins

Galactopyranosyl – cholesteryloxy substituted porphyrin [68] [Fig. (**6A**)] was obtained by coupling of galactosyl and cholesteryl dipyrromethanes with imminium ion and $K_3[Fe(CN)_6]$ oxidation. The capability of forming vesicle-like structures or aggregates was investigated. The split of Soret band indicated that face-to-face (minor) and edge-to-edge (major) orientations coexisted.

In a continuing study, mono(*para*-6'-galactosylphenyl)porphyrin [Fig. (**6B**)] was made in a similar manner [69]. The uptake of **6A** & **6B** in phosphatidylethanolamine (PE) & DMPC liposomes was detected by fluorescence spectroscopy. Porphyrin **6B** was efficiently incorporated into the liposomes while compound **6A** did not work well in

either liposome. By using dialysis and ultrasound techniques, porphyrin vesicles were

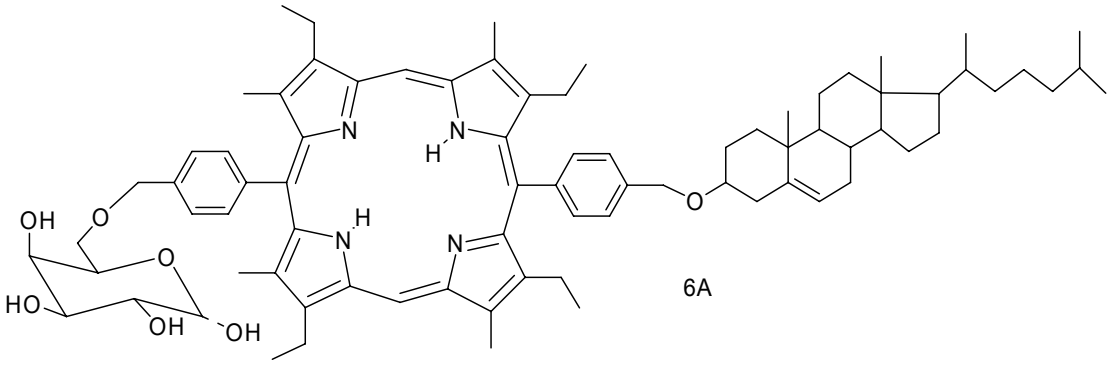

Figure 6A. Galactopyranosyl – cholesteryloxy substituted porphyrin [68].

formed, but the dilution method only led to formation of a mixture of different types of aggregates. Since lipoproteins are of importance in receptor mediated endocytosis for cell uptake, the binding constant of compound **6B** was tested against high density lipoprotein (HDL), low density lipoprotein (LDL) and very low density lipoprotein (VLDL). It had the strongest binding toward VLDL and LDL, but to a lesser extend toward HDL. This feature may facilitate selective drug delivery to cancer cells, since tumor cells are well known to have significant amount of LDL receptors.

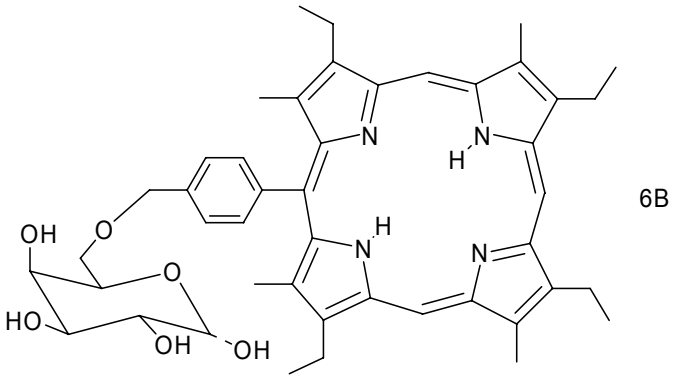

Figure 6B. Mono (*para*-6'-galactose) phenyl porphyrin [69].

This research reinforced the importance of drug design in balancing between hydrophobic and hydrophilic moieties for efficient drug delivery and uptake by cancer

cells. The fact that cholesterol substituted porphyrin (**6A**) did not incorporate well into liposomes suggests that cholesterol may not be a good choice for substitution though it is an active component in cell membranes. Cholesterol is very lipophilic and can bind well to the membrane, but it stabilizes the membrane and likely prevents the porphyrin macrocycle further intercalating into the membrane. The drug will not be as effective if the singlet oxygen production site is not in the cell vicinity, due to the short life time of singlet oxygen (about 1-3 μs).

vii. The Effects of Mono Carbohydrate Substituted Porphyrins on Liposomes

In order to study aggregation properties of glycoporphyrins and their incorporations into cell membrane models, a series of mono carbohydrate substituted porphyrins [Fig. (**7**)] were synthesized by the reactions between nickel *meso*-

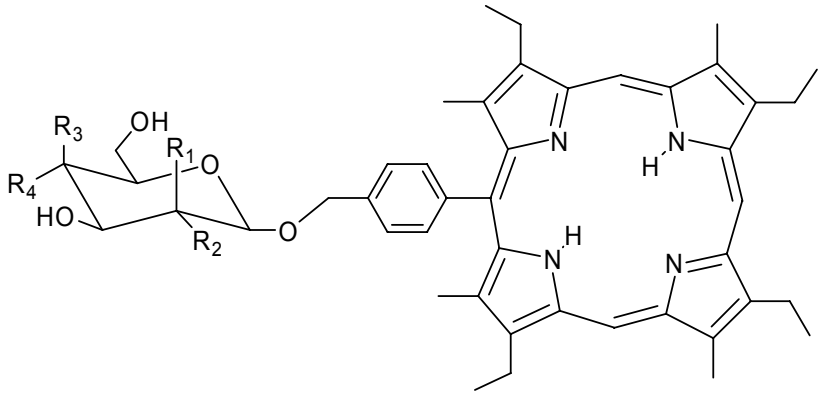

	R_1	R_2	R_3	R_4	
7A	OH	H	H	OH	Mannose derivative
7B	H	OH	OH	H	Galactose derivative
7C	H	OH	H	OH	Glucose derivative
7D	H	NHAc	H	OH	N-acetyl glucosamine derivative
7E	H	OH	H	α(1,4')Glu	Maltose derivative
7F	H	OH	H	β(1,4')Gal	Lactose derivative
7G	H	OH	H	β(1,4')Glu	Cellobiose derivative

Figure 7. Mono carbohydrate substituted porphyrins [70].

mono(hydroxymethoxyphenyl)porphyrin and different glycosyl imidates with $ZnCl_2$ as a catalyst [70]. The carbohydrate substituents include mannose, galatose, glucose, N-acetyl glucosamine, maltose, lactose and cellobiose. All compounds formed stable aggregates in a self-assembling process in aqueous solution. This process is not affected by the nature of the sugar moieties, but only by the configuration of the anomeric carbon atom. PE and DMPC liposomes were used as cell membrane models, which all compounds incorporated very efficiently into, mainly as monomers. All the estimated binding constants were much greater than those reported for hematoporphyrin. Among these compounds, the porphyrin bearing a cellobiose (**7G**) exhibited the greatest binding constant in both types of liposomes.

Though liposomes are good simplified models for cell membrane, they do not well represent the complexity of real cell membrane. In this research, the cellobiose derivative has the highest binding constant toward PE and DMPC liposomes, which only indicates that it has a better incorporation into the bilayer, but doest not imply any increased cellular uptake, and not even a better binding to cell membrane.

viii. Peptidic glycosylated porphyrins

Peptidic glycosylated porphyrins are promising PDT reagents, since not only sugar moieties but peptides are also active components in cell recognition. Two series of glucosyl TPPs bearing amino acid residues [71] were synthesized. In the first series glycoporphyrins were made using a tailored Lindsey method [53] (BF_3OEt_2/CH_2Cl_2, 18h, then *p*-choranil). The nitro groups were reduced to amines, which were coupled with N-Fmoc-$_L$-alanine by DCC. Fmoc, the alanine protecting group, was selectively removed

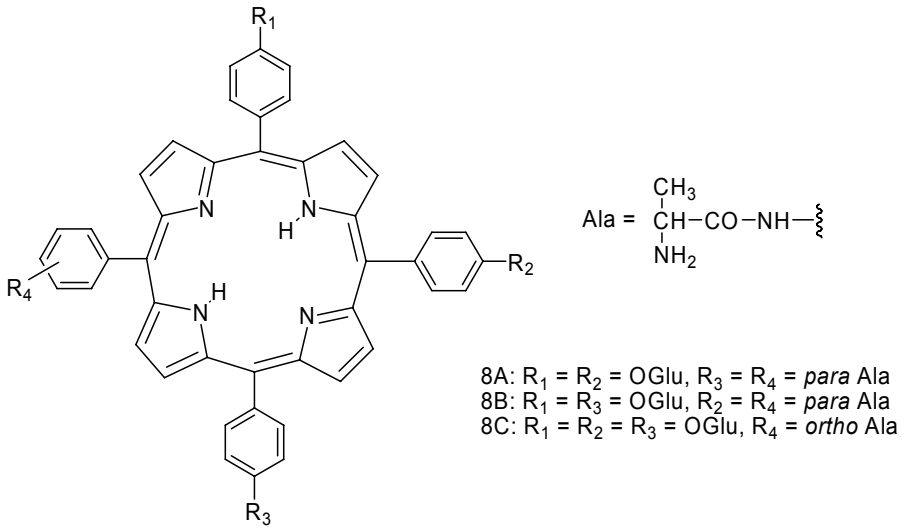

Figure 8. *Cis*- and *trans*- bis(*para*-glucosylphenyl) bis(*para*-alaninylphenyl) porphyrin and mono(*ortho*-alaninylphenyl) tris(*para*-glucosylphenyl) porphyrin [71, 72].

with morpholine, and the acetate groups on glucose moieties were cleaved by NaOMe. In the second series mono(nitrophenyl)tritolylporphyrins were reduced to give the corresponding aminoporphyrins, which were then coupled with N-Fmoc-$_L$-serine substituted tetra-acetyl-glucose by DCC. Fmoc was removed in a similar manner as the first series and acetyl groups on the glucose were removed by hydrazine. Thus, mono(glucosylaryl)tritolylporphyrins were successfully obtained, where the glucose moiety is separated from the aryl substituent by a serine unit. The photocytotoxicity of these porphyrins were tested against K562 human chronic myelogenous leukemia cells. Though all the compounds induced limited immediate cell death when compared to the effect of hematoporphyrin, *cis*- and *trans*- bis(*para*-glucosylphenyl)bis(*para*-alaninylphenyl)porphyrin (**8A** & **8B**) and mono(*ortho*-alaninylphenyl)tris(*para*-glucosylphenyl)porphyrin (**8C**) [Fig. (**8**)] led to a high percentage of cell death when checked 24 hours after irradiation, which are comparable to those observed with hematoporphyrin when irradiation was longer than 60 minutes.

By the same procedure, four peptidic glucosylated porphyrins were obtained [72] and they are mono(*ortho*- or *para*-glucosylphenyl)tris(*para*-alaninylphenyl)porphyrins and mono(*ortho*- or *para*-alaninyl)tris(*para*-glucosylphenyl)porphyrins. The photocytotoxicity of these synthetic porphyrins was again investigated against K562 human chronic myelogenous leukemia cells by a PI permeability assay using flow cytometry. With all the four porphyrins, delayed cell death was observed 24 hours following the irradiation. Among the four, mono(*ortho*-alaninylphenyl)tris(*para*-glucosylphenyl)porphyrin (**8C**) had the most photocytotoxicity and was the most promising compound for PDT. The effects on cell death of the other three porphyrins were comparable to the results observed with the same concentration (2 μM) of hematoporphyrin. These results were only observed when the irradiation time was greater than 60 minutes for hematoporphyrin and the tested compounds.

A recent study [73] has attached an arginine-glycine-aspartate (RGD) sequence to tris(*para*-glucosylphenyl)porphyrin, which was synthesized by the Little modification of the Adler method [74, 75]. RGD is a small peptide responsible for integrin binding to extracellular matrix (ECM), which is critical for cell adhesion, migration, growth and differentiation. RGD is appended to the *meso*-tris(*para*-glucosylphenyl)porphyrin in either *ortho*- or *para*- position of the remaining *meso* phenyl group by an efficient solid-phase strategy based on the use of Wang resin. The photocytotoxicity of these porphyrins was evaluated in K562 human chronic myelogenous leukemia cell line. After irradiation, the PI permeable cells detected by flow cytometry were counted as dead. While there is no immediate effect, the delayed effects of both 2 μM RGD-glucose conjugated

porphyrins were comparable with 1.2 μg/ml Photofrin®. The immediate cell death is counted as necrosis, whereas the delayed action is most likely due to apoptosis.

Peptidic porphyrins have drawn attention in recent years for potential PDT agents [76-78]. The idea is based on the fact that amino acids/peptides are cell recognizable elements, therefore may facilitate drugs incorporation into cell membrane. Combining amino acids/peptides with carbohydrate as substituents for porphyrins to target PDT is still a fairly new area of research. More combinations are needed for a summarizable conclusion.

ix. Oligosaccharide Porphyrins

Porphyrins bearing oligosaccharide also have been reported. In trying to obtain the right lipophilicity of porphyrins for PDT, a *meso*-TPP having both hexa-maltosyl and decyl hydrocarbon chain moieties [Fig. (**9**)] was synthesized via dipyrromethane coupling

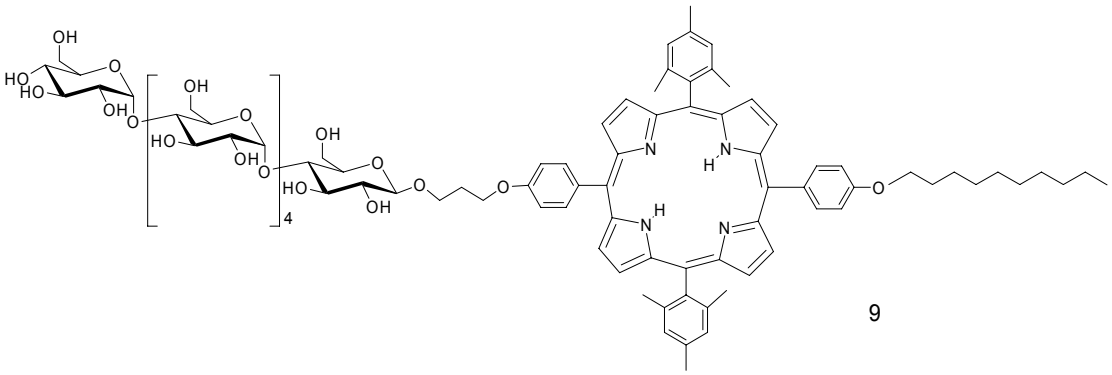

Figure 9. Meso-TPP bearing hexa-maltosyl and decyl chain [79].

[79]. Studies on HeLa cells showed that porphyrin **9** exhibited photocytotoxicity with low cytotoxicity in the dark.

With the exception of specific recognition from the cell membrane, oligosaccharides together with porphyrin core are probably too big and polar for efficient binding/incorporation into the cell membrane, and passive transport through the membrane may be even tougher.

x. Summary of O-Glyco Porphyrins

O-glycosidic porphyrins also have been synthesized and evaluated for the catalysis of alkene oxidation [80, 81], and for metal ion binding [67, 82, 83], but mostly for potential Photodynamic Therapy agents [84-86]. In designing effective drugs for PDT, solubility and cell binding/uptake are important features to be considered. Using sugar substituents can certainly increase the drug solubility in aqueous solution for efficient drug delivery. Moreover, since carbohydrates are cell components, glycosylation of porphyrins may lead to specific interaction between the drug and membrane receptors to increase the drug efficacy. For nonspecific interactions between the drugs and cell membranes, amphiphilicity is the most important character. On one hand by selecting different nature and number of sugar moieties, a wide range of hydrophilicity can be obtained. On the other hand, there is a huge pool of organic substituent groups that can lead to a variety of hydrophobicities. Balancing the two, subtle differences in amphiphilicity can be achieved.

To summarize the above studies, in general:

(1) Of all the possible carbohydrate and peptide derivatives available to append onto porphyrins for PDT, glucose might be a priority to start with because of the increased energetic requirement of cancer cells results in increased glycolysis.

(2) When molecule geometry is a concern, flat structures (*para* substituted derivatives) are usually better than globular structures (*ortho* substituted derivatives).

(3) Proper lipophilicity is essential in designing potent PDT agents. Highly hydrophobic or hydrophilic ones are not desirable, at least in carbohydrate porphyrins.

(4) Mono-, di- or tri- glycosylated porphyrins are normally better than tetra- or octa-glycosylated ones.

(5) Among di-glyco substituted porphyrins, *cis*-(5,10 substitution) isomer usually has greater biological effects than the *trans*-(5,15 substitution) isomer (through there are cases where they have similar biological activity).

(6) While peptidic porphyrins can be promising PDT agents, carbohydrate-peptide conjugated porphyrins may afford even better candidates for PDT.

In general, the problems with O-glycoside based compounds arise from the lability of the link and disappointing synthetic yields.

II. Carbon-Carbon Linkage

As discussed above, O-glycosidic porphyrins have been explored extensively in their synthetic approach and biological evaluation. A perceived problem with O-glycosides is the inherent possibility for glycosyl cleavage by acids, and in biological systems by glycohydrolases. Partial hydrolysis of the O-saccharides is also caused by the Lewis acid usually used in the synthesis, which decreases the yields of these structures. To overcome these drawbacks of O-glycosides, researchers have focused on C-glycosylated porphyrins as potential PDT agents.

Two C-*meso* glyco-conjugated phenyl porphyrins were prepared by using Ramberg-Bäcklund [87, 88] and Lindsey [53, 89] methods for the key conversions [Fig.

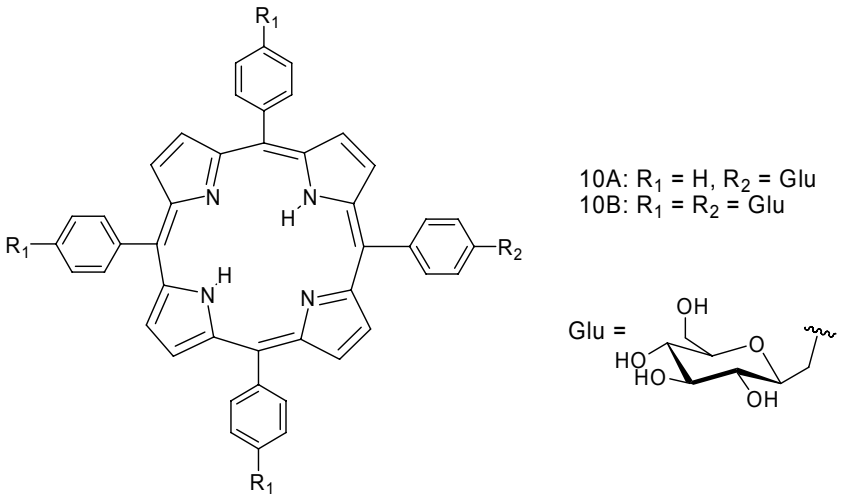

Figure 10. C-glycoconjugated porphyrins prepared by Ramberg-Bäcklund and Lindsey methods [90].

(**10**)] [90]. This is so far the only method to accomplish the direct attachment of C-glycosides onto TPPs. Standard plasmid photocleavage assays were carried out to evaluate their photoactivity. Though the photoactivity of DNA cleavage was poor, they are still promising candidates to test *in vitro* for their photocytotoxicity.

Adapting protocols of the MacDonald condensation [91, 92] or the Lindsey [53] method, porphyrins bearing two uridinyl groups or four furanosyl moieties coupled through robust carbon-carbon bonds were successfully constructed [93]. Together with their metallo species, the ability to photocleave DNA was investigated. Upon visible light irradiation, two palladium derivatives [Fig. (**11**)] proved to be strong DNA photocleavers by cleaving form I supercoiled double strand plasmid DNA into form II nicked circular DNA.

While there have been other reports of the synthesis of C-glycosylated porphyrins for PDT, where the carbohydrate moieties linked directly on *meso*-position of tetrapyrroles [94-97], the biological activities were not reported. Chiral recognition, asymmetric catalysis and transport domains [98, 99] were a few other targets of this type

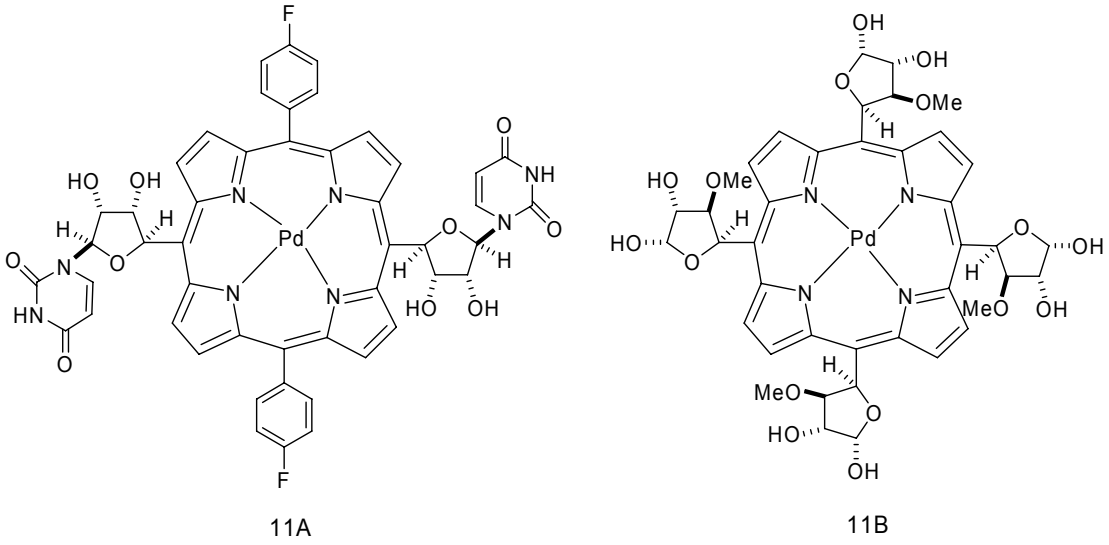

Figure 11. Palladium C-glycosylated porphyrins as strong DNA photocleavers [93].

of research. Since the preparation can be more complicated, the C-glycosidic porphyrins are less studied than O-glycosidic porphyrins. Nonetheless, because C-glycoconjugated porphyrins are not hydrolysable, are resistant to enzymatic cleavage, yet are conformationally similar to the O-glycoconjugated compounds, they remain promising PDT agents.

III. Thioether Linkage

Similar to C-glyco porphyrins, replacing the oxygen with a sulfur atom at the sugar anomeric position yields S-glycosylated porphyrins. The S-glyco porphyrins are

also resistant to endogenous hydrolysis catalyzed by glycosidases [100] and more stable with acid and base compare to their O-glyco analogues.

A series of thioglycosylated *meso*-arylporphyrins [Fig. (**12**)] with a spacer arm linkage between macrocycle and carbohydrate moieties [101] were prepared in four steps by the Little method [74]. Their photocytotoxicity was tested against yeast *S. cerevisiæ*. Yeast cells were preincubated with different porphyrins and their PI permeability were examined after irradiation by flow cytometry. Cells stained with PI were counted as non-viable ones. All six porphyrins exhibited photocytotoxicity to yeast cells, yet a delayed effect compared to hematoporphyrin. It's noteworthy that all the *ortho*-glyco substituted compounds displayed a stronger activity than the corresponding *para*-isomers. This is in

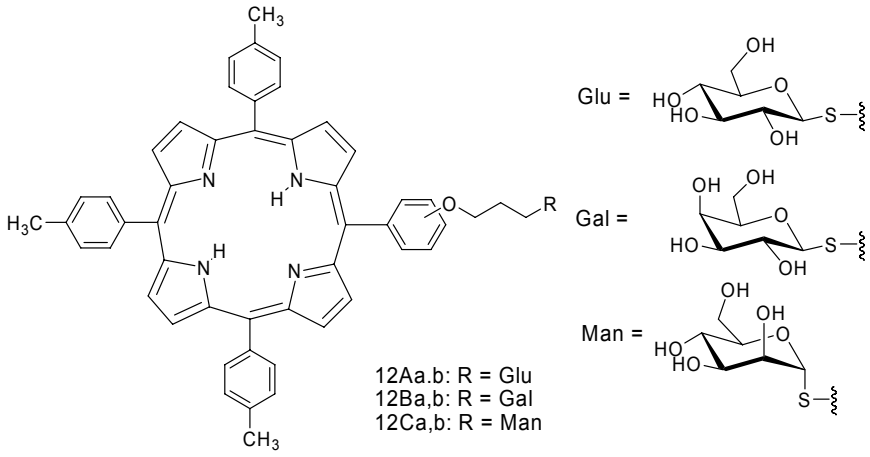

Figure 12. Thioglycosylated *meso*-arylporphyrins. (a and b refer to *ortho* and *para* positions, respectively.) [101, 102]

contrast to observations on O-glycosylated porphyrins, where in most cases molecules with sugar moieties directly anchored on the *ortho* position of TPPs were less efficient PDT agents than their *para*-substituted counterparts. The hydrocarbon spacer arm between TPPs and carbohydrate moiety in this research program must provide extra space for free rotation to generate a nonspherical geometry. Plus, there is only one

saccharide substitution as opposed to the tetra-substitutttion, which is much more capable to form a globular structure. Therefore the *ortho*-isomers bind to or penetrate into cell membranes. As we have mentioned above in Section I ii, studies on fungus cannot be inferred to the cancer cell due to the highly different cell wall/membrane system.

In continuing efforts to make S-glycosidic porphyrins [102], thiosugar groups were attached to isohematoporphyrin derivatives [Fig. (**13**)]. Thioglucosylated porphyrins **12Aa,b** were chosen as examples to test enzymatic hydrolysis of β–glucosidic bond by β–glucosidase. Contrary to their O-glucosylated counterparts **3Aa,b** where formation of

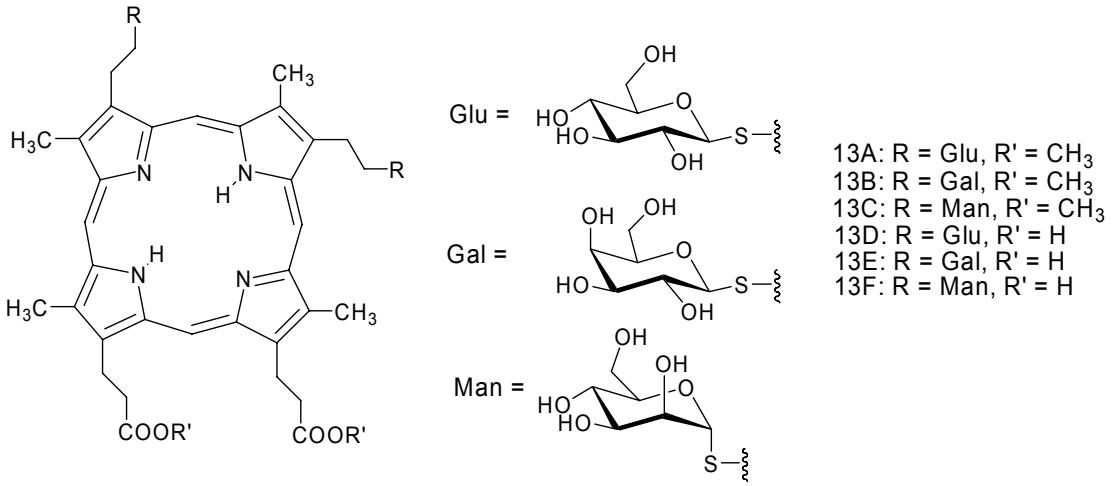

Figure 13. Thioglycosylated isohematoporphyrin derivatives [102].

glucose was observed, no cleavage was found with S-glyco-porphyrins. All the porphyrins in Fig. (**12**) & Fig. (**13**) were tested against K562 chronic leukemia cells for their *in vitro* photocytotoxicity by PI permeability. Their efficiency at 2 μM was comparable with Photofrin® at 1.2 μg/ml. Among the TPP thioglycosyl derivatives in Fig. (**12**), all *ortho*- isomers **12Aa**, **12Ba**, **12Ca** were active, yet only one *para*- isomer **12Ab** was effective. Among the thioglycosylated isohematoporphyrin derivatives in Fig. (**13**),

only the ones with ester functional group (**13A**, **13B** & **13C**) were photoactive. Moreover, the latter compounds were found to be more potent than Photofrin®. Those carboxylic acid appended porphyrins (**13D**, **13E** & **13F**) did not exhibit any photoactivity. It might be that these porphyrins partially exist in anionic form in aqueous medium and can be repelled by the negatively charged lipids on cell membranes; therefore prevent them from diffusing into the cells. In both cases, the nature of sugar did not play an essential role in biological activity. The high activities of the S-glyco porphyrins in this research program, especially those isohematoporphyrin derivatives, produced promising PDT agents. Their high bio-effects may partially due to the non-hydrolysable S-glyco substituents of porphyrins, which resist degradation while residing on the membrane or in the cell (if they were transported into the cell); i.e. they are not readily metabolized.

A simple direct glycosylation with high yield [90] was realized by reacting 1-thioglucose or 1-thiogalactose with *meso*-tetrakis(pentafluorophenyl)porphyrin at room temperature in DMF to afford **14A** & **14B** [Fig. (**14**)]. Though these two are not excellent DNA photocleavers, their proper lipophilicity and carbohydrate specificity lead them to be potent PDT agents (Chen & Drain, data not published).

S-glycoconjugated porphyrins are a class of potential drugs for PDT due to their non-hydrolysable character, though more varieties are yet to come. At this point it is reasonable to speculate that the S-glycoconjugated and C-glycoconjugated porphyrins will have similar binding characteristics as their O-glycoconjugated analogues. However, it is premature to predict that they will display the same biological activity.

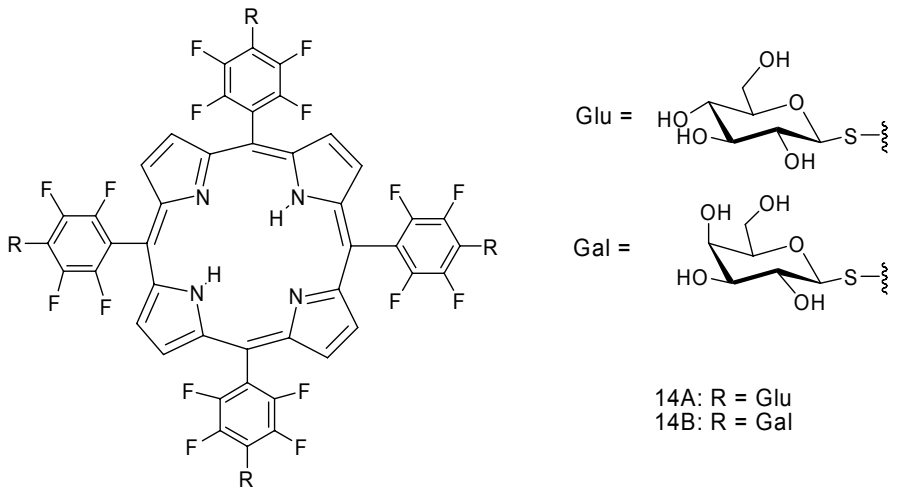

Figure 14. Fluorinated thioglycosyl porphyrins [90].

IV. Other Linkages:

i. Ester Linkage:

Two strapped porphyrins [103] with ester linkage connected by trehalose [Fig. (**15**)] were synthesized and their photocytotoxicity was evaluated against K562 human

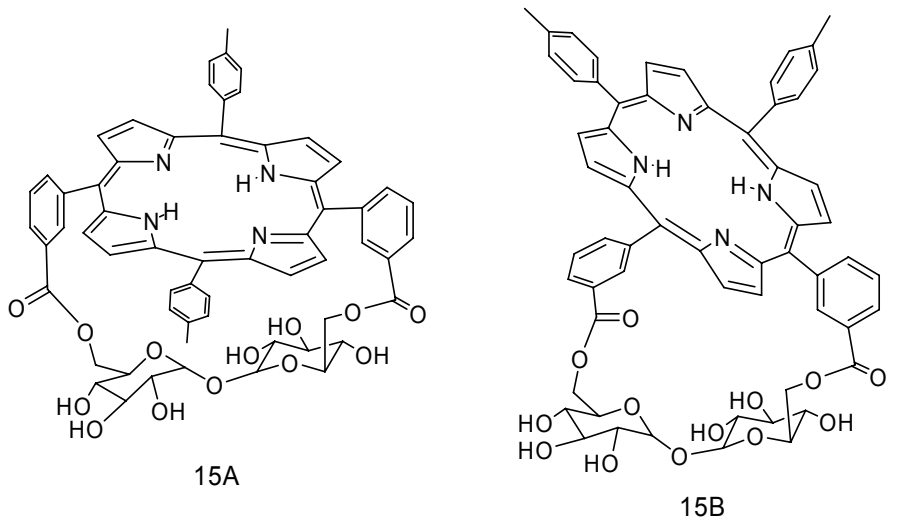

Figure 15. Two strapped glycosylated porphyrins [103].

chronic myelogenous leukemia cells by the PI permeability assay and compared with hematoporphyrin. The *trans*-strapped isomer **15A** displayed cell killing effect despite a

more delayed response time than the hematoporphyrin. There are reports that trehalose – even at relatively low concentration – may bind to the surface of DMPC and DMPC/DMPG liposomes [104]. It is difficult to explain why the *trans*-strapped porphyrin has a better biological effect than the *cis*-strapped porphyrin. The differences may arise from the differences in molecular dynamics.

Another series of ester linked galactosyl porphyrins [105] were successfully prepared [Fig. (**16**)], though no biological evaluation was available. The wide range of solubility of these compounds provides another group of candidates to study structure-activity relationships for PDT.

ii. Nitrogen linkage:

Synthesis of four neutral or cationic porphyrins bearing ribose or 2-deoxyribose was achieved [Fig. (**17**)] [106]. The presence of a furanose unit containing 3'- and 5'- OH groups creates a potential to further synthesize porphyrinyl oligonucleotides. There has been quite an effort in preparing porphyrinyl nucleosides, nucleotides and olignuclotides

[107-110]. For review, one can refer to the work in "*Trends in Heterocyclic Chemistry*" [111].

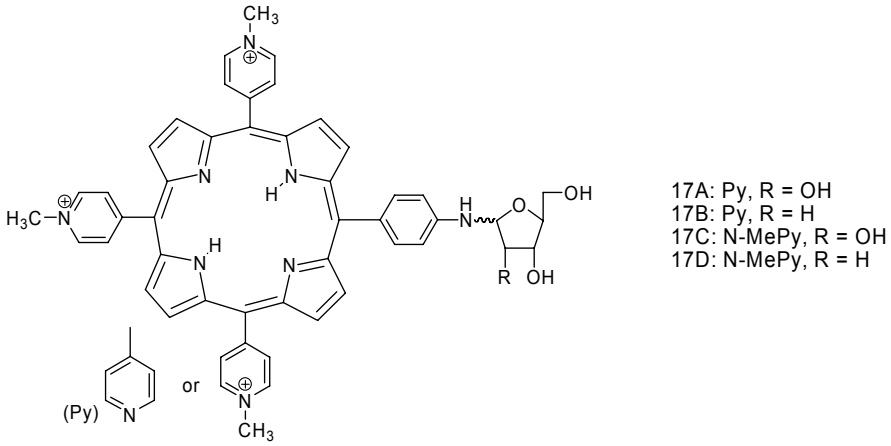

Figure 17. N-glycosylated porphyrins [106].

iii. Amide linkage:

Octalacto-TPP and octamalto-TPP derivatives [Fig. (**18**)] were obtained by reactions of lactonolactone and maltonolactone with tetrakis(3,5-

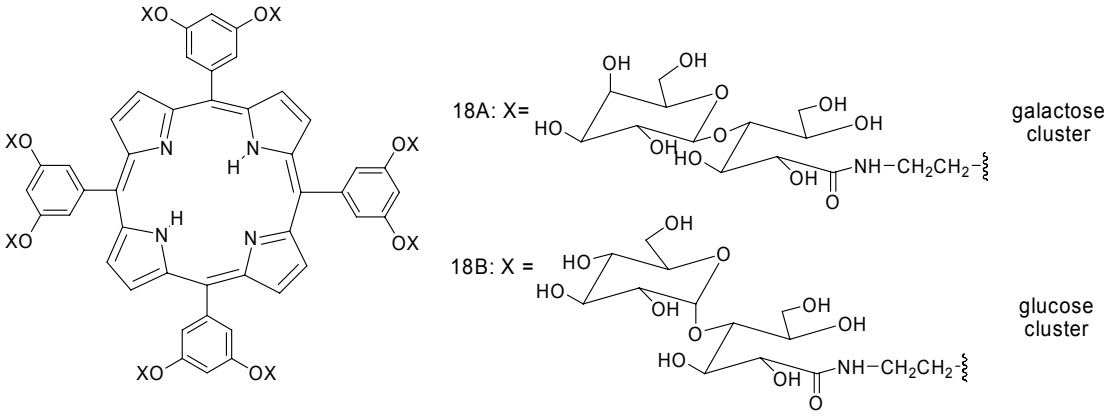

Figure 18. Amide-linked octa(galactose) and octa(glucose) derivatives of TPPs [112].

diaminoethyloxyphenyl)porphyrin, which was derived from the corresponding nitriles [112]. These porphyrin glycoconjugates are remarkably water-soluble. Therefore, the

hydrophobicity (which leads to nonspecific binding to the cell) is masked by the increase in saccharide multivalency. Fluorescence microscopy was used to investigate the interaction between these porphyrins and rat hepatoma cells (RLC-16), an example of hepatocytes (liver cells), which are well known to have receptors for the terminal galactose residues of asialoglycoproteins. It was shown that the galactose cluster **18A** was captured by the cells, while glucose cluster **18B** was not. The porphyrinyl saccharide cluster **18A** and **18B** are neutral and highly hydrophilic, where neither electrostatic nor hydrophobic force for nonspecific incorporation into the cells works effectively. So, the adsorption of galactose cluster **18A** on the cells was solely due to specific interaction of the galactose residues on **18A** and the galactoside receptor sites on the cell membranes. These results indicate that incorporation of different sugars may direct the porphyrins toward different cell types. These results are important because they demonstrate that specific interactions (in this case galactose and its receptor on the RLC-16 cell membrane) can be exploited to increase the selectivity of porphyrins to tumor cells. These results are in sharp contrast to those discussed in previous sections where the passive, diffusional uptake decreases with hydrophilicity. Perhaps these observations indicate that this approach can be made more general to target other cancer cells.

The research on carbohydrate moieties attached to the porphyrin macrocycle by amide linkage [113] is only marginally touched. No systematic study has been conducted at this time.

Summary:

We have discussed glycosylated porphyrins where the carbohydrate moieties are anchored to the porphyrin macrocycles by ether, carbon-carbon, thioether linkage, or linkages involving other heteroatoms. Major research efforts have been focused on O-glycosidic porphyrins due to the natural appearance of O-glycosides and their relative ease of synthesis. Malignant cells, liposomes mimicking cell membranes, or lipoproteins functioning in receptor mediated endocytosis are the majorities of biological systems used to evaluate PDT effects. Because of the lack of standardized protocols for PDT efficiency, comparison of results from different labs is difficult. However, understanding the chemistry and structure-activity relationships are key for designing efficient and potent drugs. We here summarize the major properties regarding saccharide-conjugated porphyrins:

(1) Sugar substituents on porphyrins provide a good solubility in aqueous solution, which may lead to elevated efficacy of drug delivery and increased efficiency of drug elimination from organisms after treatment.

(2) Current research on glycosidic porphyrins indicates that, in general, lipophilicity plays a key role and correlates with biological activity. The variety of substitution positions on both porphyrin macrocycles and/or phenyl groups in TPPs affords the possibility to create a large number of compounds of varying lipophilicity. The large number of naturally occurring carbohydrate moieties also affords the possibility to vary not only the lipophilicity but the means to target specific cell types. A wide range of well-established organic aryl or alkyl groups provides the hydrophobic residues. By balancing these two factors, subtle changes of lipophilicity on glyco-porphyrins can be achieved.

The two extremes, either too hydrophilic or too lipophilic, are generally ineffective in passive cellular or liposomal uptake. Mono-, di-, or tri- glycosylated porphyrins are usually more efficient than tetra- or octa- sugar substituted porphyrins, which might be due to the proper lipophilicity. Amphiphilic compounds may slow down the process of crossing the membrane, but residing in the membrane may very well be sufficient for the drug to exhibit efficient PDT effects.

(3) In the research discussed here, charged glyco-porphyrins, either positively or negatively charged in aqueous medium, displayed less photo activity than their neutral counterparts. Cationic glycol-porphyrins remain promising, yet more research is needed.

(4) Compounds with flat structure (e.g. sugar moieties anchored directly on the *para* positions of phenyl groups in TPPs) are better PDT candidates than those with spherical geometry (e.g. glyco-substitutions attached directly to the *ortho* positions of phenyl groups in TPPs, which also leads to different atropoisomers). One may assume that the globular structure prevents the drug from intercalating into the cell membrane or further diffusing into the cells. Yet, they can be taken up by active transport.

(5) Asymmetrically substituted (more than one functional moiety) derivatives are usually better than symmetrically substituted (with only one functional group) derivatives. This property may be related to their higher amphiphilicity.

(6) Interestingly several examples presented above show that *cis*-(5,10-substituted) glyco-porphyrins have far better biological activity than the *trans*-(5,15-substituted) isomers, while these two isomers are only different in positioning of sugar substituents. It may well be that the well-separated polar and apolar groups assist their penetrating ability to the cell membranes, and correlates with difference in the partition coefficients.

(7) The specific recognition of glycosylated porphyrins by cell membrane receptors is dependent on cell type. On the other hand, cancer cells in general have a high need for glucose due to their elevated metabolic rate. So, glucose-appended porphyrins may have an increased incorporation due to specific interaction. In the cases where there is no special enzyme to recognize a specific saccharide, the nature of carbohydrate moieties is not key to the observed biological effects.

(8) Porphyrins conjugated to both peptides and carbohydrates afford the opportunity to target different receptors on the same cell membrane.

(9) C- and S- glycosidic porphyrins are excellent mimics of O-glycosylated porphyrins, where the hydrolytically labile acetal moiety of the sugar is substituted with a functionality more stable toward hydrolysis by acids, bases and glycosidases. This property may increase the selectivity and reduce the dosage needed for PDT.

Thus, as a class of promising PDT agents, glyco-conjugated porphyrins have a great potential in developing commercialized drugs for Photodynamic Therapy. While continuing to explore more in the chemistry, future investigation of the lead compounds should be carried out in localization of the drug within the cell, the mechanism of photocytotoxicity, the pharmacokinetics and possibly biological effects on animal models.

References:

1. Mauzerall, D. C. *Clin. Dermat.*, **1998**, *16*, 195.

2. Chen, X.; Drain, C. M. In *Encyclopedia of Nanoscience and Nanotechnology*, Nalwa, H. S., Ed.; American Scientific Publishers: **2004**; Vol. *9*, pp. 593-616.

3. Perutz, M. F.; Fermi, G.; Luisi, B.; Shaanan, B.; Liddington, R. C. *Acc. Chem. Res.*, **1987**, *20*, 309.

4. Ungashe, S. B.; Groves, J. T. *Adv. Inorg. Biochem.*, **1994**, *9*, 317.

5. Boxer, S. G. *Biophys. Biochim.*, **1983**, *726*, 265.

6. Drain, C. M.; Sable, D. B.; Corden, B. B. *Inorg. Chem.*, **1988**, *27 (14)*, 2396.

7. Lane, N. *Sci. Am.*, **2003**, *288 (1)*, 38.

8. Drain, C. M.; Nifiatis, F.; Vasenko, A.; Batteas, J. D. *Angew. Chem. Int. Edit. Engl.*, **1998**, *37*, 2344.

9. Milic, T. N.; Chi, N.; Yablon, D. G.; Flynn, G. W.; Batteas, J. D.; Drain, C. M. *Angew. Chem. Int. Edit. Engl.*, **2002**, *41*, 2117.

10. Drain, C. M.; Russel, K. C.; Lehn, J.-M. *Chem. Commun.*, **1996**, 337.

11. Drain, C. M. *Proc. Natl. Acad. Sci. USA*, **2002**, *99 (8)*, 5178.

12. Gong, X.; Milic, T.; Xu, C.; Batteas, J. D.; Drain, C. M. *J. Am. Chem. Soc.*, **2002**, *124 (48)*, 14290.

13. Diskin-Posner, Y.; Dahal, S.; Goldberg, I. *Angew. Chem. Int. Edit. Engl.*, **2000**, *39 (7)*, 1288.

14. Drain, C. M.; Hupp, J. T.; Suslick, K. S.; Wasielewski, M. R.; Chen, X. *J. Porphyrins Phthalocyanines*, **2002**, *6*, 243.

15. Rakow, N. A.; Suslick, K. S. *Nature*, **2000**, *406 (6797)*, 710.

16. Kral, V.; Sessler, J. L.; Furuta, H. *J. Am. Chem. Soc.*, **1992**, *114*, 8704.

17. Wall, R. K.; Shelton, A. H.; Bonaccorsi, L. C.; Bejune, S. A.; Dube, D.; McMillin, D. R. *J. Am. Chem. Soc*, **2001**, *123*, 11480.

18. Guliaev, A. B.; Leontis, N. B. *Biochemistry*, **1999**, *38 (47)*, 15425.

19. Drain, C. M.; Gong, X.; Ruta, V.; Soll, C. E.; Chicoineau, P. F. *J. Comb. Chem.*, **1999**, *1*, 286.

20. Brown, M. *Drug Discovery Today*, **2003**, *8 (17)*, 767.

21. Oleinick, N. L.; Morris, R. L.; Belichenko, I. *Photochem. Photobiol. Sci.*, **2002**, *1 (1)*, 1.

22. Jori, G. *J. Photochem. Photobiol. B*, **1996**, *36*, 87.

23. Mody, T. D. *J. Porphyrins Phthalocyanines*, **2000**, *4*, 362.

24. Thacker, P. D. *Drug Discovery Today*, **2003**, *8 (5)*, 190.

25. Pandey, R. K. *J. Porphyrins Phthalocyanines*, **2000**, *4 (4)*, 368.

26. MacDonald, I. J.; Dougherty, T. J. *J. Porphyrins Phthalocyanines*, **2001**, *5 (2)*, 105.

27. Neurath, A. R.; Strick, N.; Debnath, A. K. *J. Mol. Recog.*, **1995**, *8*, 345.

28. Vzorov, A. N.; Dixon, D. W.; Trommel, J. S.; Marzilli, L. G.; Compans, R. W. *Antimicrob. Agents Chemother.*, **2002**, *46 (12)*, 3917.

29. Sternberg, E. D.; Dolphin, D.; Bruckner, C. *Tetrahedron*, **1998**, *54*, 4151.

30. Osterloh, J.; Vicente, M. G. H. *J. Porphyrins Phthalocyanines*, **2002**, *6*, 305.

31. Bonnett, R. *Chem. Soc. Rev.*, **1995**, 19.

32. Moan, J.; Christensen, T. *Tumor Res.*, **1980**, *15*, 1.

33. Piette, J.; Volanti, C.; Vantieghem, A.; Matroule, J.-Y.; Habraken, Y.; Agostinis, P. *Biochem. Pharmacol.*, **2003**, *66*, 1651.

34. Granville, D. J.; Hunt, D. W. C. *Curr. Opin. Drug Discovery Develop.*, **2000**, *3 (2)*, 232.

35. Moor, A. C. E. *J. Photochem. Photobiol. B*, **2000**, *57*, 1.

36. Nyman, E. S.; Hynninen, P. H. *J. Photochem. Photobiol. B*, **2004**, *73*, 1.

37. Pandey, R. K.; Zheng, G. In *The Porphyrin Handbook*, Kadish, K. M., Smith, K. M. and Guilard, R., Ed.; Academic Press: New York. **2000**; Vol. *6*, pp. 157-230.

38. Dougherty, T. J. *Photochem. Photobiol.*, **1993**, *58 (6)*, 895.

39. Salva, K. A. *Clin. Dermat.*, **2002**, *20*, 571.

40. Rouhi, A. M. *Chem. Eng. News*, **1998**, *Nov. 2*, 22.

41. Prinsep, M. R.; Caplan, F. R.; Moore, R. E.; Patterson, G. M. L.; Smith, C. D. *J. Am. Chem. Soc.*, **1992**, *114*, 385.

42. Drain, C. M.; Mauzerall, D. C. *Biophys. J.*, **1992**, *63*, 1544.

43. Momenteau, M.; Oulmi, D.; Maillard, P.; Croisy, A. *SPIE*, **1994**, *2325 Photodynamic Therapy of Cancer II*, 13.

44. Baláž, S. *Perspect. Drug Discov. Des.*, **2000**, *19 (1)*, 157.

45. Testa, B.; Crivori, P.; Reist, M.; Carrupt, P.-A. *Perspect. Drug Discov. Des.*, **2000**, *19 (1)*, 179.

46. Drain, C. M.; Mauzerall, D. C. *Biophys. J.*, **1992**, *63*, 1556.

47. Konan, Y. N.; Gurny, R.; Allemann, E. *J. Photochem. Photobiol. B*, **2002**, *66*, 89.

48. Boyle, R. W.; Dolphin, D. *Photochem. Photobiol.*, **1996**, *64 (3)*, 469.

49. Valenzeno, D. P. *Photochem. Photobiol.*, **1987**, *46 (1)*, 147.

50. Drain, C. M.; Mauzerall, D. C. *Proc. Natl. Acad. Sci. USA*, **1989**, *86*, 6959.

51. Ricchelli, F. *J. Photochem. Photobiol. B*, **1995**, *29*, 109.

52. Maillard, P.; Guerquin-Kern, J.-L.; Huel, C.; Momenteau, M. *J. Org. Chem.*, **1993**, *58*, 2774.

53. Lindsey, J. S.; Schreiman, I. C.; Hsu, H. C.; Kearney, P. C.; Marguerettaz, A. M. *J. Org. Chem.*, **1987**, *52 (5)*, 827.

54. Wagner, R. W.; Lawrence, D. S.; Lindsey, J. S. *Tetrahedron Lett.*, **1987**, *28*, 3069.

55. Oulmi, D.; Maillard, P.; Guerquin-Kern, J.-L.; Huel, C.; Momenteau, M. *J. Org. Chem.*, **1995**, *60 (6)*, 1554.

56. Csik, G.; Balog, E.; Voszka, I.; Tolgyesi, F.; Oulmi, D.; Maillard, P.; Momenteau, M. *J. Photochem. Photobiol. B*, **1998**, *44*, 216.

57. Voszka, I.; Galantai, R.; Maillard, P.; Csik, G. *J. Photochem. Photobiol. B*, **1999**, *52*, 92.

58. Gaud, O.; Granet, R.; Kaouadji, M.; Krausz, P.; Blais, J.-C.; Bolbach, G. *Can. J. Chem.*, **1996**, *74*, 481.

59. Bourhim, A.; Gaud, O.; Granet, R.; Krausz, P.; Spiro, M. *Synlett*, **1993**, 563.

60. Carre, V.; Gaud, O.; Sylvain, I.; Bourdon, O.; Spiro, M.; Blais, J.; Granet, R.; Krausz, P.; Guilloton, M. *J. Photochem. Photobiol. B*, **1999**, *48*, 57.

61. Sol, V.; Branland, P.; Granet, R.; Kaldapa, C.; Verneuil, B.; Krausz, P. *Bioorg. Med. Chem. Lett.*, **1998**, *8*, 3007.

62. Malik, Z.; Ladan, H.; Nitzan, Y. *J. Photochem. Photobiol. B*, **1992**, *14 (3)*, 262.

63. Driaf, K.; Krausz, P.; Verneuil, B.; Spiro, M.; Blais, J. C.; Bolbach, G. *Tetrahedron Lett.*, **1993**, *34 (6)*, 1027.

64. Driaf, K.; Granet, R.; Krausz, P.; Kaouadji, M.; Thomasson, F.; Chulia, A. J.; Verneuil, B.; Spiro, M.; Blais, J.-C.; Bolbach, G. *Can. J. Chem.*, **1996**, *74*, 1550.

65. Kaldapa, C.; Blais, J. C.; Carre, V.; Granet, R.; Sol, V.; Guilloton, M.; Spiro, M.; Krausz, P. *Tetrahedron Lett.*, **2000**, *41*, 331.

66. Mikata, Y.; Onchi, Y.; Tabata, K.; Ogura, S.-i.; Okura, I.; Ono, H.; Yano, S. *Tetrahedron Lett.*, **1998**, *39*, 4505.

67. Kohata, K.; Higashio, H.; Yamaguchi, Y.; Koketsu, M.; Odashima, T. *Bull. Chem. Soc. Jpn.*, **1994**, *67*, 668.

68. Hombrecher, H. K.; Schell, C. *Bioorg. Med. Chem. Lett.*, **1996**, *6 (11)*, 1199.

69. Schell, C.; Hombrecher, H. K. *Bioorg. Med. Chem.*, **1999**, *7*, 1857.

70. Schell, C.; Hombrecher, H. K. *Chem.-Eur. J.*, **1999**, *5 (2)*, 587.

71. Sol, V.; Blais, J. C.; Carre, V.; Granet, R.; Guilloton, M.; Spiro, M.; Krausz, P. *J. Org. Chem.*, **1999**, *64 (12)*, 4431.

72. Sol, V.; Blais, J. C.; Bolbach, G.; Carre, V.; Granet, R.; Guilloton, M.; Spiro, M.; Krausz, P. *Tetrahedron Lett.*, **1997**, *38 (36)*, 6391.

73. Chaleix, V.; Sol, V.; Huang, Y.-M.; Guilloton, M.; Granet, R.; Blais, J. C.; Krausz, P. *Eur. J. Org. Chem.*, **2003**, 1486.

74. Little, R. G.; Anton, J. A.; Loach, P. A.; Ibers, J. A. *J. Heterocycl. Chem.*, **1975**, *12*, 345.

75. Adler, A. D.; Longo, F. R.; Finarelli, J. D.; Goldmacher, J.; Assour, J.; Korsakoff, L. *J. Org. Chem.*, **1967**, *32*, 476.

76. Perree-Fauvet, M.; Verchere-Beaur, C.; Tarnaud, E.; Anneheim-Herbelin, G.; Bone, N.; Gaudemer, A. *Tetrahedron*, **1996**, *52 (43)*, 13569.

77. Verchere-Beaur, C.; Perree-Fauvet, M.; Tarnaud, E.; Anneheim-Herbelin, G.; Bone, N.; Gaudemer, A. *Tetrahedron*, **1996**, *52 (43)*, 13589.

78. Zoladek, T.; Nhi, N. B.; Jagletto, I.; Graczyk, A.; Rytka, J. *Photochem. Photobiol.*, **1997**, *66 (2)*, 253.

79. Hamazawa, A.; Kinoshita, I.; Breedlove, B.; Isobe, K.; Shibata, M.; Baba, Y.; Kakuchi, T.; Hirohara, S.; Obata, M.; Mikata, Y.; Yano, S. *Chem. Lett.*, **2002**, *31 (3)*, 388.

80. Maillard, P.; Vilain, S.; Huel, C.; Momenteau, M. *J. Org. Chem.*, **1994**, *59*, 2887.

81. Maillard, P.; Guerquin-Kern, J. L.; Momenteau, M. *Tetrahedron Lett.*, **1991**, *32 (37)*, 4901.

82. Kohata, K.; Yamaguchi, Y.; Higashio, H.; Odashima, T.; Ishii, H. *Chem. Lett.*, **1992**, 477.

83. Maillard, P.; Guerquin-Kern, J.-L.; Momenteau, M.; Gaspard, S. *J. Am. Chem. Soc.*, **1989**, *111*, 9125.

84. Fulling, G.; Schroder, D.; Franck, B. *Angew. Chem. Int. Edit. Engl.*, **1989**, *28 (11)*, 1519.

85. Hombrecher, H. K.; Schell, C. *Carbohydr. Polymers*, **1997**, *34 (4)*, 422.

86. Bourhim, A.; Czernecki, S.; Krausz, P.; Viari, A.; Vigny, P. *J. Carbohydr. Chem.*, **1990**, *9 (5)*, 761.

87. Belica, P. S.; Franck, R. W. *Tetrahedron Lett.*, **1998**, *39*, 8225.

88. Yang, G.; Franck, R. W.; Byun, H.-S.; Bittman, R.; Samadder, P.; Arthur, G. *Org. Lett.*, **1999**, *1*, 2149.

89. Li, F.; Yang, K.; Tyhonas, J. S.; MacCrum, K. A.; Lindsey, J. S. *Tetrahedron*, **1997**, *53*, 12339.

90. Pasetto, P.; Chen, X.; Drain, C. M.; Franck, R. W. *Chem. Commun.*, **2001**, 81.

91. Arsenault, G. P.; Bullock, E.; MacDonald, S. F. *J. Am Chem. Soc.*, **1960**, *82*, 4384.

92. Littler, B. J.; Ciringh, Y.; Lindsey, J. S. *J. Org. Chem.*, **1999**, *64*, 2864.

93. Cornia, M.; Menozzi, M.; Ragg, E.; Mazzini, S.; Scarafoni, A.; Zanardi, F.; Casiraghi, G. *Tetrahedron*, **2000**, *56*, 3977.

94. Ono, N.; Bougauchi, M.; Maruyama, K. *Tetrahedron Lett.*, **1992**, *33 (12)*, 1629.

95. Maillard, P.; Huel, C.; Momenteau, M. *Tetrahedron Lett.*, **1992**, *33 (52)*, 8081.

96. Cornia, M.; Valenti, C.; Capacchi, S.; Cozzini, P. *Tetrahedron*, **1998**, *54*, 8091.

97. Casiraghi, G.; Cornia, M.; Zanardi, F.; Rassu, G.; Ragg, E.; Bortolini, R. *J. Org. Chem.*, **1994**, *59*, 1801.

98. Cornia, M.; Casiraghi, G.; Binacchi, S.; Zanardi, F.; Rassu, G. *J. Org. Chem.*, **1994**, *59*, 1226.

99. Casiraghi, G.; Cornia, M.; Rassu, G.; Sante, C. D.; Spanu, P. *Tetrahedron*, **1992**, *48 (27)*, 5619.

100. Defaye, J.; Gelas, J. In *Studies in Natural Products Chemistry*, Atta-ur-Rahman, Ed.; Elsevier Science Publishers B. V.: Amsterdam. **1991**; Vol. *8*, pp. 315-357.

101. Sylvain, I.; Benhaddou, R.; Carre, V.; Cottaz, S.; Driguez, H.; Granet, R.; Guilloton, M.; Krausz, P. *J. Porphyrins Phthalocyanines*, **1999**, *3*, 1.

102. Sylvain, I.; Zerrouki, R.; Granet, R.; Huang, Y. M.; Lagorce, J.-F.; Guilloton, M.; Blais, J.-C.; Krausz, P. *Bioorg. Med. Chem.*, **2002**, *10*, 57.

103. Davoust, E.; Granet, R.; Krausz, P.; Carre, V.; Guilloton, M. *Tetrahedron Lett.*, **1999**, *40*, 2513.

104. Bardos-Nagy, I.; Galantai, R.; Fidy, J. *Biochimica et Biophysica Acta*, **2001**, *1512*, 125.

105. Hombrecher, H. K.; Ohm, S.; Koll, D. *Tetrahedron*, **1996**, *52 (15)*, 5441.

106. Li, H.; Czuchajowski, L. *Tetrahedron Lett.*, **1994**, *35 (11)*, 1629.

107. Czuchajowski, L.; Habdas, J.; Niedbala, H.; Wandrekar, V. *Tetrahedron Lett.*, **1991**, *32 (51)*, 7511.

108. Czuchajowski, L.; Niedbala, H. *Bioorg. Med. Chem. Lett.*, **1992**, *2 (12)*, 1645.

109. Czuchajowski, L.; Palka, A.; Morra, M.; Wandrekar, V. *Tetrahedron Lett.*, **1993**, *34 (34)*, 5409.

110. Czuchajowski, L.; Habdas, J.; Niedbala, H.; Wandrekar, V. *J. Heterocycl. Chem.*, **1992**, *29*, 479.

111. Li, H.; Czuchajowski, L. *Trends Heterocyc. Chem.*, **1999**, *6*, 57.

112. Fujimoto, K.; Miyata, T.; Aoyama, Y. *J. Am. Chem. Soc.*, **2000**, *122*, 3558.

113. Fuhrhop, J.-H.; Demoulin, C.; Boettcher, C.; Koning, J.; Siggel, U. *J. Am. Chem. Soc.*, **1992**, *114*, 4159.

Appendices:

Appendix I. Examples of photosensitizers in various phases of clinical trials.

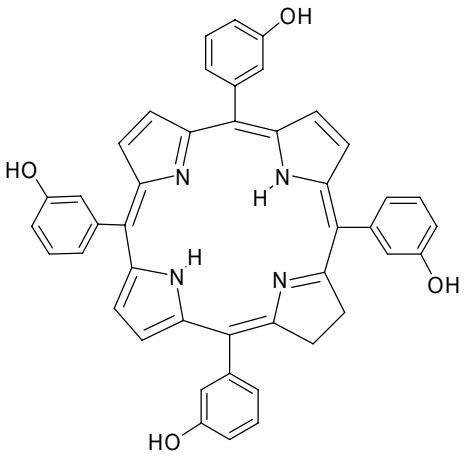

meta-Tetrahydroxyphenylchlorin (*m*-THPC)
(Foscan)

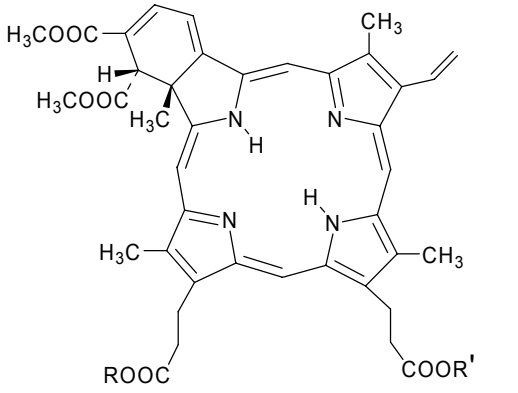

R=CH_3, R'=H and R=H, R'=CH_3 (Mixture)
Benzoporphyrin derivatives
(Visudyne)

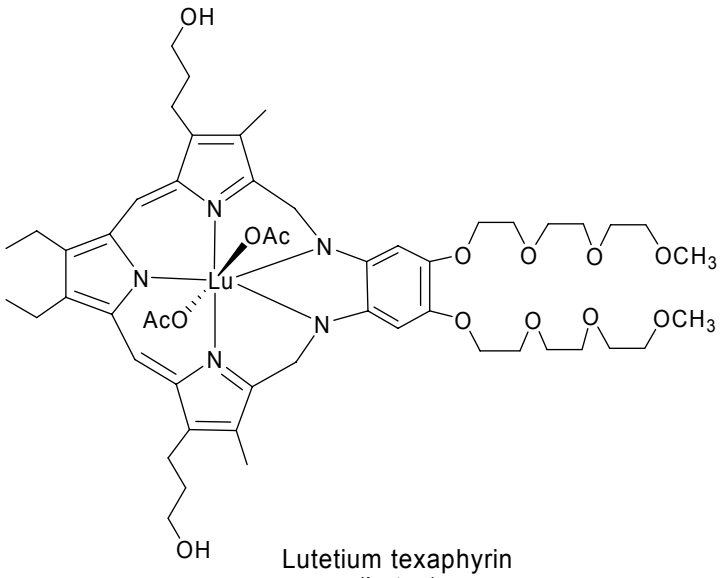

Lutetium texaphyrin
(Lutex)

Appendix II. Synthesis of Photofrin®.

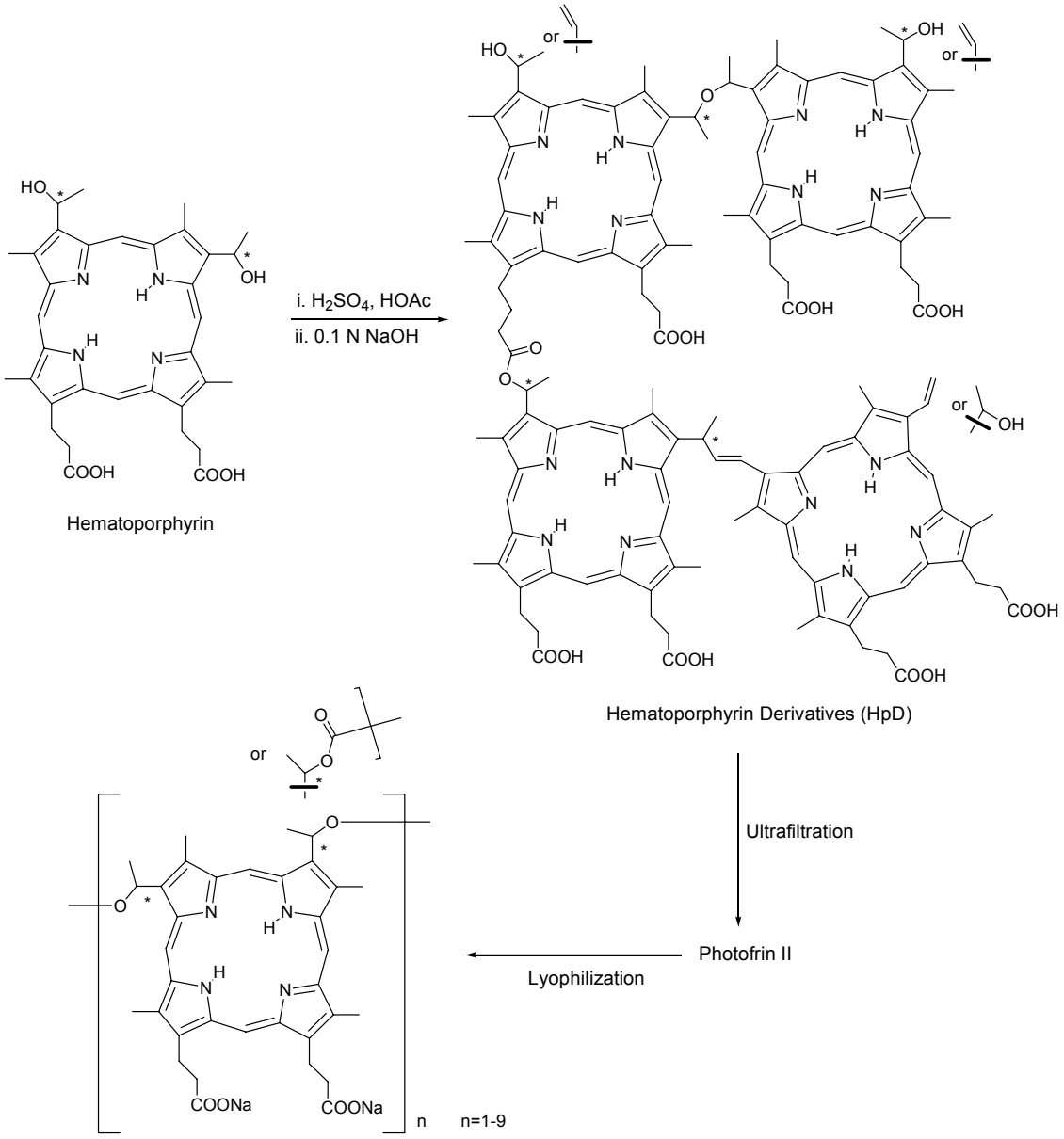

Appendix III. Different multichromophoric systems. (Note: Any *meso*-substitution is not co-planar to the macrocycle.)

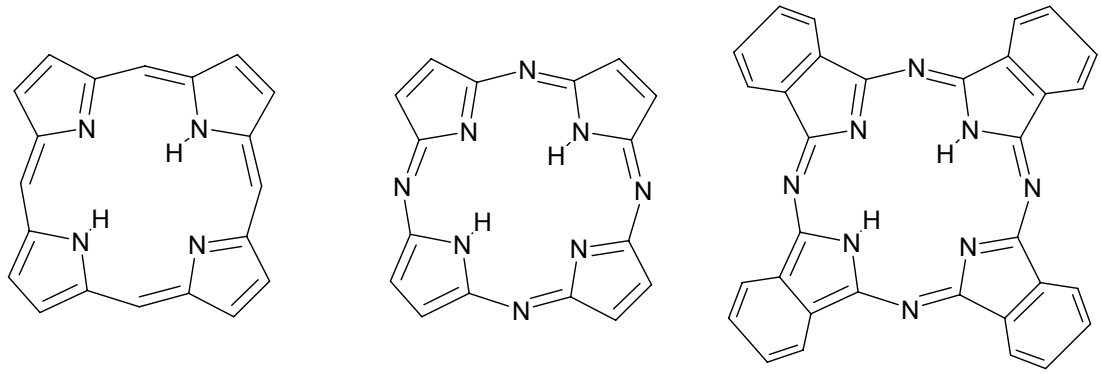

Porphyrin Porphyrazine Phthalocyanine

Appendix IV. Structures of carbohydrates.

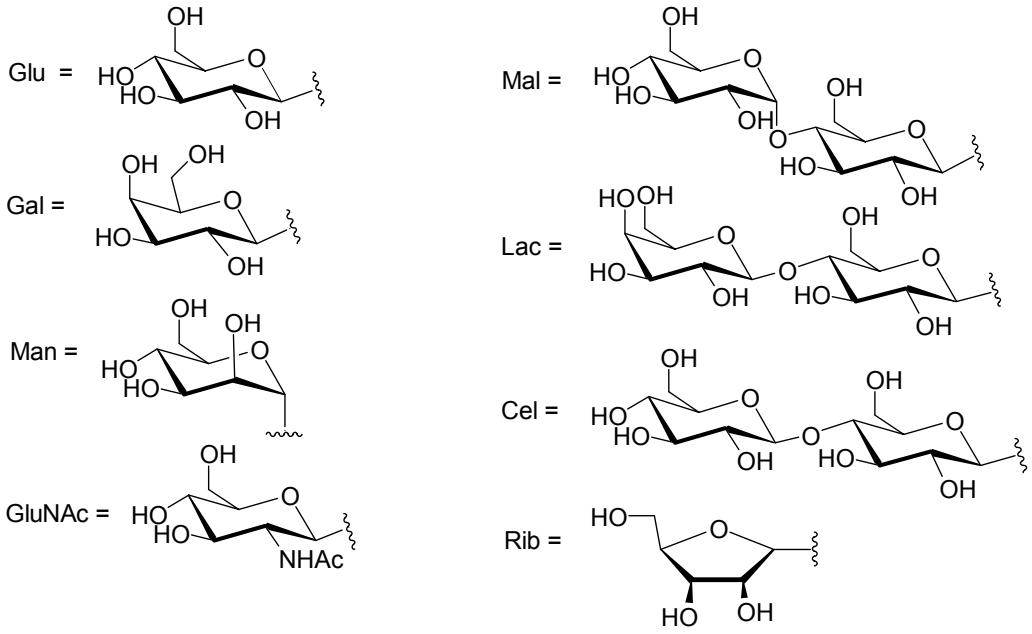

Chapter 2

Efficient Synthesis and Photodynamic Activity of Porphyrin-Saccharide Conjugates:

Targeting and Incapacitating Cancer Cells

Abstract:

Since the role of saccharides in cell recognition, metabolism, and cell labeling is well established, the conjugation of saccharides to drugs is an active area of research. Thus, one goal in the use of saccharide-drug conjugates is to impart a greater specificity toward a given cell type or other targets. Though widely used to treat some cancers and age related macular degeneration, the drugs used in Photo Dynamic Therapy (PDT) display poor chemical selectivity towards the intended targets, and uptake by cells most likely arises from passive, diffusional processes. Instead, the specific irradiation of the target tissues, and the formation of the toxic species *in situ*, are the primary factors that modulate the selectivity in the present mode of PDT. We report herein a two step method to make non-hydrolyzable saccharide-porphyrin conjugates in high yields using a tetra(pentafluorophenyl)porphyrin and the thio derivative of the sugar. As a demonstration of their properties, the selective uptake (and/or binding) of these compounds to several cancer cell types was examined, followed by an investigation of their photodynamic properties. As expected, different malignant cell types take up one type of saccharide-porphyrin conjugate preferentially over others; e.g. human breast cancer cells (MDA-MB-231) absorb a tetraglucose-porphyrin conjugate over the corresponding galactose derivative. Doseametric studies reveal that these saccharide-

porphyrin conjugates exhibit varying PDT responses depending on drug concentration and irradiation energy. (1) Using 20 μM conjugate and greater irradiation energy induces cell death by necrosis. (2) When 10-20 μM conjugate and less irradiation energy are used, both necrosis and apoptosis are observed. (3) Using 10 μM and the least irradiation energy, a significant reduction in cell migration is observed, which indicates a reduction in aggressiveness of the cancer cells.

Introduction:

The uptake of exogenous molecules such as drugs into cells can arise from a variety of mechanisms that can be broadly classified as mediated and nonmediated transport. Mediated uptake requires that target molecules be recognized by specific intermolecular interactions, selected, and shuttled across the cell membrane by receptors. Thus molecules may be targeted toward these receptors by appending appropriate substrate moieties. Conversely, nonmediated uptake involves diffusion at some point in the process and arises from non-specific cell-molecule interactions. Because of the lipid membrane core, the more lipophilic a molecule, the lower the barrier to traversing through the cell membrane, whereas amphipathic molecules will nominally bind at the interface or polar region and have greater barriers to crossing the membrane (*1, 2*).

Photodynamic Therapy (PDT) is a rapidly growing methodology to treat age related macular degeneration, various skin disorders, and an increasing number of cancers that are accessible to irradiation with visible light (*3*). Though in various stages of development, other applications are envisaged; for example as antibiotic and antiviral treatments (*4, 5*). A benzoporphyrin derivative is used in the treatment of age related

macular degeneration (*6*) and the PDT agent Photofrin®, which is approved for use in a variety of cancers, is a complex mixture of hematoporphyrin IX oligomers with issues of dosaging and selectivity (*7*). There are several other porphyrinoid derivatives and related compounds that are in various phases of testing and in clinical trials for both treatment and imaging applications; including chlorins (reduced porphyrins) and texaphyrins (expanded porphyrins) (*8-10*).

In general terms, the PDT concept is that the therapeutic compound has low toxicity until it is activated by light, whereupon it becomes very reactive and toxic, or it activates other indigenous species to become reactive and toxic (*6, 7, 11*). The selectivity in any application arises from the compound specificity for the target and the selective irradiation of the target by light. Specificity for target tissues is poor for most PDT agents and arises largely from non-specific passive uptake modulated by increased metabolic activity of cancer cells – as demonstrated by the strong correlation between the hydrophobicity and *in vitro* activity. For PDT applications, there is a general agreement that the major role of porphyrinoid compounds is to photosensitize the formation of the highly reactive singlet oxygen species via a transfer of energy from the triplet excited state of the porphyrinoid to ground state, triplet oxygen. Singlet oxygen is a powerful oxidant that reacts with many biomolecular species such as the double bonds in lipids, aromatic amino acids, both the phosphate backbone and bases of nucleic acids, and other species such as flavenoids. Enzymes designed to reduce oxidative stress such as super oxide dismutase, and antioxidants may reduce the amounts of singlet oxygen in the cell thereby modulate PDT efficiency. In some cases PDT may cause cell death by making the cells anoxic, or by the initiation of apoptosis. Most porphyrins have remarkably high

quantum yields for triplet formation, >60%. The yield of the triplet state can be increased by the incorporation of some metals into the core and/or by replacing some of the hydrogen atoms with halogens or other heavy atoms that enhance intersystem crossing from the initially formed singlet state to the triplet state. Since fluorinated porphyrin derivatives generally have greater triplet quantum yields than most free base porphyrinic systems (*12*), these compounds may be more potent photo sensitizers.

Because of the poor selectivity for target tissue, dosing concerns, and the large market, much effort has been directed toward the discovery and implementation of next generation of PDT agents (*3, 8, 13-15*). Despite these research efforts and a better understanding of how the present Photofrin mixture works, there is a paucity of progress in making porphyrinoid compounds more selective for the target tumor tissues, yet stable *in vivo*. Although the role of lipophilicity in enhancing PDT activity is not well understood, it likely arises from enhanced affinity for cell membranes and concomitant increased cellular uptake due to the lower energetic costs of traversing the low dielectric of the membrane (*1, 2, 16*). Liposomes and nanoparticles are a means to circumvent solubility problems, and many new compounds under investigation are amphipathic or hydrophobic, but selectivity remains an issue (*17*). A cadre of glycosylated porphyrins has been reported in recent years (*18-23*) because of the advantages of appending cellular recognition elements to a drug, yet hydrolysis of the sugars from the O-glycosidic porphyrin derivatives remains problematic – both *in vivo* and during synthesis/purification (*24*). Drugs bearing saccharides appended via O-glycoside linkages generally have short half-lives because this bond is readily hydrolyzed by a variety of enzymatic and non-enzymatic acid/base reactions. Most cancer cells are dependent on

glucose uptake to fulfill their energy requirements; as such glycolysis is increased in cancer cells compared with normal cells. Glucose enters cells via a family of functional glucose transporters. In this regard, breast cancer cells are not exceptional and are known to have increased glucose utilization and uptake due to an increased number of transporters (*25*). Porphyrins with several sugar moieties at appropriate positions can be amphipathic to facilitate passive uptake, and the sugars may mediate specific interactions with cancer cell membranes and active uptake of the compound (*26*). In order to surmount the hydrolysis problem, saccharide-drug conjugates using C- or S- glycoside linkages have been made, including several porphyrin derivatives (*23, 27-30*), but for the majority of cases the synthetic yield of these conjugates is poor as well.

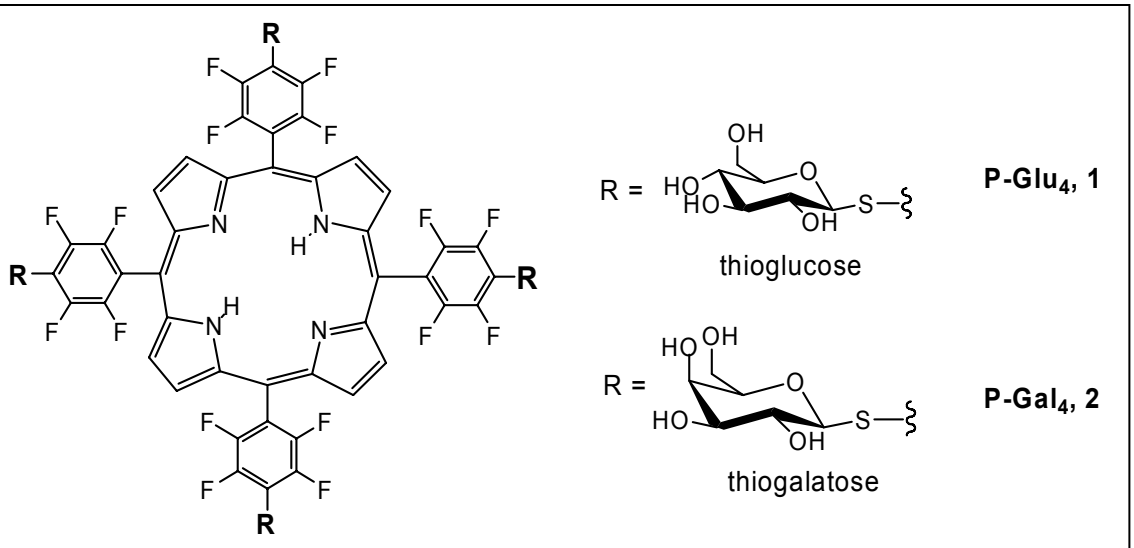

Scheme 1. Structures of P-Glu_4 & P-Gal_4.

To address many of the aforementioned issues of selectivity, amphipathicity, and hydrolytic stability in the design and efficacy of drugs such as those for PDT, we report herein the synthesis and the manifold activities of two porphyrin-saccharide conjugates (Scheme 1): 5,10,15,20-tetrakis (4,1'-thio-glucose-2,3,5,6-tetrafluorophenyl)porphyrin (P-Glu_4) and 5,10,15,20-tetrakis (4,1'-thio-galactose-2,3,5,6-tetrafluorophenyl)porphyrin

(P-Gal$_4$). A simple, two-step reaction affords a porphyrin bearing four saccharide moieties conjugated via an S-glycoside bond in high yields (Scheme 2). The reaction is general for a variety of saccharides and other nucleophiles such as amines.

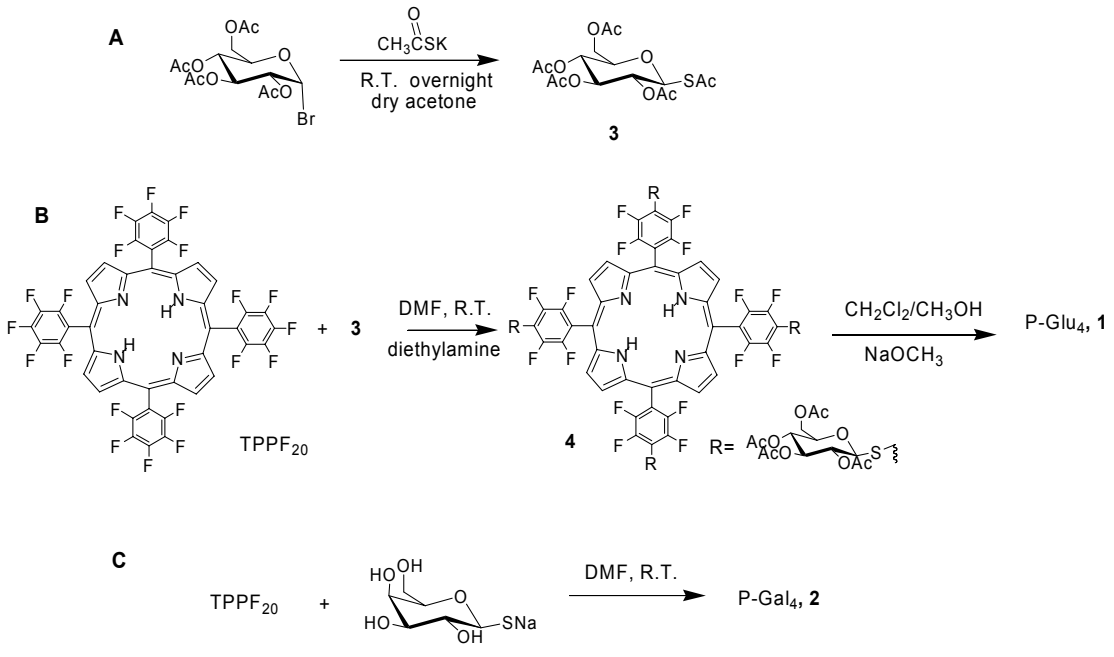

Scheme 2. The thioacetate sugar derivative (A) is more stable than the free thiol. (B) Synthesis of P-Glu$_4$ & P-Gal$_4$ can be accomplished using the protected sugar followed by deprotection, or directly by using the unprotected sugar (C).

These porphyrin-S-saccharide derivatives exhibit enhanced binding to a human breast cancer cell line compared to several widely studied non-saccharide derivatives, such as the tetra(4-methoxyphenyl)porphyrin (supporting information). These studies also show that the glucose-appended porphyrin is preferentially taken up compared to the galactose-appended derivative, wherein it displays significantly enhanced photodynamic activity in terms of inducing necrosis and apoptosis. Studies reveal that the cellular responses are dependent on the dosage of these compounds, length of irradiation with white light, and the degree of uptake. 20 μM doses of P-Glu$_4$ and ~11.3 kJ m^{-2} (20 minutes at 0.94 mW cm^{-2} irradiation using white light from a ~ 13 watt fluorescent bulb) result in necrosis. 20

μM doses of the same derivative and ~1.6 kJ m^{-2} (10 minutes at 0.27 mW cm^{-2}) irradiation results in apoptosis. Still lower concentrations and shorter irradiation times, 10 μM doses of P-Glu_4 and 0.75 kJ m^{-2} (5 minutes at 0.25 mW cm^{-2}) significantly reduces cell mobility, which is an indicator of reduced aggressiveness. Also, a normal rat fibroblast cell line absorbs less of the conjugates than the transformed version of the cell line.

Experimental Procedures:

Materials. All chemicals were purchased from Sigma-Aldrich. Dulbecco's Modified Eagle Medium (DMEM) and antimycotic for cell culture were from GibcoBRL. Bovine calf serum was obtained from HyClone. PBS was obtained from Invitrogen. The 13W fluorescent bulb was from Sanco. The antibody against poly-(ADP ribose) polymerase (PARP) was from Cell Signaling Technology. Biocoat filters were purchased from Becton Dichinson Labware and the Diff-Quik® stain set was from Dade Behring Inc.

Instrumentation. Steady state fluorescence spectra were generally taken on 1 μM of porphyrin in methanol, with excitation at the maximum UV-VIS absorbance (Soret band), and recorded on a Fluorolog 3, Jobin -SPEX Instruments S.A., Inc. UV-visible spectra were collected on a Varian Bio3 spectrophotometer. Flash column chromatography was performed using 230-400 mesh ASTM Merck silica gel-60. ^1H NMRs were recorded on a Varian 300MHz instrument in $CDCl_3$. Electron spray ionization mass spectrometry used an Aligent Technologies HP-1100 LC/MSD instrument.

Porphyrin Synthesis and Characterization. 5,10,15,20-tetrakis-(4-1'-thio-glucosyl-2,3,5,6-tetrafluorophenyl)porphyrin (P-Glu_4, **1**). 2,3,4,6-tetra-O-acetyl-glucosyl bromide (7.0 g, 0.017 mol) mixed with potassium thioacetate (4.0 g, 0.035 mol) in 20 mL dry acetone overnight at room temperature afforded 2,3,4,6-tetra-O-acetyl-glucosyl thioacetate (**3**) after removal of the solvent and purification over a 5 x 20 cm silica gel column using hexane/ethyl acetate (2:1) as eluent. A 8:1 solution of **3** (167 mg, 410.4 μmol) and 5,10,15,20-tetrakis(pentafluorophenyl)porphyrin ($TPPF_{20}$) (50 mg, 51.3 μmol) in 10mL DMF was stirred overnight at room temperature to yield 5,10,15,20-tetrakis-(4-1'-thio-2',3',4',6'-tetraacetylglucosyl-2,3,5,6-tetrafluorophenyl)porphyrin (**4**). Compound **4** was purified by column chromatography using 2 x 15 cm silica gel column hexane/ethyl acetate (2:3) as eluent, treated with 16 equivalents (1 equivalent per acetate group) $NaOCH_3$ at room temperature in 9:1 v/v solution of methanol/methylene chloride for 1 hour to afford P-Glu_4 in quantitative yield (Scheme 2). The product was neutralized by pH 7.2 ammonium acetate buffer. The overall yield after three steps was 88%. P-Glu_4: UV-Visible in methanol $\lambda(\varepsilon\ cm^{-1}M^{-1})$: 410nm ($1.83 \times 10^5$), Alternatively, the unprotected sodium thioglucose can be used as a starting material to make **1**, as described below for the galactose derivative.

5,10,15,20-tetrakis-(4-1'-thio-galactosyl-2,3,5,6-tetrafluorophenyl)porphyrin (P-Gal_4, **2**) was synthesized as described previously (*24*) (Scheme 2) by stirring a 8:1 solution of the sodium thiogalactose (54 mg, 246.4 μmol) with $TPPF_{20}$ (30 mg, 30.8 μmol), respectively, in 5 mL DMF at room temperature overnight and purified over a 1 x 10 cm silica gel column using ethyl acetate/methanol (17:3) as eluent. The yield was 92%. In order to accurately characterize the compounds by NMR, the tetra-2,3,4,6-

acetylgalactose derivatives were synthesized by mixing acetic anhydride (84.4 mg, 78 μL, 826.2 μmol), DMAP (9 mg, 73.4 μmol and P-Gal_4 (10mg, 45.9 μmol) (48:1.6:1) at room temperature in 10 mL pyridine for 1 hour to afford 5,10,15,20-tetrakis-(4-1'-thio-2',3',4',6'-tetraacetylgalactosyl-2,3,5,6-tetrafluorophenyl) porphyrin (**5**). Compound **5** was purified by column chromatography using a 1 x 8 cm silica gel column and hexane/ethyl acetate (1:2) as eluent. When **5** was made directly, deprotection was accomplished using 16 equivalents $NaOCH_3$ (1 equivalent per acetate group) at room temperature in 9:1 v/v solution of methanol/methylene chloride for 1 hour to afford P-Gal_4 in quantitative yield (Scheme 2). The product was neutralized by pH 7.2 ammonium acetate buffer. P-Gal_4: UV-Visible in methanol $\lambda(\varepsilon\ cm^{-1}M^{-1})$: 410nm ($1.74 \times 10^4$).

For compounds **4** and **5**, electron spray ionization mass spectrometry, ^1H NMR, UV-visible, and fluorescence spectra were consistent with the reported structures. For compounds **1** and **2** made via hydrolysis of the protected sugar or directly, mass, UV-visible, and fluorescence spectra confirmed the structure.

Octanol/water partition coefficient. A small amount (~1 mg) of dry porphyrin was dissolved in 3 mL 1-octanol by sonication and 3 mL distilled water (or pH 4.75 LiAc buffer) was added to the solution. The saturated mixture was shaken vigorously and centrifuged for 10 minutes to accelerate the separation of the water and organic layers. The absorption of the porphyrin Soret bands in each layer was measured by UV-VIS spectroscopy. The ratio of the absorption in 1-octanol over the absorption in water or buffer is the reported octanol/water partition coefficient.

Cell culture. Cells were maintained in Dulbecco's Modified Eagle Medium (DMEM), 10% bovine calf serum, 1% antimycotic at 37^0C and in 5% CO_2 atmosphere (*31*). For experiments, $2x10^5$ cells/mL were seeded in cell culture plates and then allowed to grow for 24 hours. For all the experiments involving porphyrins, the conjugate was added to the cells 24 hours prior to experiments to allow them to be taken up by the cells.

Fluorescence imaging cells. Cells were plated onto cover slips in cell culture dishes. Porphyrins (dissolved in methanol) were added to the cultures to a final concentration of 2 to 20 μM. Twenty-four hours later cells were washed twice with PBS (136 mM NaCl, 2.6 mM KCl, 1.4 mM KH_2PO_4, 4.2 mM Na_2HPO_4) and fixed in 4% paraformaldehyde solution in PBS for 20 min at room temperature. The cells were then washed with PBS 5 times (*32, 33*). The cover slips were mounted in Dako fluorescen mounting medium, put onto slides, air dried, and then visualized using a Nikon Optiphot 2 fluorescence microscope where images were captured as high quality (>100kb) JPEG files. (Excitation: 505-565nm and Emission: 565-685nm). For comparison and to record cell morphology, images were also captured as JPEG images using a phase contrast light microscope. For each set of experiments, cells were cultured and the fluorescence images were taken under identical culture and microscopic conditions.

For quantitative studies, the image intensities of the cells in the fluorescence micrographs were calculated by Scientific Image software, developed by Advanced Science & Technology (*34*). This program can analyze images in JPEG format as briefly outlined below.

1. The Red, Green, Blue (R, G, B) components of several selected cell regions in the first image were averaged to get (Rc, Gc, Bc).

2. For the same image several regions of background were selected and (R, G, B) for the background regions are averaged to get (Rb, Gb, Bb). The background intensity was considered as noise, which was subtracted from the intensity of the cell region. This gives the background adjusted (R1, G1, B1) for the first image.

3. For the second image (R2, G2 B2) was obtained in the same way.

4. For each image, the absolute intensity, expressed as a (R, G, B) vector, was obtained as the scalar value of the vector.

5. The relative fluorescence intensity between two images was taken as the ratio of the absolute intensity of two images.

6. Additionally, the ratios for the red, green, and blue components of two images can be separately calculated in a straightforward manner.

The data were calculated from the original RGB data of the unprocessed images. For publication purpose, the images were enhanced using Microsoft Photo Editor® using the same parameters for each set of images.

Photocytotoxicity assay. Cell viability was quantified by trypan blue exclusion. After various treatments, cells were harvested with trypsin. Trypan blue was added to cells at a concentration of 0.4% w/v. The mixture was incubated at room temperature for 10 min

and trypan blue uptake (counted as dead cells) was determined by counting on a hemacytometer.

Western blot. Cells were treated with porphyrin for 24 hours, rinsed and irradiated as described in the text. 9 Hours after irradiation, cells were washed with cold PBS (136 mM NaCl, 2.6 mM KCl, 1.4 mM KH_2PO_4, 4.2 mM Na_2HPO_4) twice before lysis with RIPA buffer (50 mM Tris-HCL, 1% NP40, 0.25% Na-deoxycholate, 150 mM NaCl, 1 mM EDTA, 1 mM PMSF, 1μg/ml Aprotinin, leupeptin, pepstatin, 1mM Na_3VO_4 and NaF). The lysates were gently rocked at 4^0C for 25 minutes, centrifuged at maximum speed for 10 minutes, and the supernatant was applied to a western blot (*35*). Equal amounts of protein were adjusted into gel-loading buffer (50 mM Tris-HCl, pH 6.8; 100 mM dithiothreitol; 2% SDS; 0.1% bromophenol blue; 10% glycerol), and then heated for 5 minutes at 100°C prior to separation by SDS-polyacrylamide gel electrophoresis using 8% acrylamide separating gels. After transferring to nitrocellulose membranes (Osmonics), membrane filters were blocked overnight at 4 ^{0}C with 5% non-fat dry milk in PBS. The nitrocellulose filters were washed three times for 5 minutes in PBS with 0.05% tween-20, and then incubated with the anti-PARP antibody for 1 hour at room temperature. Anti-mouse IgG conjugated with horseradish peroxidase was used as a secondary antibody. The bands were visualized using an enhanced chemiluminescent detection system (Amersham).

Cell migration assay. Cell migration was measured as the ability of cells to migrate through a Biocoat filter (8.0 micron pore size) (*36*). Cells were treated with porphyrin 24 hours prior to the assay and kept in the dark. After rinsing and removal of cells from a 60-mm cell culture plate using a balanced salt solution containing 0.5% (w/v) trypsin and

0.2% (w/v) EDTA, $2x10^4$ cells in 250 μL of cell culture medium (0.5% serum) were placed in the upper compartment of a Biocoat filter. 750 μL of cell culture medium was placed in the lower compartment of the filter. Cells were irradiated under 13W fluorescent white light and left to migrate for 18 hours. The filters were maintained at 37^0C in a humidified atmosphere containing 95% air, 5% CO_2. After treatment, the filters were removed, and cells that had not migrated through to the underside of the filter were removed from the upper compartment by wiping the filter with a cotton bud. The filters were washed twice with PBS, and then incubated in staining buffer Diff-Quik Fixative, Diff-Quik Solution I and Diff-Quik Solution II for 0.5 min each at room temperature. The filters were then washed twice in PBS and air dried. The cells that had migrated to the opposite side of the filter were visualized using a phase contract light microscope and images were taken.

Results and Discussion:

Synthesis and Characterization

Because of the potential to target various cell types, other S-glycosylated porphyrins have been examined as possible agents for PDT (*29, 30*). But, one of the goals herein is to develop high-yielding reactions that are general for the appending of any thio-sugar to 5,10,15,20-tetra(pentafluorophenyl)porphyrin ($TPPF_{20}$), which is commercially available and can be routinely made in large quantities either by the Adler (*37*), or Lindsey(*38*) methods. Changing the link between the aromatic and sugar moieties from oxygen to sulfur is known to increase the stability of the conjugate to acid hydrolysis. Since sulfur is a weaker Lewis base than oxygen it has a lower affinity for protons, thus less readily

forms the conjugate acid required for the hydrolysis transition-state (*39*). The same is true for reactions with glycosidases, as enzymes that act on the corresponding O-analogues do not usually cleave 1-thio saccharides (*39*).

The synthesis begins with $TPPF_{20}$ since the *para* fluoro group is known to be reactive towards nucleophilic substitution reactions (*40, 41*), and we have previously exploited this property to make a variety of porphyrin derivatives (*24*). The present work focuses on the preparation of S-glycosylated porphyrins, in which the hydrolytically labile acetal moiety of the sugar is replaced with a functionality that is significantly more stable toward acids, bases and enzymes. These properties may both increase the selectivity compared to simple amphipathic compounds and reduce the dosages needed for PDT agents compared to O-linked saccharides. Two sugar-porphyrin conjugates, **1** ($P\text{-}Glu_4$) and **2** ($P\text{-}Gal_4$), are made as shown in Scheme 2. The synthesis is straight forward, and >85% yields are routinely obtained starting from $TPPF_{20}$ and the thioacetate of the protected sugar in DMF with 20 eq. (~1%) diethylamine to deprotect the thiol moiety *in situ*. Both $P\text{-}Glu_4$ and $P\text{-}Gal_4$ and their protected intermediates were fully characterized. (The NMR data of protected intermediates are at the end of this section.) Either the acetate protected or the free sugar can be used in the synthesis of $P\text{-}Glu_4$ and $P\text{-}Gal_4$ (Scheme 2). The protected sugars enhance the reproducibility of the reaction yields and aid in characterization of the products by NMR, but necessitate a deprotection step. The removal of the acetate protecting groups with $NaOCH_3$ is quantitative, and is followed by neutralization with a pH 7.2 ammonium acetate buffer. A large excess of $NaOCH_3$ should be avoided as it partially cleaves the porphyrin-saccharide conjugate. The ~30% broadening of the Soret band and the ~ 3 nm red shifts of Q bands compared to the

starting porphyrin in the UV-VIS spectrum of e.g. P-Glu_4 in methanol (Figure 1A) shows that there is some small amount of aggregation even at μM concentrations. The

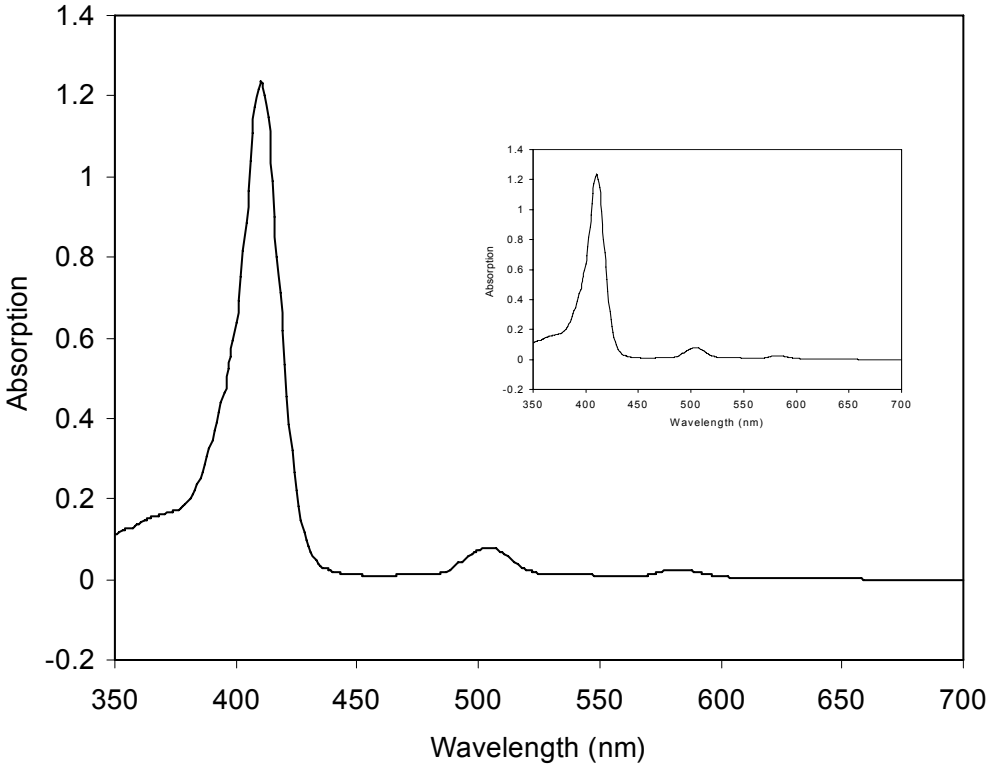

Figure 1A. UV-visible spectrum of ~ 2 μM P-Glu_4 in methanol, where the inset is x 5.

hydrophobic porphyrin core surrounded by the hydrophilic sugar moieties likely allows π stacking of the macrocycles to form dimers or small aggregates. Similar aggregation is observed in water.

The fluorescence intensity of $TPPF_{20}$ is ~37% of the non-fluorinated analogue, TPP, because of the differences in the energetics of the frontier orbitals and an increase in inter-system crossing to the triplet state. The triplet quantum yield for TPP is 80% $\pm$ 10%, and for $TPPF_{20}$ is >80% (*12*). The fluorescence intensity of both P-Glu_4 and P-Gal_4 is quenched a further ~5% compared to $TPPF_{20}$ under identical instrumental and

concentration conditions (Figure 1B). Using fluorescence as an indirect indicator, this observation suggests that P-Glu_4 and P-Gal_4 have even greater quantum yields of triplet than $TPPF_{20}$ and this is likely due to the four sulfur atoms and the heavy atom effect. Of course, these values should only be taken as relative indications of the degrees of the

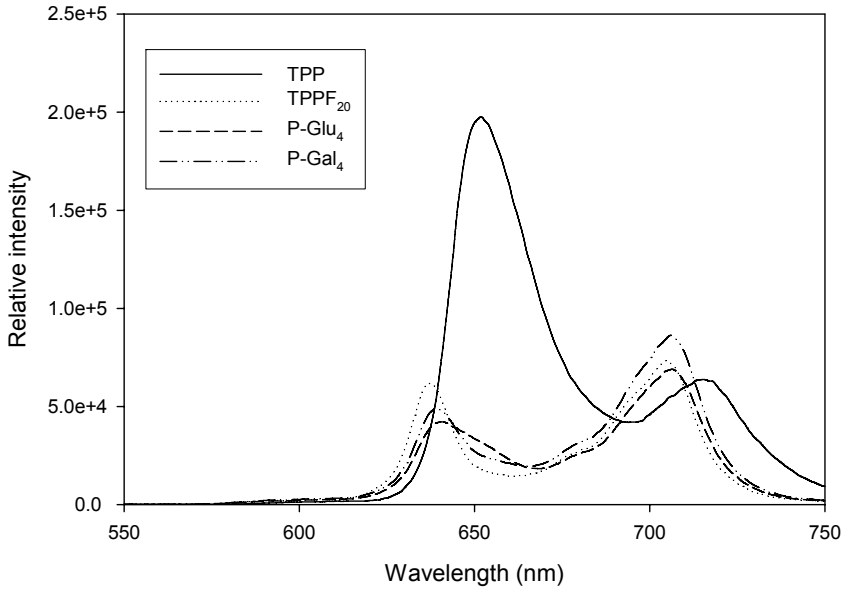

Figure 1B. Fluorescence emission spectra of TPP, $TPPF_{20}$, P-Glu_4 and P-Gal_4. The concentrations were 0.813 μM, 0.718 μM, 0.360 μM and 0.336μM respectively, in methanol, taken under identical instrumental conditions, and the spectra are normalized to the same molarity.

excited state decay pathway via the triplet manifold. Thus the quantum yields of singlet oxygen for **1** and **2** are expected to be correspondingly greater compared to simple TPP derivatives, i.e. the increased number of porphyrins in the triplet excited state will presumably produce more singlet oxygen for a given amount of dye. The photophysical properties of porphyrins and the mechanism of singlet oxygen formation pertaining to PDT have been well reviewed (*3, 8, 13*). Even though the fluorescence quantum yield of these free base porphyrins is ~10%, the large extinction coefficient (~2×10^5 $M^{-1}cm^{-1}$) and

long integration times allows the observation of nM quantities of these dyes by fluorescence microscopy.

These two conjugates are stable to hydrolysis between pH 4.75 and 9. Solutions of both P-Glu_4 and P-Gal_4 in methanol are photo chemically stable in refluxing methanol for six hours under ambient light 21.6 kJ m^{-2} (0.1 mW cm^{-2}) as judged by ESI-MS. This confirms our hypothesis that these conjugates are stable under these conditions. Other saccharide appended porphyrins assembled via oxygen linkages are known to be labile under similar conditions (*30*). Photolysis experiments on P-Glu_4 indicate little oxidation of the sulfur or cleavage of the sugar from the porphyrin under the conditions used for the treatment of the cells.

There are numerous reports on the correlation of amphipathic character of PDT agents with cell uptake and/or efficacy of PDT (*27, 42-45*). The octanol/water partition coefficients for each derivative are the same in unbuffered water and pH 4.75 buffer (in unbuffered water P-Glu_4 is 204 $\pm$ 10 and P-Gal_4 is 158 $\pm$ 20; while in pH 4.75 buffer P-Glu_4 is 199 $\pm$ 10 and P-Gal_4 is 156 $\pm$ 10). Since the region around cancer cells is often acidic due to the increase metabolic rate (*8, 13, 46*), the unchanged partition coefficients at lower pH indicate that any passive uptake of these compounds by cancer cells will be unaffected. This property arises from the hydrophobic core surrounded by the four hydrophilic groups, the ionization potentials of the hydroxy groups, and somewhat because of the 16 remaining fluoro groups. This is different from porphyrins conjugated to saccharides via an alkane tether with either oxygen or sulfur linkages (*29, 30, 47-49*). The ~ 20% difference in the partition coefficient means that P-Glu_4 is slightly more

lipophilic than P-Gal_4, and this may account for a small fraction of the differences noted below.

NMR data:

5,10,15,20-tetrakis-(4-1'-thio-tetraacetate-glucose-2,3,5,6-tetrafluorophenyl)porphyrin. ^{1}H-NMR($CDCl_3$, 300 MHz): δ9.02 (s, 8H), pyrrole βH; δ5.38 (d, J=8.79Hz, 4H), H_1×4; δ5.22 (m,12H), $H_2H_3H_4$×4; δ5.32 (d, J=3.30Hz, 8H), $2H_6$×4; δ3.91 (m, 4H), H_5×4; δ2.23 (s, 12H) OAc×4; δ2.10 (s, 12H), OAc×4; δ2.09 (s, 12H), OAc×4; δ2.08 (s, 12H), OAc×4; δ-2.86 (s, 2H), pyrrole NH. ESI-MS calcd. 2351, found 2351.

5,10,15,20-tetrakis-(4-1'-thio-tetraacetate-galactose-2,3,5,6-tetrafluorophenyl)porphyrin, ^{1}H-NMR($CDCl_3$, 300 MHz): δ8.92 (s, 8H), pyrrole βH; δ5.47 (d, J=3.30Hz, 4H), H_4×4; δ5.41 (t, J=9.88Hz, 4H), H_2×4; δ5.14 (m, 8H), H_1H_3×4; δ4.26 (m, 4H), H_6×4; δ4.15 (m, 4H), H_6×4; δ4.05 (t, J=6.59Hz, 4H), H_5×4; δ2.18 (s, 12H), OAc×4; δ2.16 (s, 12H), OAc×4; δ2.00 (s, 12H), OAc×4; δ1.96 (s, 12H), OAc×4; δ-2.94 (s, 2H), pyrrole NH. ESI-MS calcd. 2351, found 2351.

MDA-MB-231 Breast Cancer Cells

P-Glu_4 vs P-Gal_4 Selectivity of Cell Uptake

The selective binding of the porphyrin-saccharide conjugates to MDA-MB-231 breast cancer cells was evaluated by fluorescence microscopy. Cells cultured under the same

conditions on glass cover slips were incubated with various concentrations of the porphyrin derivatives under identical conditions. After rinsing the unbound compounds from the cells on the cover slips and fixing the cells, fluorescence images of the cells were taken. The observed fluorescence intensity was taken to be proportional to the quantity of porphyrin bound to the cells, and was quantified by comparing the integrated RGB vectors for identical areas (see experimental procedures).

The fluorescence microscopy images (Figure 2) clearly show that both porphyrin-

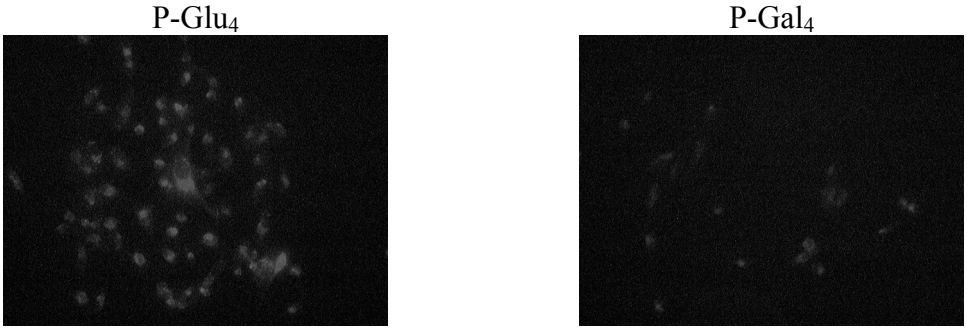

Figure 2: P-Glu_4 is preferentially taken up by human breast cancer MDA-MB-231 cells over P-Gal_4. Cells were treated with 10 μM glycosylated porphyrin for 24 hours, rinsed, and fixed with a 4 % paraformaldehyde solution. Fluorescence images were taken under identical conditions. R,G,B vector analysis of the unmodified images indicates the average relative fluorescence intensity, taken to be proportional to the extent of conjugate uptake by these cells, is 2.3 : 1 for P-Glu_4 : P-Gal_4.

saccharide conjugates bind to human breast cancer (MDA-MB-231) cells, but these cells take up more than twice as much P-Glu_4 than P-Gal_4 when incubated with 10 μM solutions for 24 hours. The RGB vector analysis, comparing the average values of >20 cells treated with each conjugate from several different experiments, indicates the uptake of P-Glu_4 by MDA-MB-231 is 2.3-fold greater than P-Gal_4.

A primary characteristic of malignant cells is an increased uptake of glucose due to increased metabolic activity, and human breast cancer cells are known to have a higher expression and functional level of glucose transporters than normal cells (*50, 51*).

Therefore, the greater binding of P-Glu_4 to MDA-MB-231 cells likely arises from the presence of a greater number of glucose transporters than galactose transporters. In addition to the increased mediated transport, there may be an increased proclivity for these cancer cells to diffuse conjugates **1** and **2** because of the more acidic environment of cancer cells and increased metabolic rate relative to healthy cells (*46, 52-54*). It has been reported that generally, an increasing hydrophobicity increases *in vitro* activity (*55*). Our observations indicate that the amphipathic nature of the free base porphyrin-sugar conjugates also plays a role in porphyrin incorporation into MDA-MB-231 cells. Neither the acetate protected porphyrin intermediates (e.g. **4**) nor $TPPF_{20}$ bind to MDA-MB-231 cancer cells as judged by fluorescence microscopy (supporting information), thus merely increasing lipophilicity does not *a priori* increase uptake by these cells. The hydrophobic porphyrins either do not enter the cells well and/or there are problems in the delivery these compounds without auxiliary drug delivery formulations such as liposomes.

A previous report found that TPPs bearing eight galactose moieties bound to rat hepatoma (liver cancer) cells (RLC-16), to a much greater extent than the corresponding glucose-porphyrin derivative (*56*). This was expected since there are galactose receptors on this particular cell line, but not glucose receptors. Combined with our observations, these results indicate that incorporation of different sugars may direct the porphyrins towards different cell types.

Photocytotoxicity: Necrosis

For cultured breast cancer MDA-MB-231 cells, the P-Glu_4 derivative is a more potent mediator of cell death upon illumination with white light than the P-Gal_4 derivative,

which is consistent with the above observations on cell uptake/binding. Since cell death can be caused directly by necrosis, and indirectly by initiating apoptosis (*57*), several assays were performed to delineate the extent of each. At 20 μM concentrations of P-Glu_4 and using 0.94 mW cm^{-2} of white light for 20 minutes (11.3 kJ m^{-2}), more than 60% of the cells are necrotic immediately after PDT treatment (within the few minutes it takes to place them under the light contrast microscope, Figure 3A) (*57*). Yet, these two assays also reveal that the number of non-viable cells continues to increase with time until it reaches nearly 100% after 24 hours, which implies that under these conditions a secondary process such as apoptosis is causing cell death, *vide infra*.

Cell viability is porphyrin-saccharide conjugate concentration dependent where the photocytotoxicity of P-Glu_4 is approximately 2-fold better than P-Gal_4 at 8-16 μM (Figure 3B). The photodynamic response of these cells is also light dose dependent, such that with extended irradiation times nearly 100% of the cells are dead (Figure 3C). These results confirm those from fluorescence microscope images – glucose-porphyrin conjugates are taken up by human breast cancer MDA-MB-231 cells more than twice as much as the corresponding galactose-porphyrin derivatives.

Photocytotoxicity: Apoptosis

In order to verify the hypothesis that apoptosis is at least partially the cause of the continued increase in non-viable cells after the cessation of light irradiation (Figure 4), milder conditions were used to decrease the number of initially formed necrotic cells. At the same 20 μM P-Glu_4 concentrations, but with 7-fold *less* total light energy (1.62 kJ m^{-2}; 0.27 mW cm^{-2} for 10 minutes) than used in the assays shown in Figures 3, cell death is

caused at least in part by apoptosis as indicated by a Poly-ADP-Ribose-Polymerase (PARP) cleavage assay. PARP is one of the best-examined targets of activated caspases and is a common indicator of the action of caspase-3 in apoptosis (*58*). PARP is a DNA repair enzyme whose expression is triggered by DNA-strand breaks. In cells undergoing apoptosis PARP is cleaved from a 113 kD peptide into 24 kD and 89 kD polypeptides. It appears plausible that cleavage of PARP facilitates the degradation of cellular DNA (*59*), which is a hallmark of apoptosis. Our PARP assay results demonstrate that apoptosis was induced in MDA-MB-231 cells by photodynamic treatment with P-Glu_4 (Figure 4). These observations are consistent with other reports (*60*) that lower doses than those needed to produce necrosis are effective in eliciting cell death. This indicates that MDA-MB-231 cell death can be affected even under low light conditions such as found when tumors are further away from the light source and the irradiation has to penetrate through more tissue.

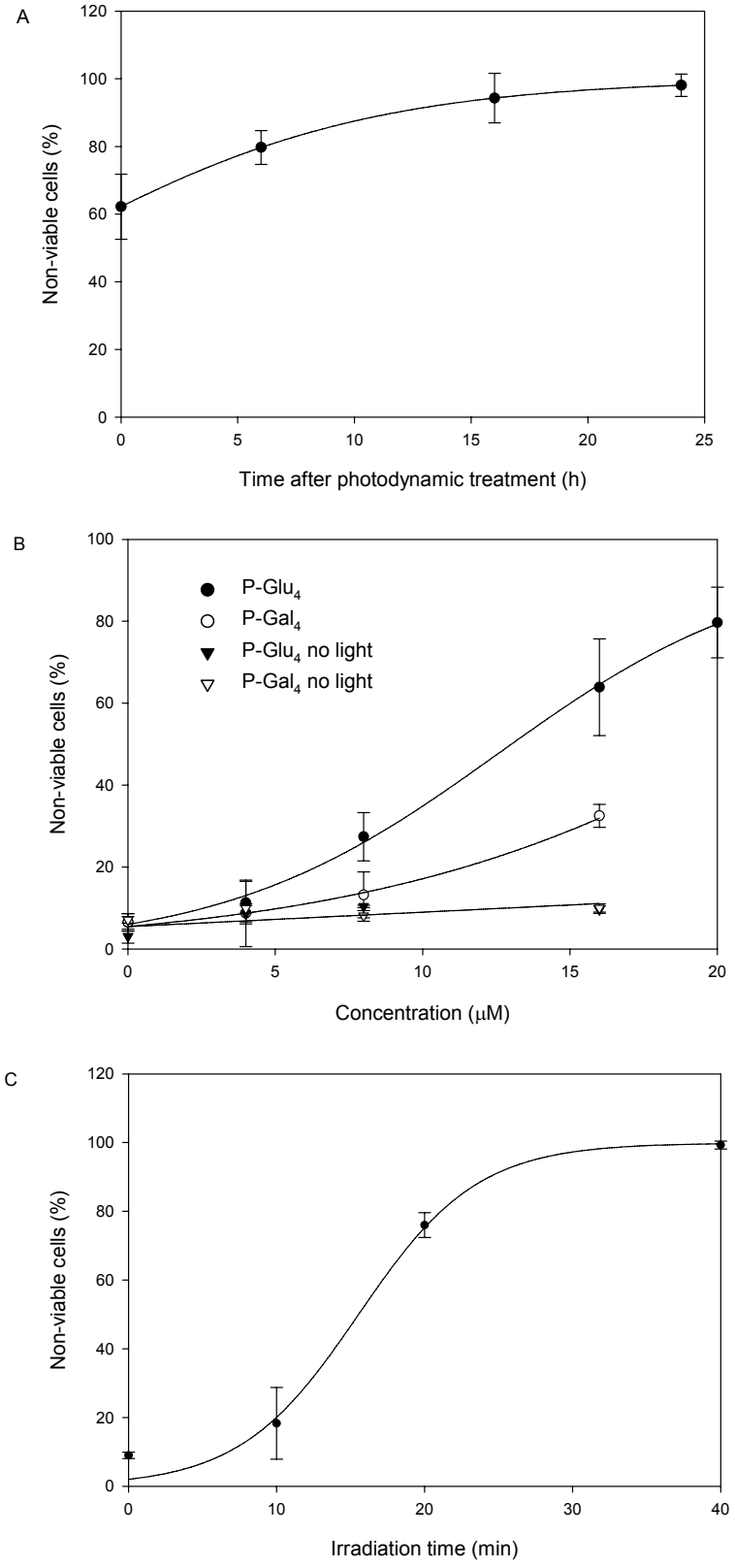

Figure 3. Photocytotoxic effects on human breast cancer MDA-MB-231 cells. Non-viable cells were counted with hemacytometer after staining with 0.4% w/v trypan blue. (A) MDA-MB-231 cells were treated with 20 μM P-Glu_4 for 24 hours, rinsed by exchanging the growth medium, and irradiated under a white 13W fluorescent light (0.94 mW cm^{-2} for 20 minutes; 11.28 kJ m^{-2}). The non-viable cells were counted at various lengths of time after photodynamic treatment. (B) MDA-MB-231 cells were treated with various concentrations of P-Glu_4 (•) or P-Gal_4 (o) for 24 hours, rinsed by exchanging the growth medium, and irradiated under a white 13W fluorescent light (0.94 mW cm^{-2} for 20 minutes; 11.28 kJ m^{-2}). Six hours after photodyamic treatment non-viable cells were counted. Control experiments with no light show that MDA-MB-231 cells remain viable in the presence of the porphyrin-saccharide conjugates (▼, ∇). (C) MDA-MB-231 cells were treated with 20 μM P-Glu_4 for 24 hours, rinsed by exchanging the growth medium, and irradiated under a white 13W fluorescent light (0.94 mW cm^{-2}) for various lengths of time. Six hours after photodynamic treatment non-viable cells were counted. Each data point represents an average ± S.D. from at least three independent measurements.

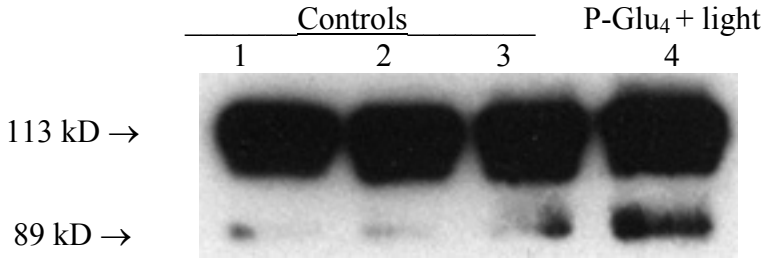

Figure 4. Detection of Poly-ADP-Ribose-Polymerase (PARP) cleavage in human breast cancer MDA-MB-231 cells as an indication of apoptosis. MDA-MB-231 cells were treated with 20 μM P-Glu_4 for 24 hours, irradiated with a 13W fluorescent light (0.27 mW cm^{-2} for 10 minutes; 1.62 kJ m^{-2}), and 9 hours after irradiation, cells were collected and lysed. The supernatant of the lysate was applied to western blot to detect PARP cleavage. Lane 1: with no irradiation or P-Glu_4; Lane 2: with irradiation but no P-Glu_4; Lane 3: with P-Glu_4 but no irradiation; Lane 4: with P-Glu_4 and irradiation.

Reduced Cell Migration

It is clear that matastatic tumor cells must retain or increase their ability to migrate and to invade across vessel walls and into tissues (*61*). Decreasing their migration can effectively decrease tumors from spreading (*61*). Using even milder conditions, where the breast cancer MDA-MD-231 cells are kept alive (as indicated by trypan blue exclusion assay) by using still less porphyrin-sugar conjugate and less total light energy (*e.g.* 10 μM P-Glu_4 with 0.75 kJ m^{-2} light irradiation, i.e. 0.25 mW cm^{-2} for 5 minutes), there is significant inhibition of cell migration. The ability of the cancer to cells migrate from one side of a porous material to the other side (*32*) is much reduced after the treatment with P-Glu_4 and irradiation (Figure 5). Control experiments show that P-Glu_4 without irradiation or irradiation without P-Glu_4 has no effect on cell migration. This result may indicate that lower levels of P-Glu_4 in the cells with less light irradiation may damage the membrane or proteins that facilitate or trigger cell migration, thus mitigating aggressiveness. The migration inhibition is porphyrin dose-dependent. Reduced cell migration indicates that the cancer cells are not as aggressive as the untreated MDA-MB-

231 cells. This character could slow down the tumor spreading to other tissues or organs (*32*), and has clinical relevance when some tumor tissues are too deep for enough light to penetrate to induce necrosis or apoptosis, since reduced aggressiveness may facilitate other treatments.

Figure 5. Low concentrations of P-Glu_4 and low light irradiation inhibit cell migration. Reduced cell migration of human breast cancer MDA-MB-231 cells after non-lethal photodynamic treatment. Cells were treated with 0 or 10 μM P-Glu_4 for 24 hours and transferred to the Biocoat filters and irradiated under 13W fluorescent light at 0.25 mW cm^{-2} for 5 minutes (0.75 kJ m^{-2}). Cells were kept in dark, left to migrate for 18 hours, and stained. The images were taken using a phase contrast light microscope.

Conclusions on MDA-MB-231 cells

These observations indicate that the uptake and photodynamic response of the porphyrin-saccharide conjugate by this breast cancer cell line is correlated with the concentration of the compound. The photodynamic response is also correlated with the amount of irradiation with white light. There are no observable effects on cells treated with the conjugates but without light nor on cells treated with light but no conjugate. These results also indicate that even at low dosage and low irradiation – such as might be found for central regions of a tumor where the drug has lower uptake and light penetrates less – these compound still may elicit desirable effects such as apoptosis and reduced aggressiveness. These results support the hypothesis that saccharides may be used to enhance the selectivity of the compound towards a given cell type, and can be predicted

using a knowledge of the target cell metabolism and/or relative abundance of receptors for a given sugar.

Normal, partially transformed, and fully transformed 3Y1 rat fibroblasts

Over expression of a tyrosine kinase is a common genetic defect in a variety of human cancers. It was demonstrated previously that 3Y1 rat fibroblasts over expressing c-Src ($3Y1^{c\text{-}Src}$) are partially transformed since elevated expression of the less active c-Src kinase is not sufficient to fully transform cells (*62*). However, when treated with tumor-promoting phorbal esters (*63*) these cells become transformed. Expression of v-Src, which is an activated kinase, fully transforms 3Y1 cells ($3Y1^{v\text{-}Src}$) (*64*). Thus, we employed a system of normal (3Y1 rat fibroblasts), partially transformed ($3Y1^{c\text{-}Src}$) and fully transformed ($3Y1^{v\text{-}Src}$) cells to evaluate the P-Glu_4 and P-Gal_4 conjugates for binding and PDT effects.

Selectivity of Cell Uptake

The three cell types on cover slips were incubated with porphyrin derivatives under identical conditions. After rinsing off the unbound compounds and fixing the cells, the uptake of the porphyrin–saccacharide conjugates by cells was evaluated by fluorescence microscopy, where the observed fluorescence intensity was taken to be proportional to the quantity of porphyrin taken up by the cells, and confirmed by the RGB vector analysis. These studies also show that P-Glu_4 is preferentially absorbed by the transformed $3Y1^{v\text{-}Src}$ cells compared to the absorption of P-Gal_4 (supporting information), so we again use the glucose derivative for further investigation. Importantly, neither of the porphyrins are taken-up by normal 3Y1 fibroblasts to the extent that they are in the

transformed 3Y1$^{v\text{-}Src}$ cells. The partially transformed 3Y1$^{c\text{-}Src}$ show an intermediate uptake (Figure 6 and 7), which indicate that these sugar-appended porphyrins are selective toward tumor over normal cells.[a]

Fluorescence image assays (Figure 6) indicate that the uptake of P-Glu$_4$ increases in the order of 3Y1 (normal rat fibroblast) < 3Y1$^{c\text{-}Src}$ (partially transformed cells) < 3Y1$^{v\text{-}Src}$ (fully transformed cells). The relative affinity of P-Glu$_4$ towards 3Y1, 3Y1$^{c\text{-}Src}$ and 3Y1$^{v\text{-}Src}$ cells is 1:2.3:3.2 according to the relative fluorescence intensity calculated by the Scientific Image program, as described in experimental procedure section. This indicates that the tumor-like 3Y1$^{v\text{-}Src}$ cells have > 3-fold greater affinity toward P-Glu$_4$ than do the corresponding normal cells; further supporting the hypothesis that saccharides can increase the selectivity of porphyrins for tumor cells over normal cells.

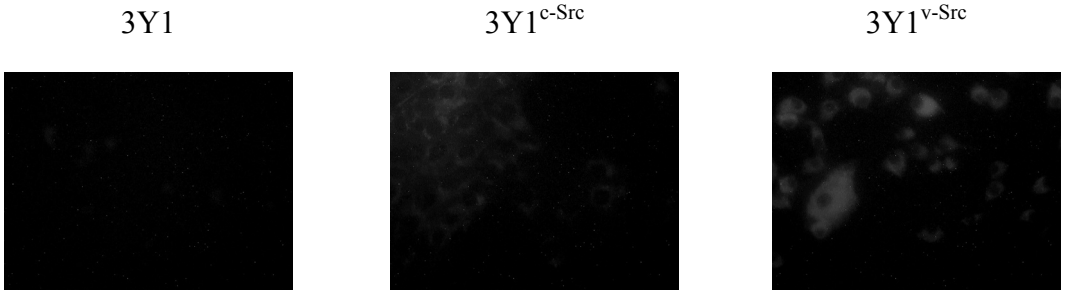

Figure 6. P-Glu$_4$ is preferentially taken up by transformed 3Y1$^{v\text{-}Src}$ cells compared to partially transformed 3Y1$^{c\text{-}Src}$ cells and non-transformed 3Y1 cells. Cells were treated with 10 μM P-Glu$_4$ for 24 hours before fixing with a 4% paraformaldehyde solution. Fluorescence images were taken under identical conditions. The relative fluorescence intensity is 1 : 2.3 : 3.2.

For malignant cells, elevated metabolic activity leads to greater uptake of glucose and this is true for 3Y1$^{v\text{-}Src}$ cells compared to 3Y1$^{c\text{-}Src}$ and 3Y1 cells. Thus glucose uptake is

[a] Fluorescence imaging assays demonstrate that normal mouse fibroblast (NIH3T3) do not take up either P-Glu$_4$ or P-Gal$_4$.

greater due to increased active transport by elevated expression and/or function of glucose transporters. The observed increase in the affinity for P-Glu_4 with increasing degree of cell transformation is consistent with this expectation: $3Y1^{v\text{-}Src}$ > $3Y1^{c\text{-}Src}$ > 3Y1. In addition to elevated active glucose transport, there may be an increased tendency for tumor (or tumor like) cells to passively absorb P-Glu_4 because of the faster growth rate and differences in the environment of tumor cells relative to normal cells. The lower pH around cancer cells, for example, may partially protonate free base porphyrins, therefore increase the hydrophilicity and assist the cationic porphyrin binding to the cell membrane containing anionic lipids. The neutral amphipathic porphyrin can cross the membrane, or since the cationic porphyrin retains much of its amphipathic nature it may also passively enter the cell. Note that P-Glu_4 is taken up to a greater extent by the $3Y1^{v\text{-}Src}$ cells, supporting the hypothesis that the glucose facilitates transport. Thus the differences in uptake cannot be ascribed solely to the small difference in octanol/water partition coefficients.

Photocytotoxicity: $3Y1^{v\text{-}Src} > 3Y1^{c\text{-}Src} > 3Y1$

Cells from the three different cell lines were treated identically. Various concentrations of P-Glu_4 were incubated with the cells for 24 hours and the medium was changed to remove any unbound conjugate. Then cells were irradiated for 7 min at 0.84 mW cm^{-2} (3.5 kJ m^{-2}). Immediately after irradiation, cells were treated with a 0.4% w/v trypan blue solution for 10 min at room temperature. Blue stained cells were counted as non-viable cells using a light microscope.

The observed phototoxicity of P-Glu_4 on the three cell lines corresponds to their uptake as determined by their fluorescence images (above). P-Glu_4 has the highest affinity toward $3Y1^{v\text{-}Src}$ cells, and ~45% of these cells are rendered non-viable under these PDT conditions using 20 μM of the conjugate. Consistent with the uptake assays, the percentage of non-viable $3Y1^{c\text{-}Src}$ and 3Y1 cells under the same PDT conditions decreases to ~30% and ~10 %, respectively (Figure 7).

Photocytotoxicity: Apoptosis

As with the MDA-MB-231 cells, a PARP cleavage assay was used as an indication of apoptosis in all three-3Y1 cell lines post photodynamic treatment (Figure 8). No PARP cleavage is observed in control experiments on the three 3Y1 cell lines (no irradiation or porphyrin, with irradiation but no porphyrin, or with porphyrin but no irradiation), which indicates that there is no apoptotic induction without both P-Glu_4 and light. Detailed analysis of the apoptotic response of these cells to photodynamic treatment with P-Glu_4 will be the subject of a later report.

The cells were incubated with 8 μM P-Glu_4 for 24 hours, whereupon the medium was changed just prior to irradiation to ensure that no unbound porphyrins remain in the medium. Cells were irradiated at 0.84 mW cm^{-2} for 3.5 min (1.764 kJ m^{-2}). Nine Hours later, the cells were collected, lysed, and the lysate analyzed by a Western Blot. As it is shown in Figure 8, there is no PARP cleavage in normal 3Y1 rat fibroblasts, an intermediate degree of PARP cleavage in the partially transformed $3Y1^{c\text{-}Src}$ cells is observed, and the transformed $3Y1^{v\text{-}Src}$ cells exhibit the most PARP cleavage.

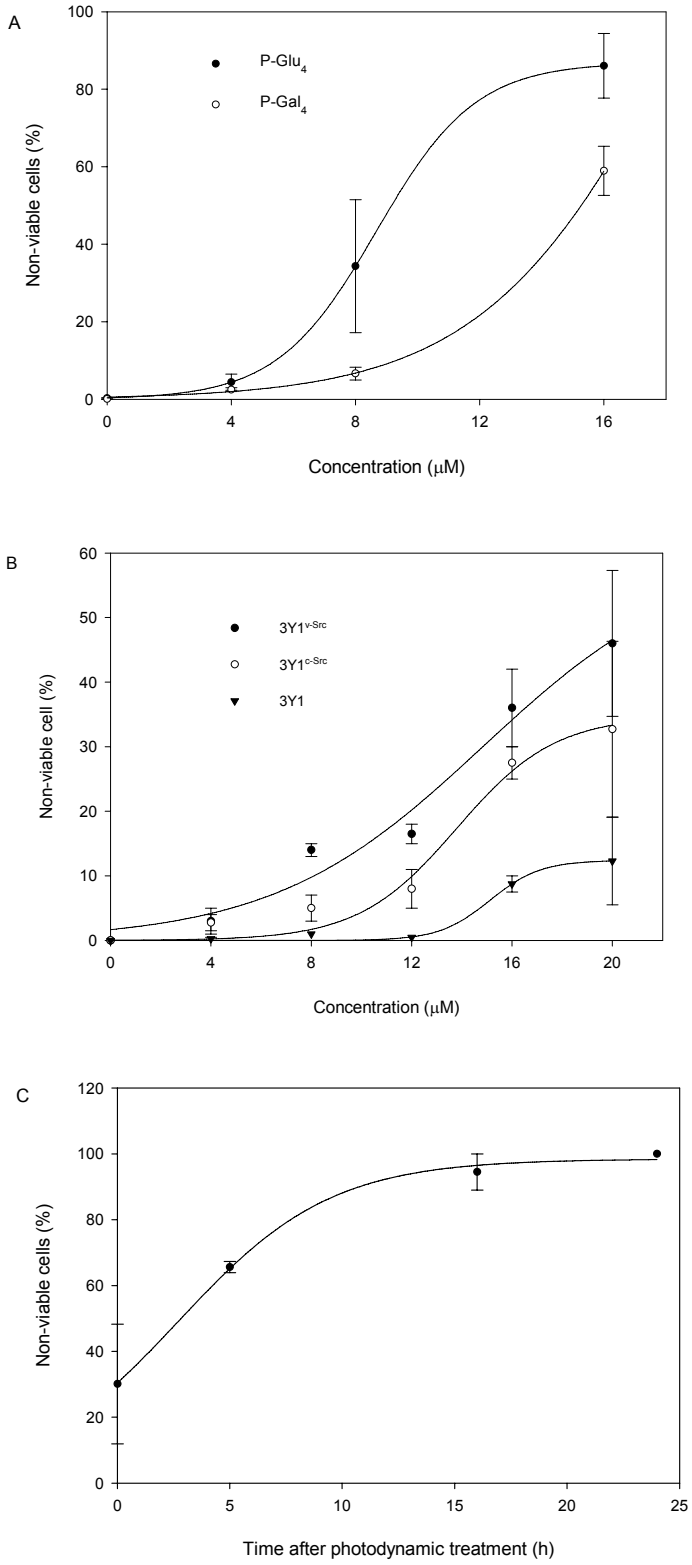

Figure 7. Photocytotoxic effects on transformed $3Y1^{v\text{-}Src}$, partially transform $3Y1^{c\text{-}Src}$ and normal 3Y1 rat fibroblasts. (A) The photocytotoxic effects of various concentrations of P-Glu_4 and P-Gal_4 on $3Y1^{v\text{-}Src}$ cells are compared using 5.76 kJ m^{-2} white light (0.96 mW cm^{-2} from a 13 W fluorescent bulb for 10 minutes), where non-viable cells were visualized with trypan blue staining 5 hours after treatment. (B) The photocytotoxic effects of various concentrations of P-Glu_4 on transformed $3Y1^{v\text{-}Src}$, partially transformed $3Y1^{c\text{-}Src}$ and normal 3Y1 cells using 3.53 kJ m^{-2} white light (0.84 mW cm^{-2} from a 13 W fluorescent bulb for 7 minutes), where necrotic cells were visualized with trypan blue staining immediately after treatment. (C) The photocytotoxic effects of 10 μM P-Glu_4 on transformed $3Y1^{v\text{-}Src}$ using 11.52 kJ m^{-2} white light (0.96 mW cm^{-2} from a 13 W fluorescent bulb for 20 minutes). Non-viable cells were counted at various lengths of time after photodynamic treatment. Each data point represents an average ± S.D. from at least three independent measurements.

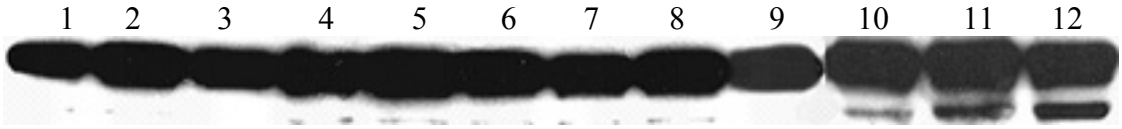

Figure 8. Different degrees of PARP cleavage in fully transformed ($3Y1^{v\text{-}Src}$), partially transformed ($3Y1^{c\text{-}Src}$) and normal (3Y1) rat fibroblasts as indications of apoptosis. 3Y1, $3Y1^{c\text{-}Src}$, $3Y1^{v\text{-}Src}$ cells were treated with 8 μM $P\text{-}Glu_4$ for 24 hours. Cells were irradiated at 0.84 mW cm^{-2} for 3.5 minutes (1.76 kJ m^{-2}), and 9 hours later the cells were collected and lysed. The supernatant of the lysate was applied to western blot to detect PARP cleavage. Lane 1: 3Y1 cells with no photodynamic treatment; Lane 2: $3Y1^{c\text{-}Src}$ cells with no photodynamic treatment; Lane 3: $3Y1^{v\text{-}Src}$ cells with no photodynamic treatment; Lane 4: 3Y1 cells with irradiation but no $P\text{-}Glu_4$; Lane 5: $3Y1^{c\text{-}Src}$ cells with irradiation but no $P\text{-}Glu_4$; Lane 6: $3Y1^{v\text{-}Src}$ cells with irradiation but no $P\text{-}Glu_4$; Lane 7: 3Y1 cells with $P\text{-}Glu_4$ but no irradiation; Lane 8: $3Y1^{c\text{-}Src}$ cells with $P\text{-}Glu_4$ but no irradiation; Lane 9: $3Y1^{v\text{-}Src}$ cells with $P\text{-}Glu_4$ but no irradiation; Lane 10: 3Y1 cells with irradiation and $P\text{-}Glu_4$; Lane 11: $3Y1^{c\text{-}Src}$ cells with irradiation and $P\text{-}Glu_4$; Lane 12: $3Y1^{v\text{-}Src}$ cells with irradiation and $P\text{-}Glu_4$.

3Y1 Conclusions

These results reinforce the MDA-MB-231 results in that the $P\text{-}Glu_4$ conjugate has good selectivity for the transformed cells over normal cells. Both necrosis and apoptosis are a consequence of the photodynamic treatment of the transformed cells and correlate with the extent of $P\text{-}Glu_4$ uptake. The extent of both necrosis and apoptosis increases in the order of fully transformed cells ($3Y1^{v\text{-}Src}$) > partially transformed cells ($3Y1^{c\text{-}Src}$) > normal rat fibroblasts (3Y1).

Conclusion

The formation of saccharide conjugates to porphyrins and related compounds can be accomplished in high yields in one or two steps by using thiosaccharides and a pentafluorophenyl group on the macrocycle. The thio linker results in a porphyrin-saccharide conjugate that is non-hydrolizable under physiological conditions – enzymatically or by reduced pH. In the present studies we used the symmetric tetra substituted $TPPF_{20}$; however, different pentafluorophenyl porphyrin substitution patterns

with 1-3 saccharides may be readily formed by using less than four equivalents of the thiosugar and chromatographic separation. These later derivatives would have different octanol/water partition coefficients, thus different activities. The significantly enhanced uptake of the P-Glu_4 derivative over the P-Gal_4 derivative by aggressive malignant MDA-MB-231 and the transformed $3Y1^{v\text{-}Src}$ cells indicates this is a viable strategy for targeting cancer cells. Importantly, the fact that normal 3Y1 fibroblasts absorbed the P-Glu_4 to a much lesser extent than the transformed $3Y1^{v\text{-}Src}$ cells indicates that discrimination between healthy and cancerous cells is achievable by using simple sugars. Furthermore, P-Glu_4 and P-Gal_4 are effective PDT agents as they induce cell death by necrosis and/or apoptosis, depending on the concentration of the conjugate and on the light exposure. At still lower concentrations of the porphyrin and light exposure, cells are rendered less aggressive as indicated by significantly reduced mobility. The apoptosis and mobility observations may indicate that the PDT methodology using P-Glu_4 or P-Gal_4 remains effective even when there is poor light penetration and low concentrations of the porphyrin-saccharide conjugate.

There are a number of reports on the potential of glycosylated porphyrins as PDT agents; however, the major conclusion that can be made is that the complex interplay between structure lipophilicity and the extent of cell binding/uptake differs widely from system to system. The field lacks a set of standardized protocols that make rigorous comparisons of results from different labs difficult if not impossible.

Abbreviations

PDT	Photo Dynamic Therapy
P-Glu_4	5,10,15,20-tetrakis (4,1'-thio-glucose-2,3,5,6-tetrafluorophenyl)porphyrin
P-Gal_4	5,10,15,20-tetrakis (4,1'-thio-galactose-2,3,5,6-tetrafluorophenyl)porphyrin
DMEM	Dulbecco's Modified Eagle Medium
PARP	poly-(ADP ribose) polymerase
$TPPF_{20}$	5,10,15,20-tetrakis(pentafluorophenyl)porphyrin
ESI-MS	Electron Spray Ionization Mass Spectroscopy
TPP	Tetraphenylporphyrin

References:

1. Drain, C. M., Christensen, B., and Mauzerall, D. C. (1989) Photogating of ionic currents across a lipid bilayer, *Proc. Natl. Acad. Sci. USA 86*, 6959-6962.
2. Drain, C. M., and Mauzerall, D. C. (1992) Photogating of ionic currents across lipid bilayers: Hydrophobic ion conductance by an ion chain mechanism, *Biophys. J. 63*, 1556-1563.
3. MacDonald, I. J., and Dougherty, T. J. (2001) Basic principles of photodynamic therapy, *J. Porphyrins Phthalocyanines 5*, 105-129.
4. Neurath, A. R., Strick, N., and Debnath, A. K. (1995) Structural requirements for and consequences of an antiviral porphyrin binding to the V3 loop of the human immunodeficiency virus (HIV-1) envelope glycoprotein gp120, *J. Mol. Recog. 8*, 345-357.
5. Vzorov, A. N., Dixon, D. W., Trommel, J. S., Marzilli, L. G., and Compans, R. W. (2002) Inactivation of human immunodeficiency virus type 1 by porphyrins, *Antimicrob. Agents Chemother. 46*, 3917-3925.
6. Pandey, R. K. (2000) Recent advances in photodynamic therapy, *J. Porphyrins Phthalocyanines 4*, 368-373.
7. Sternberg, E. D., Dolphin, D., and Bruckner, C. (1998) Porphyrin-based photosensitizers for use in photodynamic therapy, *Tetrahedron 54*, 4151-4202.
8. Bonnett, R. (1995) Photosensitizers of the porphyrin and phthalocyanine series for photodynamic therapy, *Chem. Soc. Rev.*, 19-33.
9. Moor, A. C. E. (2000) Signaling pathways in cell death and survival after photodynamic therapy, *J. Photochem. Photobiol. B: Biol. 57*, 1-13.

10. Mody, T. D. (2000) Pharmaceutical development and medical applications of porphyrin-type macrocycles, *J. Porphyrins Phthalocyanines 4*, 362-367.

11. Jori, G. (1996) Tumor photosensitizers: approaches to enhance the selectivity and efficiency of photodynamic therapy, *J. Photochem. Photobiol. B: Biol. 36*, 87-93.

12. Yang, S. I., Seth, J., Strachan, J.-P., Gentlemann, S., Kim, D., Holten, D., Lindsey, J. S., and Bocian, D. F. (1999) Ground and excited state electronic properties of halogenated tetraarylporphyrins. Tuning the building blocks for porphyrin-based photonic devices., *J. Porphyrins Phthalocyanines. 3*, 117-147

13. Dougherty, T. J. (1993) Yearly review Photodynamic therapy, *Photochem. Photobiol. 58*, 895-900.

14. Granville, D. J., and Hunt, D. W. C. (2000) Porphyrin-mediated photosensitization - Taking the apoptosis fast lane, *Curr. Opin. Drug Discovery Develop. 3*, 232-243.

15. Salva, K. A. (2002) Photodynamic therapy; Unapproved uses, dosages, or indications, *Clin. Dermat. 20*, 571-581.

16. Mauzerall, D. C., and Drain, C. M. (1992) Photogating of ionic currents across lipid bilayers: Electrostatics of ions and dipoles inside the membrane, *Biophys. J. 63*, 1544-1555.

17. Gong, X., Milic, T., Xu, C., Batteas, J. D., and Drain, C. M. (2002) Preparation and characterization of porphyrin nanoparticles, *J. Am. Chem. Soc. 124*, 14290-14291.

18. Hombrecher, H. K., and Schell, C. (1997) Carbohydrate substituted porphyrins. Synthesis, characterization and lipoprotein binding properties, *Carbohydr. Polymers 34*, 422-423.

19. Sol, V., Blais, J. C., Carre, V., Granet, R., Guilloton, M., Spiro, M., and Krausz, P. (1999) Synthesis, spectroscopy, and photocytotoxicity of glycosylated amino acid porphyrin derivatives as promising molecules for cancer phototherapy, *J. Org. Chem. 64*, 4431-4444.

20. Schell, C., and Hombrecher, H. K. (1999) Synthesis and investigation of glycosylated mono- and diarylporphyrins for photodynamic therapy, *Bioorg. Med. Chem. 7*, 1857-1865.

21. Mikata, Y., Onchi, Y., Tabata, K., Ogura, S.-i., Okura, I., Ono, H., and Yano, S. (1998) Sugar-dependent photocytotoxic property of tetra- and octa-glycoconjugated tetraphenylporphyrins, *Tetrahedron Lett. 39*, 4505-4508.

22. Maillard, P., Vilain, S., Huel, C., and Momenteau, M. (1994) Efficient preparation of the alpha, alpha, alpha, alpha-atropoisomer of meso-tetrakis[2-(2,3,4,6-tetraacetyl-O-beta-glucosyl)phenyl]porphyrin, *J. Org. Chem. 59*, 2887-2890.

23. Chen, X., and Drain, C. M. (2004) Photodynamic therapy using carbohydrate conjugated porphyrins, *Drug Design Review - Online 1*, 215-234, http://www.bentham.org/ddro/.

24. Pasetto, P., Chen, X., Drain, C. M., and Franck, R. W. (2001) Synthesis of hydrolytically stable porphyrin C- and S-glycoconjugates in high yields, *Chem. Commun.*, 81-82.

25. Brown, R. S., and Wahl, R. L. (1993) Overexpression of Glut-1 glucose transporter in human breast cancer. An immunohistochemical study, *Cancer 72*, 2979-2985.

26. Sharon, M., and Lis, H. (1989) Lectins as cell recognition molecules, *Science 246*, 227-234.

27. Cornia, M., Valenti, C., Capacchi, S., and Cozzini, P. (1998) Synthesis, characterisation and conformational studies of lipophilic, amphiphilic and water-soluble C-glyco-conjugated porphyrins, *Tetrahedron 54*, 8091-8106.

28. Cornia, M., Menozzi, M., Ragg, E., Mazzini, S., Scarafoni, A., Zanardi, F., and Casiraghi, G. (2000) Synthesis and utility of novel C-*meso*-glycosylated metalloporphyrins, *Tetrahedron 56*, 3977-3983.

29. Sylvain, I., Benhaddou, R., Carre, V., Cottaz, S., Driguez, H., Granet, R., Guilloton, M., and Krausz, P. (1999) Synthesis and biological evaluation of thioglycosylated meso- arylporphyrins, *J. Porphyrins Phthalocyanines 3*, 1 - 4.

30. Sylvain, I., Zerrouki, R., Granet, R., Huang, Y. M., Lagorce, J.-F., Guilloton, M., Blais, J.-C., and Krausz, P. (2002) Synthesis and biological evaluation of thioglycosylated porphyrins for an application in photodynamic therapy, *Bioorg. Med. Chem. 10*, 57-69.

31. Hornia, A., Lu, Z., Sukezane, T., Zhong, M., Joseph, T., Frankel, P., and Foster, D. A. (1999) Antagonistic effects of protein kinase C alpha and delta on both transformation and phospholipase D activity mediated by the epidermal growth factor receptor, *Mol. Cell Biol. 19*, 7672-7680.

32. Shen, Y., Xu, L., and Foster, D. A. (2001) Role for phospholipase D in receptor-mediated endocytosis, *Mol. Cell Biol. 21*, 595-602.

33. Willingham, M. C., and Pastan, I. (1985) *An Atlas of Immunofluorescence in Cultured Cells*, Academic Press, Orlando.

34. Qian, G. (2003), Advanced Science & Technology, http://www.howardast.com, New York.

35. Lu, Z., Hornia, A., Joseph, T., Sukezane, T., Frankel, P., Zhong, M., Bychenok, S., Xu, L., Feig, L. A., and Foster, D. A. (2000) Phospholipase D and RalA cooperate with the epidermal growth factor receptor to transform 3Y1 rat fibroblasts, *Mol. Cell Biol. 20*, 462-467.

36. Shen, Y., Zheng, Y., and Foster, D. A. (2002) Phospholipase D2 stimulates cell protrusion in v-Src-transformed cells, *Biochem. Biophys. Res. Commun. 293*, 201-206.

37. Adler, A. D., Sklar, L., Longo, F. R., Finarelli, J. D., and Finarelli, M. G. (1968) A mechanistic study of the synthesis of meso-tetraphenylporphin, *5*, 669-677.

38. Lindsey, J. S., Schreiman, I. C., Hsu, H. C., Kearney, P. C., and Marguerettaz, A. M. (1987) Rothemund and Adler-Longo reactions revisited: synthesis of tetraphenylporphyrins under equilibrium conditions, *J. Org. Chem. 52*, 827-836.

39. Defaye, J., and Gelas, J. (1991) Thio-oligosaccharides: Their Synthesis and Reactions with Enzymes, in *Studies in Natural Products Chemistry* (Atta-ur-Rahman, Ed.) pp 315-357, Elsevier Science Publishers B. V., Amsterdam.

40. Shaw, S. J., Edwards, C., and Boyle, R. W. (1999) Regioselective synthesis of multifunctionalised porphyrins - coupling of mono-(pentafluorophenyl)porphyrins to electrophiles, *Tet. Lett. 40*, 7585-7586.

41. Shaw, S. J., Elgie, K. J., Edwards, C., and Boyle, R. W. (1999) Mono-(pentafluorophenyl)porphyyrins - Useful intermediates in the regioselective synthesis of multifunctionalised porphyrins, *Tet. Lett. 40*, 1595-1596.

42. Momenteau, M., Oulmi, D., Maillard, P., and Croisy, A. F. (1994) In vitro photobiological activity of a new series of photosensitizers: the glycoconjugated porphyrins, *Proc. SPIE 2325 Photodynamic Therapy of Cancer II*, 13-23.

43. Adams, K. R., Berenbaum, M. C., Bonnett, R., Nizhnik, A. N., Salgado, A., and Valles, M. A. (1992) Second generation tumour photosensitisers: the synthesis and biological activity of octaalkyl chlorins and bacteriochlorins with graded amphiphilic character, *J. Chem. Soc., Perkin Trans. 1*, 1465-1470.

44. Oulmi, D., Maillard, P., Guerquin-Kern, J.-L., Huel, C., and Momenteau, M. (1995) Glycoconjugated porphyrins. 3. synthesis of flat amphiphilic mixed meso-(glycosylated aryl)arylporphyrins and mixed meso-(glycosylated aryl)alkylporphyrins bearing some mono- and disaccharide groups, *J. Org. Chem. 60*, 1554-1564.

45. Drain, C. M., Gong, X., Ruta, V., Soll, C. E., and Chicoineau, P. F. (1999) Combinatorial synthesis and modification of functional porphyrin libraries: identification of new, amphipathic motifs for biomolecule binding, *J. Comb. Chem. 1*, 286-290.

46. Maziere, J. C., Santus, R., Morliere, P., Reyftmann, J. P., Candide, C., Mora, L., Salmon, S., Maziere, C., Gatt, S., and Dubertret, L. (1990) Cellular uptake and photosensitizing properties of anticancer porphyrins in cell membranes and low and high density lipoproteins, *J. Photochem. Photobiol. B: Biol. 6*, 61-68.

47. Bourhim, A., Gaud, O., Granet, R., Krausz, P., and Spiro, M. (1993) Synthesis of new glycosylated porphyrin derivatives with a hydrocarbon spacer arm, *Synlett*, 563-564.

48. Gaud, O., Granet, R., Kaouadji, M., Krausz, P., Blais, J.-C., and Bolbach, G. (1996) Synthese et analyse structurale de nouvelles meso-arylporphyrines glycosylees en vue de I'application en phototherapie des cancers, *Can. J. Chem. 74*, 481-499.

49. Carre, V., Gaud, O., Sylvain, I., Bourdon, O., Spiro, M., Blais, J., Granet, R., Krausz, P., and Guilloton, M. (1999) Fungicidal properties of meso-arylglycosylporphyrins: influence of sugar substituents on photoinduced damage in the yeast Saccharomyces cerevisia, *J. Photochem. Photobiol. B: Biol. 48*, 57-62.

50. Grover-McKay, M., Walsh, S. A., Seftor, E. A., Thomas, P. A., and Hendrix, M. J. (1998) Role for glucose transporter 1 protein in human breast cancer, *Pathol. Oncol. Res. 4*, 115-120.

51. Younes, M., Brown, R. W., Mody, D. R., Fernandez, L., and Laucirica, R. (1995) GLUT1 expression in human breast carcinoma: correlation with known prognostic markers, *Anticancer Res. 15*, 2895-2898.

52. Brault, D. (1990) Physical chemistry of porphyrins and their interactions with membranes: the importance of pH, *J. Photochem. Photobiol. B: Biol. 6*, 79-86.

53. Bohmer, R. M., and Morstyn, G. (1985) Uptake of hematoporphyrin derivative by normal and malignant cells: effect of serum, pH, temperature, and cell size, *Cancer Res. 45*, 5328-5334.

54. Friberg, E. G., Cunderlikova, B., Pettersen, E. O., and Moan, J. (2003) pH effects on the cellular uptake of four photosensitizing drugs evaluated for use in photodynamic therapy of cancer, *Cancer Lett. 195*, 73-80.

55. Pandey, R. K., and Zheng, G. (2000) Porphyrins as photosensitizers in photodynamic therapy, in *The Porphyrin Handbook* (Kadish, K. M., Smith, K. M., and Guilard, R., Eds.) pp 157-230, Academic Press, New York.

56. Fujimoto, K., Miyata, T., and Aoyama, Y. (2000) Saccharide-directed cell recognition and molecular delivery using macrocyclic saccharide clusters: masking of hydrophobicity to enhance the saccharide specificity, *J. Am. Chem. Soc. 122*, 3558-3559.

57. Kroemer, G., Dallaporta, B., and Resche-Rigon, M. (1998) The mitochondrial death/life regulator in apoptosis and necrosis, *Annu. Rev. Physiol. 60*, 619-642.

58. Yu, S.-W., Wang, H., Poitras, M. F., Coombs, C., Bowers, W. J., Federoff, H. J., Poirier, G. G., Dawson, T. M., and Dawson, V. L. (2002) Mediation of poly(ADP-ribose) polymerase-1–dependent cell death by apoptosis-inducing factor, *Science 297*, 259-263.

59. de Murcia, G., and Menissier de Murcia, J. (1994) Poly(ADP-ribose) polymerase: a molecular nick-sensor, *Trends Biochem. Sci. 19*, 172-176.

60. Oleinick, N. L., Morris, R. L., and Belichenko, I. (2002) The role of apoptosis in response to photodynamic therapy: what, where, why, and how, *Photochem. Photobiol. Sci. 1*, 1-21.

61. Ridley, A. J., Schwartz, M. A., Burridge, K., Firtel, R. A., Ginsberg, M. H., Borisy, G., Parsons, J. T., and Horwitz, A. R. (2003) Cell migration: integrating signals from front to back, *Science 302*, 1704-1709.

62. Zhong, M., Joseph, T., Jackson, D., Beychenok, S., and Foster, D. A. (2002) Elevated phospholipase D activity induces apoptosis in normal rat fibroblasts, *Biochem. Biophys. Res. Commun. 298*, 474-477.

63. Zhong, M., Lu, Z., and Foster, D. A. (2002) Downregulating PKC delta provides a PI3K/Akt-indepentdent survival signal that overcomes apoptotic signals generated by c-Src overexpression, *Oncogene 21*, 1071-1078.

64. Zhong, M., Shen, Y., Zheng, Y., Joseph, T., Jackson, D., and Foster, D. A. (2003) Phospholipase D prevents apoptosis in v-Src-tranformed rat fibroblasts and MDA-MB-231 breast cancer cells, *Biochem. Biophys. Res. Commun. 302*, 615-619.

65. Pandey, R. K., and Zheng, G. (2000) Porphyrins as photosensitizers in photodynamic therapy, in *The porphyrin handbook* (Guilard, R., Ed.) pp 157-, Academic Press.

66. Lipscomb, L. A., Zhou, F. X., Presnell, S. R., Woo, R. J., Peek, M. E., Plaskon, R. R., and Williams, L. D. (1996) Structure of DNA-porphyrin complex, *Biochem. 35*, 2818-2823.

Supporting Information:

1. Low affinity of non-saccharide porphyrins to MDA-MB-231 human breast cancer cells, compared to P-Glu_4.

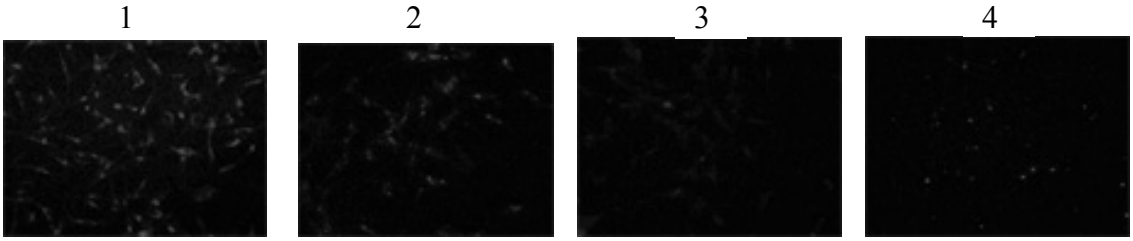

1. P-Glu_4
2. meso-tetra (4-Carboxyphenyl)porphyrin tetramethyl ester
3. meso-tetra(4-Methoxyphenyl)porphyrin
4. $TPPF_{20}$

2. Low affinity of acetyl protected tetra-glucose porphyrin to MDA-MB-231 human breast cancer cells, compared to unprotected tetra-glucose porphyrin (P-Glu_4).

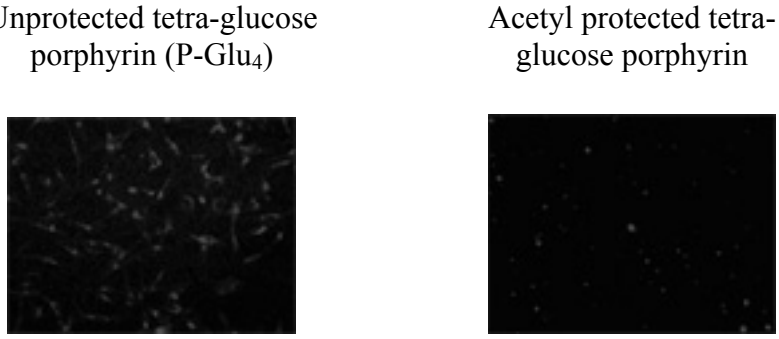

3. Low affinity of P-Gal_4 to fully transformed $3Y1^{v\text{-}Src}$ rat fibroblast, compared to P-Glu_4.

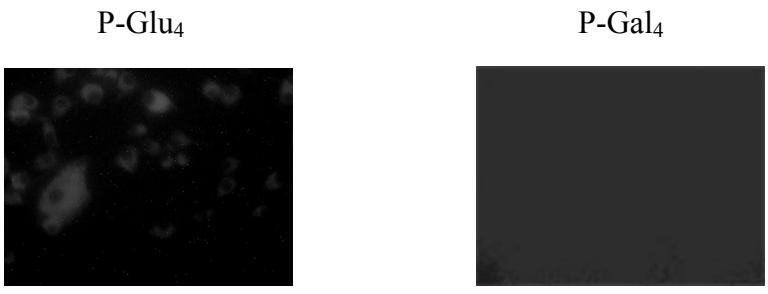

4. Extinction coefficients of $TPPF_{20}$, P-Glu_4 and P-Gal_4.

ε (L/mol·cm)	Soret Band	Q_1	Q_2	Q_3	Q_4
$TPPF_{20}$ (CH_2Cl_2)	6.50×10^5	4.46×10^4	4.47×10^3	1.51×10^4	3.20×10^3
$TPPF_{20}$ (CH_3OH)	6.22×10^5	4.49×10^4	5.92×10^3	1.50×10^4	3.30×10^3
P-Glu_4 (CH_3OH)	1.83×10^5	1.31×10^4	3.81×10^3	4.87×10^3	3.19×10^3
P-Glu_4 (H_2O)	1.30×10^5	1.06×10^4	2.21×10^3	3.98×10^3	2.12×10^3
P-Gal_4 (CH_3OH)	1.74×10^5	1.18×10^4	1.82×10^3	3.57×10^3	1.26×10^3
P-Gal_4 (H_2O)	1.38×10^5	0.866×10^4	1.71×10^3	3.09×10^3	0.973×10^3

λmax	Soret Band	Q_1	Q_2	Q_3	Q_4
$TPPF_{20}$ (CH_2Cl_2)	411	506	535	582	623
$TPPF_{20}$ (CH_3OH)	406	503	534	579	632
P-Glu_4 (CH_3OH)	410	505	535	583	647
P-Glu_4 (H_2O)	410	508	541	584	646
P-Gal_4 (CH3OH)	410	504	536	582	648
P-Gal_4 (H_2O)	410	508	538	577	641

5. MALDI mass spectra of P-Glu_4 and P-Gal_4.

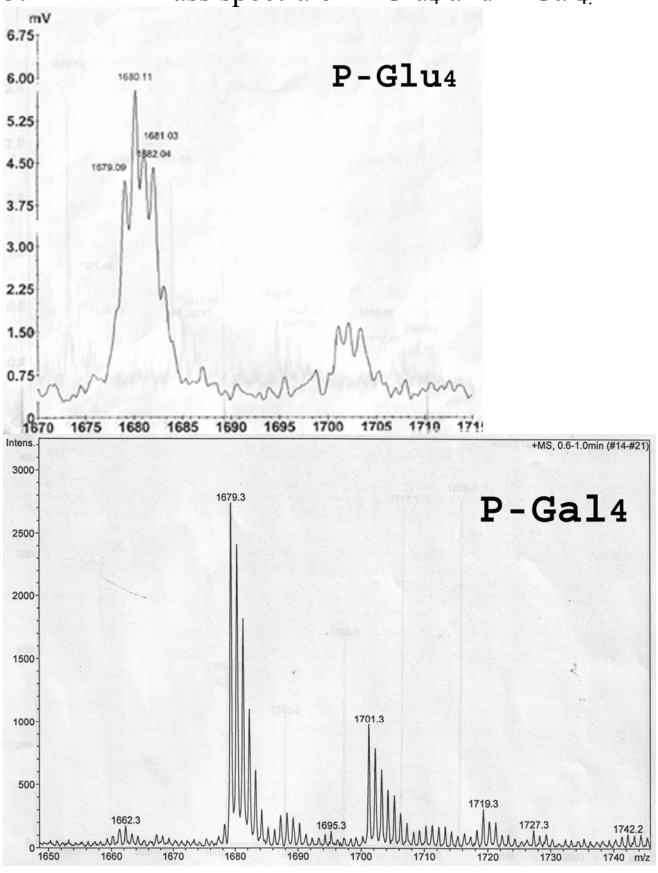

The peaks at 1701 are Na^+ (+23) from the parent peaks, which is typical for sugar porphyrins.

6. Low affinity of P-Glu_4 to mouse NIH3T3 fibroblast (right), compared to human breast cancer MDA-MB-231 cells (left).

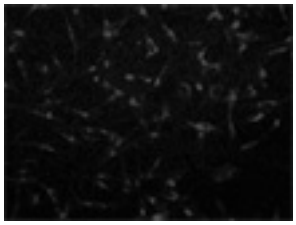

Appendices

Different solvent effects on human breast cancer MDA-MB-231 cells

5% (v/v) Solvent was add to the medium and 24 hours later, cell growth was observed using a phase contrast microscope. Tested solvents and their effects on cells on a general scale are listed in Table 1. In general, any organic solvent shouldn't exceed 2% to avoid any stress on normal cell growth.

Table 1. Different solvent effects on human breast cancer MDA-MB-231 cells.

Effect	*Solvent(s) (5% v/v)*	*Observation*
Very good	DME (ethylene glycol dimethyl ether)	Cells proliferate and their morphology is as normal as the control.
Good	Methanol, acetonitrile	Cells may proliferate at a slightly slower speed, but their morphology is normal.
Fair	Ethanol, acetone	Cells proliferate at a significant slower speed.
Poor	THF, DMF, DMSO, 2-Chloroethanol	Cells stop proliferating and their morphology appear to be unhealthy.

Optimal incubation time of P-Glu_4 with human breast cancer MDA-MB-231 cells for maximum uptake judged by fluorescence images

Judged by fluorescence images, 24 hours incubation time of porphyrin (represented by P-Glu_4) is the best condition for maximal drug uptake by human breast cancer MDA-MB-231 cells (Appendix I). Incubation time longer than 24 hours did not indicate any better uptake. For the convenience of experiments, 24-hour incubation time is routinely used.

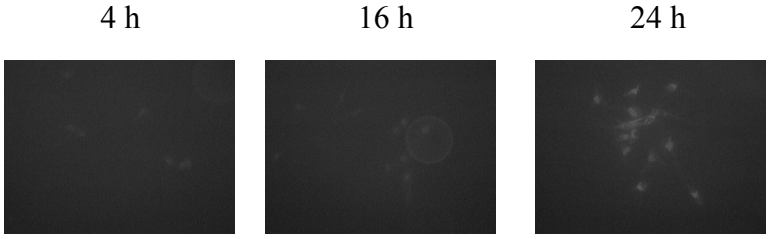

Appendix I. Twenty-four hours incubation time of P-Glu_4 with human breast cancer cells is the best condition for maximal drug uptake.

Different porphyrins affinities to human breast cancer MDA-MB-231 cells judged by fluorescence images

Different porphyrins (dissolved in DME, methanol or aqueous solution) were added to the cultures to a final concentration of 2 to 20 μM, when cells reached about 80% confluence. Twenty-four hours later cells were fixed and imaged as described in the text. The tested porphyrins structures and images are shown in Table 2. Our observation for porphyrins having two charges are: when positive charged moieties are on the same side (5,10), they bind to/enter cells much more efficiently than when the charged groups are on opposite sides (Table 2: images of **1** & **2**) and better than the tetracationic species (Table 2: image of **7**). The hydrophobic porphyrins either do not enter the cells well or there are problems in the delivery of these compounds. (They tend to aggregate even in DMSO.) Those hydrophilic porphyrins do not bind/enter the cells well as their partition coefficient (hydrocarbon/water) is very small. This has also been well documented (*65*).

Table 2. Different porphyrins affinities to human breast cancer MDA-MB-231 cells: fluorescence images and structures.

1. 5,10-di(4-N-methylpyridyl)-15-(4-hydroxyphenyl)-20-(4-methylphenyl)porphyrin (2μM)	**2**. 5,15-di(4-N-methylpyridyl)-10-(4-hydroxyphenyl)-20-(4-methylphenyl)porphyrin (2μM)
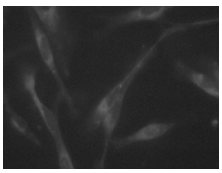 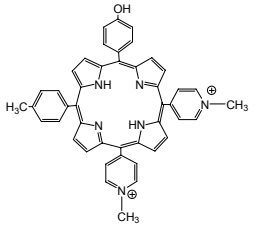	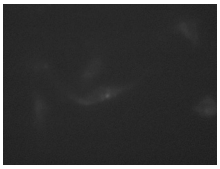 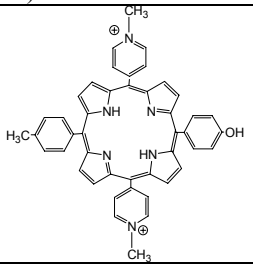
3. 5,10,15,20-tetrakis[4-(2'-acetamido-3',4',6'-tri-O-acetyl-1'-S-acetyl-2'-deoxy-1'-thiogluco)-2,3,5,6-tetrafluorophenyl]porphyrin (20μM)	**4**. 5,10,15,20-tetrakis[4-(2',3',4'-tri-O-acetyl'-xylosyl thio)-2,3,5,6-tetrafluorophenyl]porphyrin (20μM)

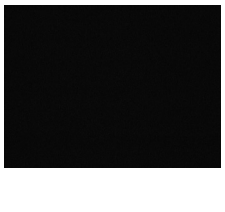 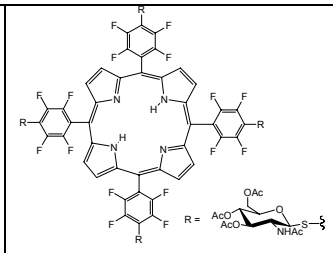	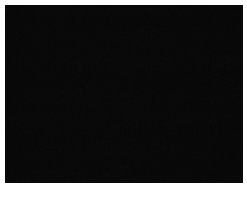 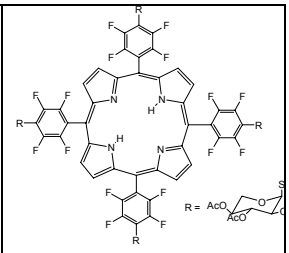
5. 5,10,15,20-tetrakis[4-(1'-thio-4'-methylphenyl)-2,3,5,6-tetrafluorophenyl]porphyrin (20μM)	**6**. 5,10,15,20-tetra(4-thiopentyl-2,3,5,6-tetrafluorophenyl)porphyrin (20μM)
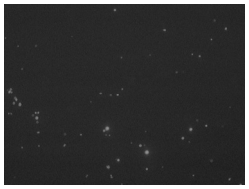 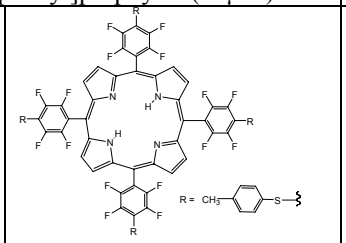	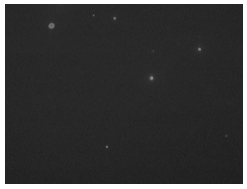 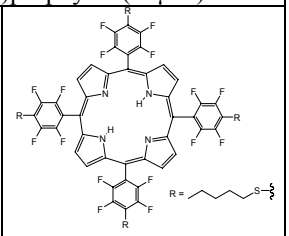
7. tetra(4-N-methylpyridinium)porphyrin (20μM)	**8**. tetra-4-carboxyphenyl porphyrin (20μM)
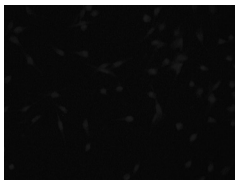 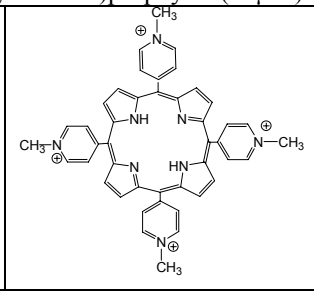	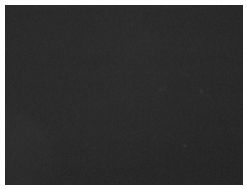 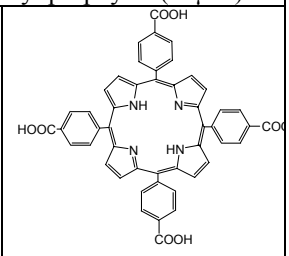
9. tetra(4-sulfonatophenyl)porphyrin (10μM)	**10**. 5,10-bis(1'-butyl-6'-uracyl)-15,20-bis(4-*tert*-butylphenyl)porphyrin (20μM)
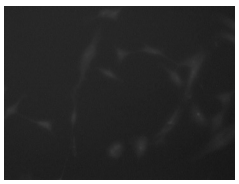 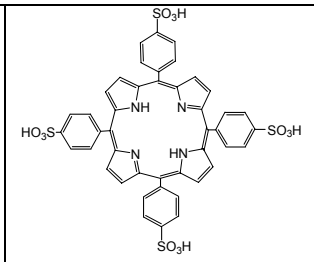	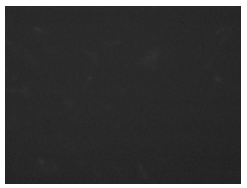 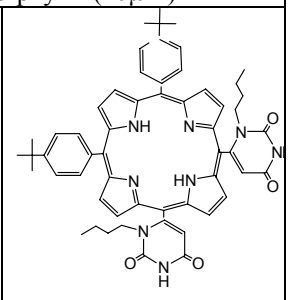
11. 5-mono(1'-butyl-6'-uracyl)-10,15,20-tri(4-*tert*-butylphenyl)porphyrin (20μM)	**12**. 5,10,15-tri(3,5-diacetamido-4-pyridyl)-20-mono(4-tert-buylphenyl)porphyrin (10μM)
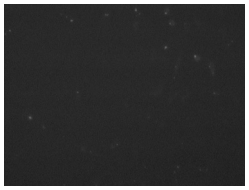 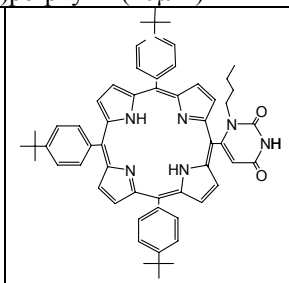	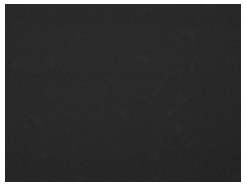 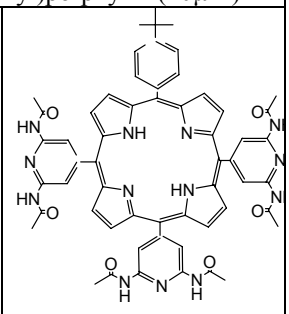
13. 5,10-bis(1'-butyl-6'-uracyl)-15,20-bis(4-*tert*-	**14**. 5,15-bis(1'-butyl-6'-uracyl)-10,20-bis(4-*tert*-

butylphenyl)porphyrin(Zn) (20μM)		butylphenyl)porphyrin(Zn) (20μM)	
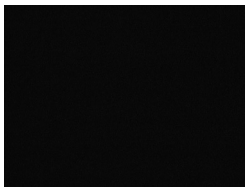	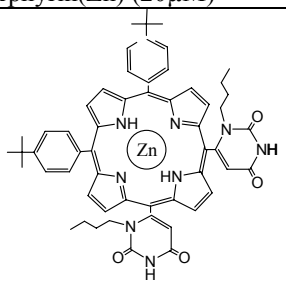	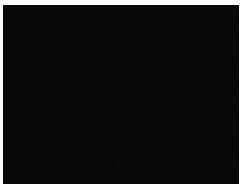	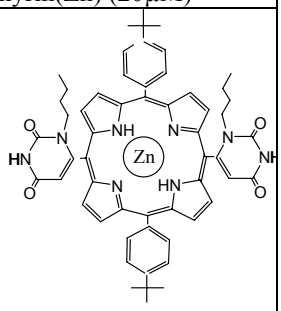
15. 5,15-di(4-N-methylpyridyl)-10,20-di(4-nitrophenyl)porphyrin (10μM)			
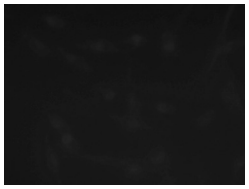	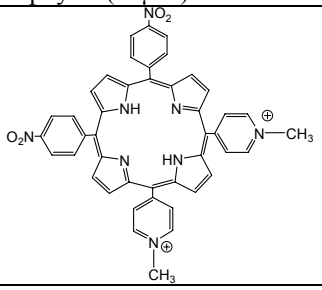		

Some of the charged porphyrins show good affinity to the cancer cells in the above images. In order to investigate the charge effect on the cell uptake, two negatively anionic porphyrins (tetra-4-carboxyphenylporphyrin and tetra-4-sulfonatophenylporphyrin) were chosen to mix with the cationic tetra(4-N-methylpyridinium)porphyrin and affinities to cancer cells of the porphyrin\ mixtures were evaluated again by fluorescence images, which are shown in Table 3. The data displayed that negatively charged porphyrins did mask some affinity of the positively charged tetra(4-N-methylpyridinium)porphyrin to the cancer cells, but not all. These results suggest that the affinity of tetra(4-N-methylpyridinium)porphyrin is partially due to the electrostatic interaction of the positively charged porphyrin with negatively charged membrane / lipids. Detailed studies are still needed to test this hypothesis. While it is known that the tetra(4-N-methylpyridinium)porphyrin binds to a variety of biopolymers such as DNA (*66*), less is known on how this porphyrin binds and/or enters cancer cell

lines. The generalization that PDT efficacy correlates with lipophilicity (*65*) indicates tetra(4-N-methylpyridinium)porphyrin ($TMePyP^{4+}$) should bind but not enter cells. However this tetra cationic porphyrin may interact with anionic lipids sufficiently to allow it to cross the low dielectric membrane core. In contrast, the tetra(4-sulfonatophenyl)porphyrin ($TSPP^{4-}$) binds to these cells at least as well as the cationic $TMePyP^{4+}$. A simple hypothesis is that a 1 : 1 stoichimetry of $TMePyP^{4+}$/ $TSPP^{4-}$ would form a zwitterionic pair in solution; therefore facilitating entry into the cells. The preliminary data (Table 3) did not indicate this hypothesis though.

Table 3. Mixtures of positively and negatively charged porphyrins and their affinities to the human breast cancer MDA-MB-231 cells. (Helps from Tal Hasson on $TSPP^{4-}$ results are appreciated.)

Mixture 1 tetra(4-N-methylpyridinium)porphyrin (10μM) + tetra-4-carboxyphenyl porphyrin (10μM)	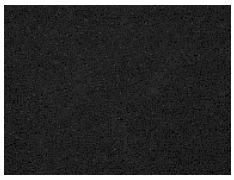
Mixture 2 tetra(4-N-methylpyridinium)porphyrin (10μM) + tetra(4-sulfonatophenyl)porphyrin (10μM)	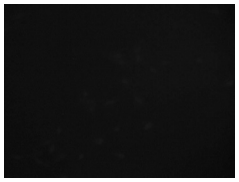

The affinity of P-Glu_4 (and/or P-Gal_4) to other cells lines

Human breast cancer MCF-7 cells

The fluorescence images shown in Appendix II demonstrated that P-Glu_4 is preferentially taken in another human breast cancer cell line --- MCF-7 cells when compared with P-Gal_4.

P-Glu_4 (10μM) P-Gal_4 (10μM)

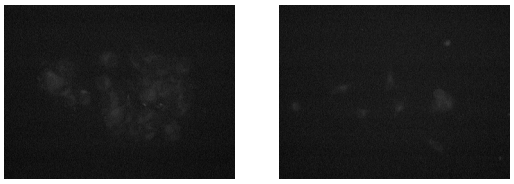

Appendix II. P-Glu_4 is preferentially taken up by human breast cancer MCF-7 cells over P-Gal_4. Fluorescence images were taken under identical conditions.

Human breast cancer 435S cells

Affinity is low for both P-Glu_4 and P-Gal_4; signals are not detectable.

Photocytotoxicities of P-Glu_4 on human breast cancer MCF-7 cells (compared to MDA-MB-231 cells)

Human breast cancer MCF-7 is a more redundant cell line than human breast cancer MDA-MB-231 cell line. MCF-7 cells are generally more vulnerable toward toxins because MDA-MB-231 cells can provide more survival signals. The concentration dependent photocytotoxicities of P-Glu_4 in MCF-7 and MDA-MB-231 cells are compared in Appendix III.

DAPI staining for rat 3Y1, 3Y1$^{c\text{-}Src}$, 3Y1$^{v\text{-}Src}$ fibroblasts

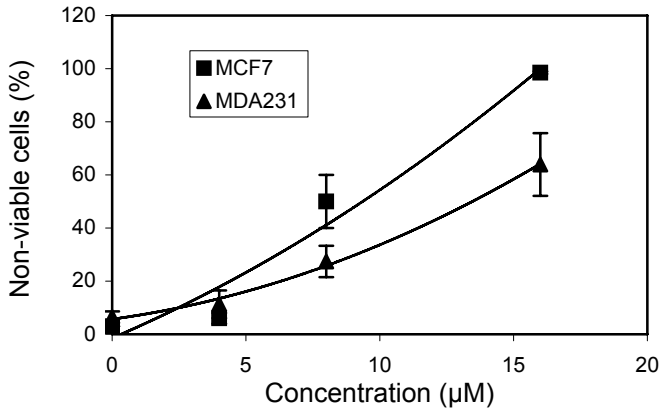

Appendix III. Human breast cancer MCF-7 cells are more vulnerable toward photodynamic treatment than human breast cancer MDA-MB-231 cells.

Chromatin condensations with the induced apoptotic cells were visualized by DAPI staining. 4 μM P-Glu$_4$ was incubated with the three cell lines for 24 hours. The cells were then rinsed, fixed and stained with DAPI solution. Fluorescence images were taken under identical conditions. Chromatin condensation is a typical morphological change in apoptotic cells. These results in Appendix IV show that the chromatin condensations are in the order of 3Y1$^{v\text{-}Src}$ (fully transformed) > 3Y1$^{c\text{-}Src}$ (partially transformed) > 3Y1 (normal) rat fibroblasts, which is an indication of the same order of apoptotic induction.

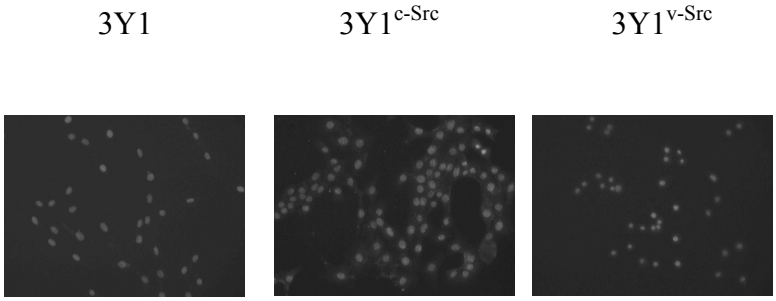

Appendix IV. Chromatin condensations visualized by DAPI staining are in the order of $3Y1^{v\text{-}Src}$ (fully transformed) > $3Y1^{c\text{-}Src}$ (partially transformed) > 3Y1 (normal) rat fibroblasts. (Controls with no photodynamic treatment have similar chromatin size within the three cell lines.)

References:

1. Pandey, R. K., and Zheng, G. (2000) Porphyrins as photosensitizers in photodynamic therapy, in *The porphyrin handbook* (Kadish, K. M., Smith, K. M., and Guilard, R., Eds.) pp 157-, Academic Press.

2. Lipscomb, L. A., Zhou, F. X., Presnell, S. R., Woo, R. J., Peek, M. E., Plaskon, R. R., and Williams, L. D. (1996) Structure of DNA-porphyrin complex, *Biochem. 35*, 2818-2823.

Chapter 3

A non-hydrolysable tetra-S-glucosylated porphyrin induces apoptosis in human breast cancer cells: photodynamic effects under low porphyrin concentrations

Abstract

A water-soluble tetra-S-glucosylated porphyrin is actively absorbed by MDA-MB-231 human breast cancer cells whereupon irradiation with visible light causes necrosis or apoptosis depending on the concentration of the porphyrin and the power of the light. With the same amount of light irradiation power (9.4 W m^{-2}), at 10-20 μM concentrations necrosis is observed, while at <10 μM concentrations, apoptosis is the predominant cause of cell death. Of the various possible pathways for the induction of apoptosis, experiments demonstrate that cytochrome c is released from the mitochondria to the cytosol, pro-caspase-3 is cleaved, poly-(ADP-ribose) polymerase is also cleaved, and the chromatin is condensed subsequent to photodynamic treatment of these cells. These data indicate that the photodynamic treatment of MDA-MB-231 cells using low concentrations of the tetra-S-glucosylated porphyrin and low light induces apoptosis at least partially from mitochondria, and other pathways.

Introduction

Apoptosis, programmed physiological cell death, is an essential and well-regulated cell function that allows for the ordered removal of superfluous, aged, or damaged cells (*1, 2*). Several million cells in the human body undergo apoptosis every second. Insufficient apoptosis may prompt oncogenesis by allowing cell accumulation

while excessive apoptosis may be the basis of degenerative diseases such as Huntington's and Alzheimer's (*2*). Apoptosis is manifested by both biochemical and morphological changes including: cell shrinkage, chromatin condensation, DNA fragmentation, plasma membrane blebbing and vesiculating, and phosphatidylserine redistribution to the cell surface. Also, the pathology of necrosis is characterized by significant degradation of membrane integrity and leakage of cell contents. The differences between necrosis and apoptosis are distinct, and are summarized in Table 1 (*1*).

Table 1. Apoptosis vs. necrosis

Apoptosis	Necrosis
• Physiological or pathological (subnectrotic damage) • Susceptibility tightly regulated • Plasma membranes near-to-intact until late • Heterophagic elimination • No leakage of cell content: little or no inflammation • Cellular enzymes participate, causing characteristic biochemical or morphological features including: ▪ chromatin condensation (pyknosis), ▪ nuclear fragmentation (karyorrhexis), ▪ regular DNA fragmentation pattern (endonucleolysis), ▪ selective protein degradation by specific proteases (capases), ▪ subtle changes in plasma membrances (loss of membrance asymmetry before loss of membrane integrity), ▪ cell shrikage, ▪ no mitochondrial swelling	Primary necrosis • Accidental • Always pathological • Unregulated or poorly regulated • Plasma membrane destroyed early • Leakage of cell contact • Inflammation • Biochemical and morphological features include: ▪ swelling of the entire cytoplasma (oncosis), ▪ mitochondrial swelling Secondary necrosis • Cytolysis secondary to apoptosis when dying cells fail to b removed by heterophagy

PhotoDynanmic Therapy (PDT) is an approved treatment for a variety of cancers that can be exposed to a high flux of light – either white or a band centered at a particular

wavelength. Since PDT has been extensively reviewed (*3-6*), it is described only in broad terms here. The concept is that the patient is dosed with a photosensitizing dye and the specificity arises largely from the selective irradiation of target tissue with light in the visible region of the electromagnetic spectrum. Upon irradiation the dye becomes reactive and/or toxic, or it photosensitizes the formation of reactive and/or toxic species *in vivo*. The chromophores used in current technologies and those in the immediate pipelines are generally not selective for cancer tissue beyond what would be expected from the greater metabolism, and are generally believed to photosensitize the formation of singlet oxygen. Singlet oxygen then reacts with a variety of cellular components including, aromatic amino acids, double bonds in lipids, a variety of redox enzymes and cofactors, both the bases and the phosphate backbones of DNA and RNA, etc. The significantly reduced oxygen concentration that results from these reactions may be a significant cause of cell death as well. In general, the percentage of necrotic cells decreases and the percentage of apoptotic cells increases to a maximum and then decreases, as the concentration of the drug and the irradiation power decrease. The localization of the photodynamic agent in the cell depends exquisitely on the exact chemical structure of the dye and any covalently bound auxiliary motifs, and this topic has been well reviewed (*5, 7*). As illustrated below, the specific localization of the photodynamic chromophore dictates to a large extent the mode of cell death.

Of the vast number of reports on apoptosis (*2*), the induction of apoptosis by photodynamic treatment constitutes a small fraction (*7-9*). Cellular responses to photodynamic treatment depend on the cell type, the specific photosensitizer, the dosage of both photosensitizer and light, and other factors. The specific subcellular localizations

of the photosensitizer dictates the sites of primary photo damage, thus the apoptosis initiation point(s). To date, the photosensitizers used in PDT are found to localize mostly in the mitochondria, lysosomes, and cell membranes (Scheme 1). Concerning apoptosis, for example, after activation of the drug localized in the mitochondria membrane, the membrane integrity and/or potential of the mitochondria may be lost, which is followed by the release of cytochrome c to the cytosol. Cytochrome c, upon binding to apoptotic protease activating factor-1 (Apaf-1) and pro-caspase-9 (cystein aspartate-specific protease), activates the caspase. The activation of caspase-9 then triggers a cascade of proteases. The induction of the caspases also triggers a variety of other responses in the

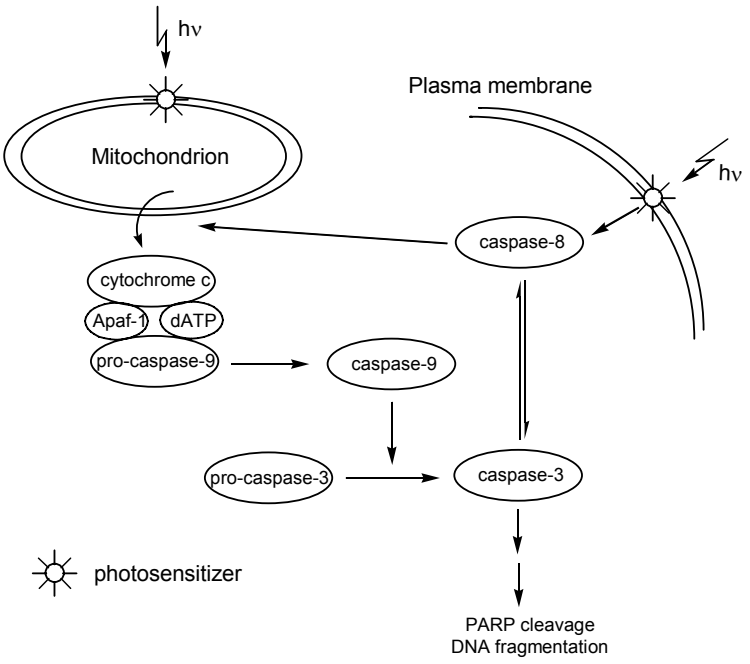

Scheme 1. Different pathways of photosensitizer-induced apoptosis.

cell via signaling pathways, such as chromatin condensation, DNA cleavage, and the cleavage of repair enzymes such as poly-(ADP ribose) polymerase (PARP). The detection of these activities is generally considered as biochemical markers of apoptosis. Release of cytochrome c from between the inner and outer membranes of the

mitochondria has been shown to accompany apoptosis in every circumstance with every cell line studied to date (*10*), though the mechanism of the release of this enzyme remains a topic of interest. The release of cytochrome c also interrupts the electron-transport chain, preventing oxidative phosphorlyation, promoting free radical production, and depriving the cell of ATP. Of the more than dozen caspases identified to date, most are expressed as proenzymes that are activated to pro-apoptotic stimuli (7). There are more than 100 caspase substrates identified, including proteins involved in cell cycle regulation, DNA repair such as PARP.

Hydrophobic photosensitizers preferentially bind the plasma membrane, and a number of signaling pathways, including apoptosis, may be induced at this level, though the mechanisms remain controversial (*9*). Apoptosis is rapidly induced at the plasma membrane level via activation of "death-inducing signaling complexes" (DISCs) that involve cell surface receptors such as Fas and tumor necrosis factor receptor (TNFR) (*9*). Several photosensitizers can localize in lysosomes, wherein the integrity of this membrane is compromised upon photodynamic treatment, and the release of lysosomal enzymes into the cytosol results. These proteolytic enzymes then initiate/cause cell death.

We previously reported that a tetraglucose-porphyrin conjugate (P-Glu_4) (Scheme 2) can be made in > 90% yield based on the starting meso-tetrakis(pentafluorophenyl)porphyrin ($TPPF_{20}$) and a thioglucose derivative, both of which can be made in large quantities and are commercially available (*11, 12*). The porphyrin-glucose bond of P-Glu_4 does not hydrolyze under physiological conditions because of the thio-linker is significantly less labile than the O-saccharide bond. Also reported was the observation that human breast cancer MDA-MB-231 cells preferentially

absorb tetraaryl porphyrins with four glucose moieties over the tetragalactose and several other hydrophilic porphyrin derivatives and possibly because of the increased expression of glucose receptors/transporters on this cancer cell line compared to healthy tissue. Doseametric studies reveal that these saccharide-porphyrin conjugates exhibit varying

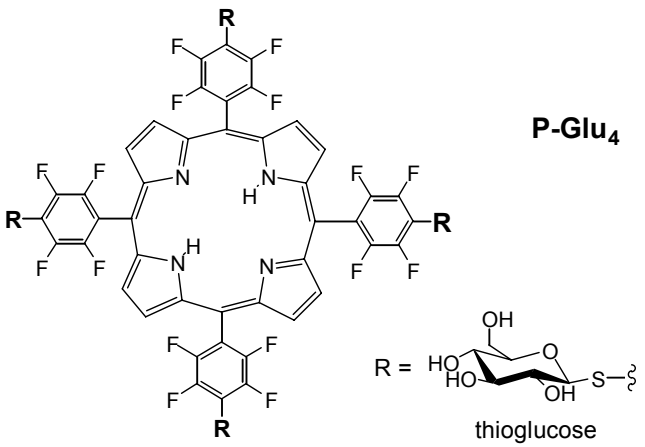

Scheme 2. Structure of P-Glu$_4$.

photodynamic responses depending on drug concentration and irradiation energy. (1) Using 20 μM conjugate and greater irradiation energy induces cell death by necrosis. (2) When 10-20 μM conjugate and less irradiation energy are used, both necrosis and apoptosis are observed. (3) Using 10 μM and the least irradiation energy, a significant reduction in cell migration is observed, which indicates a reduction in aggressiveness of the cancer cells.

Research on porphyrins with sugar moieties has been of great interest in the last decade. Glycosylated porphyrins can have greater water solubility than most naturally occurring and synthetic, *meso* substituted, porphyrins. This property can not only increase the efficacy of drug delivery but also assist the drug elimination from the organism after treatment. The proper lipophilicity of neutral saccharide conjugated porphyrins enable

them to permeate better in both lipophilic and hydrophilic biological structures. Furthermore, they can have specific interactions with proteins on cell membranes and thus exhibit specific targeting of cancer cells (*13*). 5,10,15,20-tetrakis-(4-1'-thio-glucosyl-2,3,5,6-tetrafluorophenyl)porphyrin (P-Glu_4) can be made in one or two steps in high yields (*14, 15*). Herein we report our investigations on the mode of apoptosis induced by P-Glu_4 in MDA-MB-231 breast cancer cells. Confocal microscopy indicates that at <10 μM the porphyrin binds predominantly to the mitochondria. The observations are (1) cytochrome c is released from the mitochondrial membrane, (2) pro-caspase-3 is cleaved, (3) the chromatin condensed, and (4) PARP is cleaved upon photodynamic treatment. These results are consistent with our hypothesis that glucosyl porphyrin conjugate (P-Glu_4) at least partially induces apoptosis through mitochondrial pathway. Other apoptosis pathways are also likely to be affected by the photodynamic treatment.

Results and Discussion

Photocytotoxicity

P-Glu_4 is a potent mediator of cell death for MDA-MB-231 cells in culture (*15*). Since cell death can be caused either directly by necrosis, or indirectly by initiating apoptosis (*1*), several assays were performed to delineate the extent of each. Cells were incubated for 24 hours with 10 μM P-Glu_4, the growth medium was exchanged to remove unbound porphyrin, and the cells were then irradiated with 0.94 mW cm^{-2} white light for 20 min (11.28 kJ m^{-2}). ~20% of the cells were necrotic immediately after photodynamic treatment (within the few minutes it takes to place them under a light contrast microscope, Figure 1A). Yet, these assays also revealed that the number of non-viable

cells continues to increase with time until nearly 100% 24 hours post irradiation, which implies that under these conditions a secondary process such as apoptosis is causing cell

A

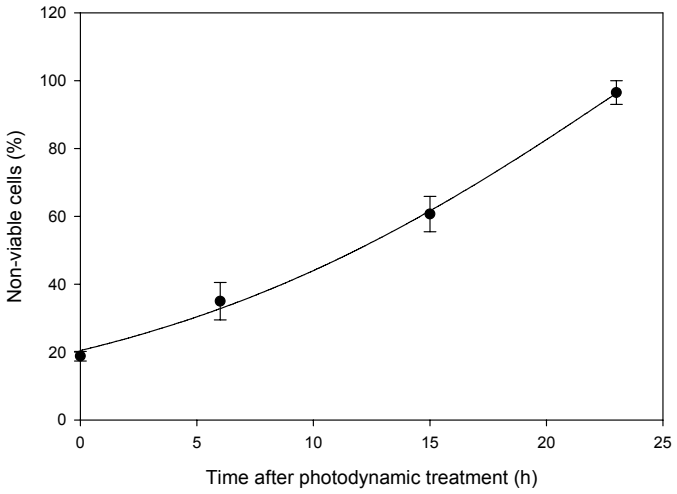

B

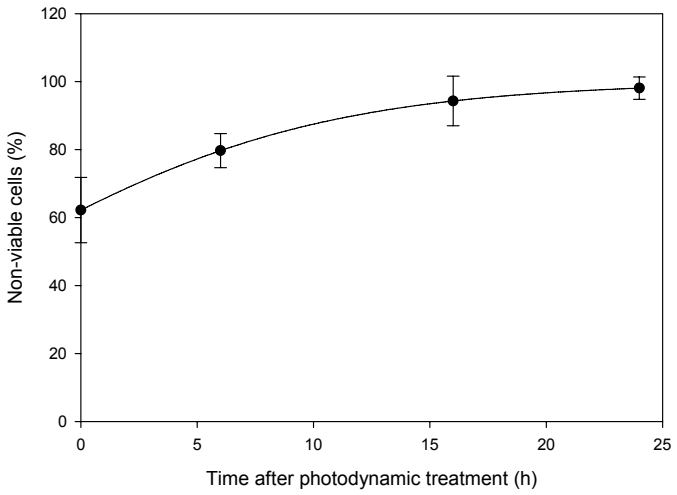

Figure 1. Photocytotoxic effects on human breast cancer MDA-MB-231 cells. Cells were treated with 10 μM (A) or 20 μM (B) P-Glu_4 for 24 hours, rinsed by exchanging the growth medium, and irradiated under a white 13W fluorescent light (0.94 mW cm^{-2} for 20 minutes; 11.28 kJ m^{-2}). The non-viable cells were counted with hemacytometer after staining with 0.4% w/v trypan blue at various lengths of time after photodynamic treatment.

death. When the porphyrin concentration was doubled to 20 μM, ~60% of the cells died from necrosis; and the non-viable cells reached 100% in 24 hours after photodynamic

treatment (Figure 1B). Control experiments show there is no significant effect without both light and the P-Glu_4.

Confocal fluorescence microscopy

MitoTracker Green® (Molecular Probes) is a dye specific to mitochondria and luminesces green when bound to mitochondria (*16*); while the P-Glu_4 porphyrin, as most free base tetraarylporphyrins, fluoresces in the red region. The combination of the two dyes allows an evaluation of the location of the glucosylated porphyrin in MDA-MB-231 human breast cancer cells. Cells on cover slips were incubated with 40 μM P-Glu_4 for 24 hours, rinsed with growth medium to remove unbound conjugate, and incubated with 40 nM Mitotracker Green in growth medium for 30 minutes. The cells were then treated with 4% paraformaldehyde in growth medium for 15 minutes and mounted. Figure 2 shows typical confocal fluorescence images of the MitoTracker Green fluorescence, the porphyrin fluorescence, and an overlay of the two images. The high concentration of the porphyrin is necessitated by the weak, ~10%, fluorescence of this compound (*15*). These experiments indicate that ~70% of P-Glu_4 is located at the mitrochondria, supporting our hypothesis that photodynamic treatment of cells with P-Glu_4 can induce apoptosis from the mitochondria.

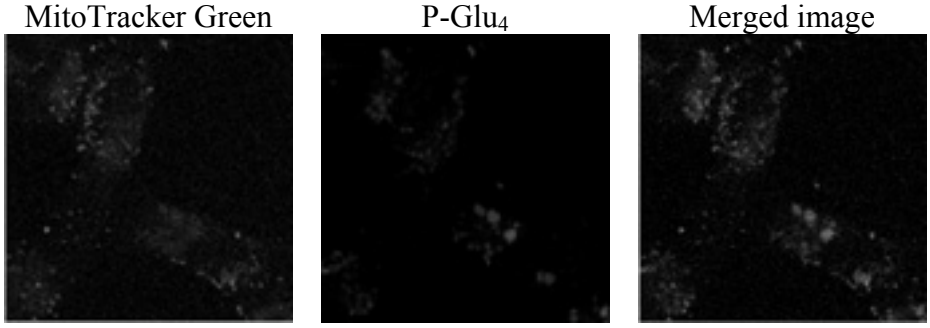

Figure 2. P-Glu_4 is partially localized in mitochondria in human breast cancer MDA-MB-231 cells. Cells were incubated with 40 μM P-Glu_4 for 24 hours, treated with 40 nM MitoTracker Green, rinsed and fixed with 4% paraformaldehyde solution. Confocal fluorescence images were taken under identical conditions.

Release of cytochrome c from the mitochondria to the cytosol

If the integrity of the mitochondrial membrane is compromised as a result of photodynamic treatment with porphyrins localized in this membrane, cytochrome c can be released to the cytosol, which in turn triggers caspase cascades and ultimately results in apoptosis. Though the mechanism of release remains under investigation, it has been demonstrated that two cytosolic proteins collaborate with cytochrome c to induce proteolytic processing and activation of caspase-3 in vitro. The MDA-MB-231 cells were treated with 8 μM of the glucose-porphyrin conjugate for 24 hours, rinsed, and irradiated for 30 minute or 60 minute durations with white light from a 13 W fluorescent bulb. Five hours later a mitochondria/cytosol fractionation kit (BioVision) was used to separate the cytosol from the mitochondria. Western blots of the cytosolic and mitochondrial fractions were then used to detect cytochrome c. These results show that mild photodynamic conditions with P-Glu_4 causes cytochrome c release from the mitochondria to the cytosol, which indicates that there is sufficient quantities of the porphyrin to disrupt the membrane integrity upon PDT (Figure 3).

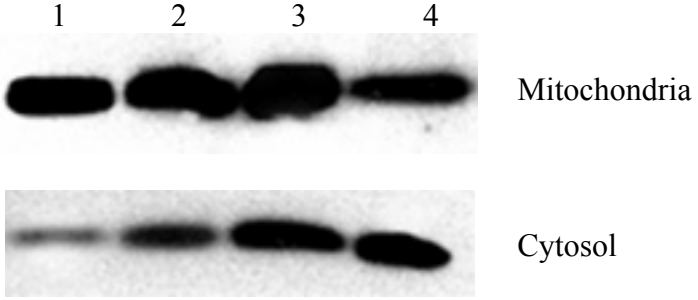

Figure 3. Cytochrome c release from mitochondria to cytosol. 0 or 4 μM P-Glu_4 was incubated with human breast cancer MDA-MB-231 cells for 24 hours and irradiated with 13W fluorescent white bulb for 30 or 60 min at 0.96 mW/cm^2 (17.28 or 34.56 kJ/m^2). 5 Hours later, mitochondria/cytosol fractionation kit was used to separate mitochondria and cytosol. The cytosol fractions were subjected to western blot to detect cytochrome c. Lane 1: control (no porphyrin, no light). Lane 2: control (4 μM porphyrin, no light) Lane 3: 4 μM porphyrin, 30min irradiation. Lane 4: 4 μM porphyrin, 60min irradiation.

Pro-caspase-3 cleavage/activation

Caspase-3 is activated during most apoptotic processes and is believed to be the main executioner caspase (*17*). Caspase-3 activation is essential for DNA fragmentation as well as chromatin condensation and plasma membrane blebbing (*18*). For these experiments the cells were treated with 0, 4, or 10 μM porphyrin conjugate, rinsed by exchanging the media, and irradiated for 20 or 40 minunte with white light. These experiments show that procaspase-3 is indeed cleaved to the active caspase after mild photodynamic treatment of MDA-MB-231 cells in the presence of P-Glu_4 (Figure 4).

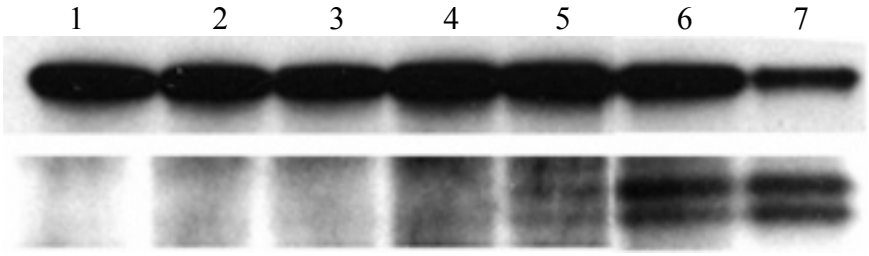

Figure 4. Detection of pro-caspase-3 cleavage. 0, 4 or 10 μM P-Glu_4 was incubated with human breast cancer MDA-MB-231 cells for 24 hours and irradiated with 13W fluorescent white bulb for 20 or 40 min at 0.96 mW/cm^2 (11.52 or 23.04 kJ/m^2). Seven hours later, cells were collected and lysed. The supernatant of the lysate was applied to a western blot to detect pro-caspase-3. Lane 1: control (no porphyrin, no irradiation). Lane 2: control (no porphyrin, 20 min irradiation. Lane 3: control (4 μM porphyrin, no irradiation). Lane 4: 4 μM porphyrin, 20 min irradiation. Lane 5: 4 μM porphyrin, 40min irradiation. Lane 6: 10 μM porphyrin, 20 min irradiation. Lane 7: 10 μM porphyrin, 40 min irradiation.

DAPI staining

To examine the morphological changes in the MDA-MB-231 chromatin after photodynamic treatment in the presence of P-Glu_4, DAPI (4'6-diamino-2-phenylindole)

staining experiments were used. DAPI binds to dA-T rich regions and is widely used as a DNA probe because of its large increase in fluorescence quantum yield upon DNA binding (*19*). The breast cancer cells were incubated with 10 μM P-Glu_4 for 24 hours, the growth medium exchanged to remove unbound porphyrin, and irradiated for 5 minutes at 0.84 mW cm^{-2} (2.52 kJ m^{-2}); these conditions are significantly milder than those used to induce necrosis. Eight hours after irradiation the cells were fixed with a 4% paraformaldehyde solution and stained with a 1 μg mL^{-1} DAPI solution. The blue DAPI fluorescence images of the photodynamic treated MDA-MB-231 cells, reveal that the nuclei are condensed and split compared to parallel control experiments (Figure 5). The observed condensed and split chromatin morphology is typical of apoptotic cells and further indicates that photodynamic treatment using low concentrations of the glucosylated porphyrin and low light irradiation is capable of inducing apoptosis.

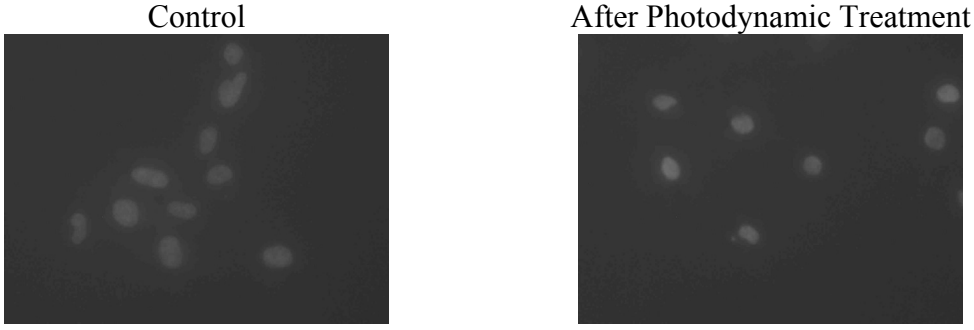

Figure 5. DAPI staining. 0 or 10 μM P-Glu_4 was incubated with human breast cancer MDA-MB-231 cells for 24 hours and irradiated for 5 min at 0.84 mW/cm^2 (2.52 kJ/m^2) 8 Hours after irradiation, cells were fixed with 4% paraformaldehyde and stained with 1 μg/ mL DAPI solution. Fluorescence images were taken under identical conditions.

PARP Cleavage

After the evidence of subcellular localization at mitochondria, cytochrome c release, pro-caspase-3 cleavage, and chromatin condensation described above, it was not

surprised to observe poly-ADP-ribose-polymerase (PARP) cleavage since these occur at the later stages of apoptosis. As shown in Figures 6, cell death is caused at least in part by apoptosis as indicated by a PARP cleavage assay. PARP is one of the best-examined targets of activated caspases and is a common indicator of the action of caspase-3 in apoptosis (*20*). PARP is a DNA repair enzyme whose expression is triggered by DNA-strand breaks. In cells undergoing apoptosis PARP is cleaved from a 113 kD peptide into 24 kD and 89 kD polypeptides. It appears plausible that cleavage of PARP facilitates the degradation of cellular DNA (*21*), which is a hallmark of apoptosis. Our PARP assay results demonstrate that apoptosis was induced in MDA-MB-231 cells by photodynamic treatment with P-Glu_4 (Figure 6).

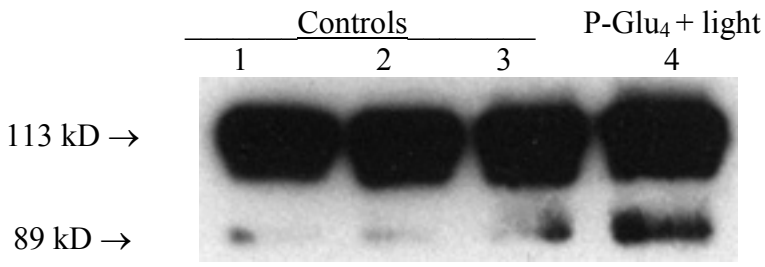

Figure 6. Detection of Poly-ADP-Ribose-Polymerase (PARP) cleavage in human breast cancer MDA-MB-231 cells as an indication of apoptosis. MDA-MB-231 cells were treated with 20 μM P-Glu_4 for 24 hours, irradiated with a 13W fluorescent light (0.27 mW cm^{-2} for 10 minutes; 1.62 kJ m^{-2}), and 9 hours after irradiation, cells were collected and lysed. The supernatant of the lysate was applied to a western blot to detect PARP cleavage. Lane 1: with no irradiation or P-Glu_4; Lane 2: with irradiation but no P-Glu_4; Lane 3: with P-Glu_4 but no irradiation; Lane 4: with P-Glu_4 and irradiation.

Discussion

The selectivity of the MDA-MB-231 cell line for P-Glu_4 over other conjugates such as P-Gal_4 can be understood in terms of the increased number of glucose transporters. The responses of this cell line differ dramatically depending on the dosage of both P-Glu_4 and light. While greater concentrations of this porphyrin and greater irradiation with white light leads directly to necrosis, lower concentrations and less light

lead to a delayed cell death predominantly by apoptosis. Since confocal microscopy data indicates that ~ 70% of the porphyrin absorbed by this cell line ends up localized at the mitochondria, and significant cytochrome c is observed in the cytosol after photodynamic treatment of MDA-MB-231 cells, it is reasonable to conclude that a significant fraction of the observed apoptosis is a consequence of the reduced integrity of the mitochondrial membrane. There are a variety of other cellular structures and/or functions that can serve as initiation points for the cascade of events that lead to apoptosis that can be affected by the remaining 30% of P-Glu_4 distributed throughout the cell. However, fluorescence microscopy indicates that little, if any, P-Glu_4 entered the cell nucleus (supporting information).

Conclusion

A two step method to make non-hydrolyzable saccharide-porphyrin conjugates in high yields using a tetra(pentafluorophenyl)porphyrin and the thio derivative of the sugar was reported (*15*). Since the S-saccharide bonds of the galactose (P-Gal_4) and xylose (P-Xyl_4) derivatives also do not hydrolyze under physiological conditions, and all three saccharide-porphyrin conjugates are robust under light because of the added oxidative stability imparted by the 16 fluoro groups, the $TPPF_{20}$ may be an ideal scaffold to build a variety of porphyrin-saccharide conjugates for diverse applications. The various causes of MDA-MB-231 cell death mediated by the glucosyl-porphyrin conjugate depend both on light energy and drug concentration; nonetheless the elimination of cancer cells, via any mechanism, is the goal. These results indicate that highly vasculated tissues near surfaces accessible to light irradiation that receive greater doses of both drug and light may be

eliminated by necrosis, whereas areas of the tumor that absorb less drug and are further away from the light source may be eliminated by apoptosis. Previous cell migration studies reveal that MDA-MB-231 cells are rendered less aggressive with yet less P-Glu_4 and lower light (*15*). Thus there is an array of responses by this breast cancer cell line that are elicited by this saccharide-porphyrin conjugate that depend on the amount of porphyrin absorbed and the amount of light reaching the cell.

Materials and Methods

Materials. All chemicals were purchased from Sigma-Aldrich. Dulbecco's Modified Eagle Medium (DMEM) and antimycotic for cell culture were obtained from GibcoBRL. Bovine calf serum was obtained from HyClone. PBS (136 mM NaCl, 2.6 mM KCl, 1.4 mM KH_2PO_4, 4.2 mM Na_2HPO_4) was obtained from Invetrogen. The 13W fluorescent bulb was from Sanco. The antibodies against PARP, cytochrome c, and pro-caspase-3 were from Cell Signaling Technology. The mitochondrial/cytosol fractionation kit was from BioVision, and MitoTracker Green was purchased for Molecular Probes.

Cell Culture. Cells were maintained in DMEM, 10% bovine calf serum, 1% antimycotic, at 37^0 C and 5% CO_2 atmosphere (12). For experiments ~2 x 10^5 cells mL^{-1} were seeded in cell culture plates and allowed to grow for 24 hours. For experiments involving the porphyrin saccharide conjugate, P-Glu_4 was added to the cells 24 hours prior to the experiments to allow it to be taken up by the cells.

Phototoxicity assays. Cell viability was quantified by trypan blue dye exclusion. After various experiments, cells were harvested with trypsin, a 0.4% w/v trypan blue solution added to the cells, and the mixture incubated at room temperature for 10

minutes. Cells that had taken up trypan blue were counted with a hemacytometer and considered non-viable.

Confocal Microscopy. Cells were plated onto cover slips in cell culture dishes. Porphyrins dissolved in methanol were added to the cultures to a final concentration of 40 μM. After incubation for 24 hours the cells were treated with MitoTracker Green in growth medium and incubated for 30 minutes under conditions outlined above. Cells were then washed twice with growth medium and incubated with a 4% paraformaldehyde solution in growth medium for 15 minutes at 37^0 C under cell growth conditions. Cells were then washed three times with PBS and mounted in Dako fluorescence mounting medium, and visualized using a Zeiss LSM510 laser scanning confocal microscope where images were captured. For MitoTracker green: excitation 488 nm, emission 505-550; for P-Glu_4: excitation at 488 nm, emission >585 nm. Since the 488 nm excitation hits an edge of the highest energy porphyrin Q band where $\varepsilon \approx 4.20 \times 10^3$ cm^{-1} M^{-1} which is 28.3-fold less than the MitroTracker green at this wavelength and the fluorescence quantum yield for P-Glu_4 is ~10%, higher concentrations of porphyrin are needed in the confocal experiments to obtain clear images.

Western blots. Cells were treated with porphyrin for 24 hours, rinsed and irradiated as described in the text. After a period of time appropriate for the given experiment, cells were washed with cold PBS twice before lysed with RIPA buffer (50 mM Tris-HCl, 1% NP40, 0.25% Na-deoxycholate, 150 mM NaCl, 1 mM EDTA, 1 mM PMSF, 1 μg mL^{-1} aprotinin, leupeptin, and pepstatin of each, 1 mM Na_3VO_4, and NaF of each). The lysates were gently rocked at 4^0 C for 25 minutes, centrifuged at maximum speed for 10 minutes, and the supernatant applied to a western blot (13). In the assay for

cytochrome c, the cytosol was further fractionated from the mitochondria with a kit designed for this purpose (purchased from Biovision) and both the cytosolic and mitochondrial fractions were examined by a western blot. Equal amounts of protein were adjusted into gel-loading buffer (50 mM Tris-HCl, pH 6.8, 100 mM dithiothreitol, 2% SDS, 0.1% bromophenol blue, 10% glycerol), and heated for five minutes at 100^0 C prior to separation by SDS-polyacrylamide (8%) gel electrophoresis. After transferring to nitrocellulose membranes (Osmonics), membrane filters were blocked overnight at 4^0C with 5% non-fat dry milk in PBS. The nitrocellulose filters were washed three times for five minutes in PBS with 0.05% Tween-20, before incubation with anti-cytochrome c, or anti-pro-caspase-3, or anti-PARP antibodies for one hour at room temperature. Anti-mouse IgG conjugated with horseradish peroxidase was used as a secondary antibody. The bands were visualized using an enhanced chemiluminescent detection system (Amersham).

DAPI Staining. Cells were placed onto cover slips in cell culture dishes. Porphyrins dissolved in methanol were added to the cultures to a final solution of 10 μM, and 24 hours later irradiated with white light from a 13 W fluorescent bulb with the energy stated in the text. The photodynamically treated cells were kept in the dark for eight hours, washed twice with PBS, and fixed with 4% paraformaldehyde solution in PBS for 20 minutes at room temperature (14, 15). The cells were then washed with PBS 5 times, permeablized by ice-cold methanol for 2 minutes, and blocked by DMEM with 10% bovine calf serum for 30 minutes at room temperature. Cells were incubated with DAPI (1 μg mL^{-1} in PBS) for 5 minutes at room temperature and washed three times. The cover slips were mounted in Dako fluorescent mounting medium, put onto slides, air

dried, and visualized using a Nikon Optiphot 2 fluorescence microscope where images were captured as high quality (>100kb) JPEG files.

Abbreviations

Apaf	apoptotic protease activating factor
Caspase	cysteine aspartate-specific proteases
PARP	poly(ADP-ribose)polymerase
DISCs	death-inducing signaling complexes
DAPI	4',6-diamidino-2-phenylindole
PBS	phosphate buffered saline
DMEM	Dulbecco's modified eagle medium
P-Glu_4	5,10,15,20-tetrakis (4,1'-thio-glucose-2,3,5,6-tetrafluorophenyl)porphyrin
$TPPF_{20}$	*meso*-tetrakis(pentafluorophenyl)porphyrin
PDT	photodynamic therapy
TNRA	tumor necrosis factor acceptor
RIPA	radioimmunoprecipitation
PMSF	phenylmethylsulfonylfluoride
EDTA	Ethylenediaminetetraacetate

References:

1. Kroemer, G., Dallaporta, B., and Resche-Rigon, M. (1998) The mitochondrial death/life regulator in apoptosis and necrosis, *Annu. Rev. Physiol. 60*, 619-642.
2. Lawen, A. (2003) Apoptosis-an introduction, *BioEssays 25*, 888-896.
3. MacDonald, I. J., and Dougherty, T. J. (2001) Basic principles of photodynamic therapy, *J. Porphyrins Phthalocyanines 5*, 105-129.
4. Sternberg, E. D., Dolphin, D., and Bruckner, C. (1998) Porphyrin-based photosensitizers for use in photodynamic therapy, *Tetrahedron 54*, 4151-4202.
5. Osterloh, J., and Vicente, M. G. H. (2002) Mechanisms of porphyrinoid localization in tumors, *J. Porphyrins Phthalocyanines 6*, 305-324.
6. Bonnett, R. (1995) Photosensitizers of the porphyrin and phthalocyanine series for photodynamic therapy, *Chem. Soc. Rev.*, 19-33.
7. Oleinick, N. L., Morris, R. L., and Belichenko, I. (2002) The role of apoptosis in response to photodynamic therapy: what, where, why, and how, *Photochem. Photobiol. Sci. 1*, 1-21.
8. Granville, D. J., and Hunt, D. W. C. (2000) Porphyrin-mediated photosensitization----Taking the apoptosis fast lane, *Curr. Opin. Drug Discovery Develop. 3*, 232-243.
9. Moor, A. C. E. (2000) Signaling pathways in cell death and survival after photodynamic therapy, *J. Photochem. Photobiol. B: Biol. 57*, 1-13.
10. Reed, J. C. (1997) Cytochrome c: Can't Live with It-Can't Live without It, *Cell 91*, 559-562.

11. Adler, A. D., Longo, F. R., Finarelli, J. D., Goldmacher, J., Assour, J., and Korsakoff, L. (1967) A simplified synthesis for meso-tetraphenylporphine, *J. Org. Chem. 32*, 476-476.

12. Lindsey, J. S., Schreiman, I. C., Hsu, H. C., Kearney, P. C., and Marguerettaz, A. M. (1987) Rothemund and Adler-Longo reactions revisited: synthesis of tetraphenylporphyrins under equilibrium conditions, *J. Org. Chem. 52*, 827-836.

13. Chen, X., and Drain, C. M. (2004) Photodynamic therapy using carbohydrate conjugated porphyrins, *Drug Design Review - Online 3*, in press, http://www.bentham.org/ddro/.

14. Pasetto, P., Chen, X., Drain, C. M., and Franck, R. W. (2001) Synthesis of hydrolytically stable porphyrin C- and S-glycoconjugates in high yields, *Chem. Commun.*, 81-82.

15. Chen, X., Hui, L., Foster, D., and Drain, C. M. (2004) Efficient synthesis and photodynamic activity of porphyrin-saccharide conjugates: targeting and incapacitating cancer cells, *Biochem. in press*.

16. Johnson, P. R., Dolman, N. J., Pope, M., Vaillant, C., Petersen, O. H., Tepikin, A. V., and Erdemli, G. (2003) Non-uniform distribution of mitochondria in pancreatic acinar cells, *Cell Tissue Res. 313*, 37-45.

17. Takahashi, A. (1999) Caspase: executioner and undertaker of apoptosis, *Int. J. Hematol. 70*, 226-232.

18. Kohler, C., Orrenius, S., and Zhivotovsky, B. (2002) Evaluation of caspase activity in apoptotic cells, *J. Immunological Methods 265*, 97-110.

19. Reddy, B. S. P., Sondhi, S. M., and Lown, J. W. (1999) Synthetic DNA minor groove-binding drugs, *Pharmacology & Therapeutics 84*, 1-111.

20. Yu, S.-W., Wang, H., Poitras, M. F., Coombs, C., Bowers, W. J., Federoff, H. J., Poirier, G. G., Dawson, T. M., and Dawson, V. L. (2002) Mediation of Poly(ADP-Ribose) Polymerase-1–Dependent Cell Death by Apoptosis-Inducing Factor, *Science 297*, 259-263.

21. de Murcia, G., and Menissier de Murcia, J. (1994) Poly(ADP-ribose) polymerase: a molecular nick-sensor, *Trends Biochem. Sci. 19*, 172-176.

Supporting Information

1. Fluorescence image of P-Glu_4 treated human breast cancer MDA-MB-231 cells. Note there is little, if any, P-Glu_4 entered the cell nucleus.

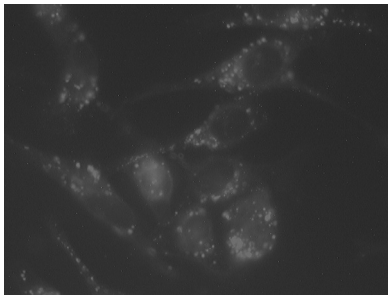

Chapter 4

Synthesis of a solution-phase combinatorial porphyrin library and selection by human breast cancer cells: New targets for Photodynamic Therapy

Abstract

High-yield, clean synthesis of solution-phase combinatorial libraries using porphyrin as the core structure are presented. The libraries feature a non-hydrolysable thioether linkage between the macrocycle and the substituents. A proof-of-principle selection method using human breast cancer cells, and MALDI-MS is also reported.

Introduction

Combinatorial chemistry is a useful tool to discover, optimize or assign molecular properties, particularly ones that are difficult to design a priori. It is based on efficient, parallel synthesis, in that many more chemical compounds can be generated in a library than the number of steps used in the synthesis. This approach to organic synthesis is in contrast to traditional organic chemistry for the past 100 years, in which several synthetic steps are designed to maximize the production of only one compound. The roots of combinatorial organic synthesis stem from the development of solid-phase peptide synthesis in 1960s (*1-3*). In past 2 decades combinatorial chemistry, linked to high-throughput screening techniques, has been developed into a powerful technology for the drug discovery process and has resulted in variety of biologically active agents (*4*).

Combinatorial libraries can be generated in a spatially separated format (solid-phase) or as pooled mixtures (solution-phase), among which the solid-phase method is obviously more straightforward in identifying active compounds. However, the

fundamental problem with this approach is that, generally, solid-phase libraries miss the synergistic effects exhibited by several compounds on systems with multiple targets. Though with disadvantages in purification, characterization and selection, other key advantages (*4*) of solution-phase combinatorial approaches include the following: (1) Unlimited number of reactions can be used, which provide maximal structural diversity. (2) Sufficient product quantities can be achieved for follow-up and different bio-assays since there is no limitation of reaction scale. (3) There is no need of large excesses of reagents and solvents that are usually required in solid-phase synthesis. (4) No need for linker management (attachment or detachment from resin). (5) Solution-phase libraries are easy to develop and monitor. Though less developed than solid-phase library synthesis, the ease of preparation and early success ensure the continuation in this field (*5*). In general, high-yielding and clean reactions are the basic requirements to develop solution-phase combinatorial libraries.

Compared to linear structured libraries, core-structured libraries are less developed. Rebek, Jr. and coworkers reported the first core-structured solution-phase libraries (*5*) using rigid core molecules as scaffolds or templates to discover a competitive inhibitor for trypsin.

As already mentioned above, purification of solution-phase libraries continues difficult. There have been different ways to tackle this problem. When there is a high yield synthesis and the impurities are inert in the following bio-assay, the libraries are usually subjected to the selection step directly without any purification. A number of methods have been developed including liquid-phase (*6*), fluorous-phase (*7*) reactions, ion exchange (*8*), and high performance liquid chromatography (HPLC) systems (*9*).

There are also cases using “scavenger reagent” (*10*), “sequestration enabling reagent” (SER) (*11*) or impurity annihilation strategy (*12*), depending on the chemical structures of the impurities.

Most characterizations of solution-phase libraries highly depend on mass spectrometry (MS), including electrospray ionization (ESI) or matrix-assisted laser desorption ionization (MALDI) since they generally produce fragmentation-free spectra with a pseudomolecular ion peak for every component (*13, 14*). Other efficient analytical methods such as NMR spectrometry, capillary electrophoresis, micro HPLC, etc. also applied to the characterization of libraries (*15, 16*). These methods may be performed on isolated fractions or directly to the entire library mixture.

Selection methods of the solution-phase libraries vary due to different bio targets (*17-19*). Usually the original libraries are divided to sublibraries by synthetic steps or by HPLC fractionation; those sublibraries or fractions with high bioactivities are reproduced and individual compounds are tested for their activity.

More recently, dynamic combinatorial chemistry (DCC) has been used to create virtual combinatorial libraries (VCLs) (*20*). VCLs are constructed using reversible covalent or coordinating bonds in the present of the target. The presence of the target shifts the equilibrium towards the formation of a given set of library members. The products of the target-directed synthesis are then “locked together by a reaction that makes the linking bonds irreversible, or less reversible. Examples include inhibitors of carbonic anhydrase (*21*) or receptors for guests (*22*).

Porphyrins are tetrapyrrole macrocycles, and porphyrin derivatives are considered excellent candidates in drug discovery as anticancer (*23-28*), antimicrobial (*29*), antiviral

(*30, 31*) theraputics, because of their potential uses as mediators of Photodynamic Therapy. The use of porphyrins in combinatorial synthesis for drug discovery is not well developed (*14*). Our laboratory reported the first solution-phase combinatorial porphyrin libraries (*13*), with organic substituents designed to impart the members with a variety of properties for binding biological components. Herein, we present core-structured solution-phase combinatorial porphyrin libraries using a new synthetic strategy and a new class of substituents – saccharides.

Saccharide-appended porphyrins are very promising PDT agents (*32-34*). Both the importance of carbohydrate-conjugated porphyrins in PDT and the advantages of using S-glycoporphyrins are discussed in previous chapters.

Results and Discussions

Synthesis of initial library

The synthesis uses *meso*-tetrakis(pentafluorophenyl)porphyrin ($TPPF_{20}$), because it can be made in large quantities and is commercially available. Because of the high reactivity of the *para* fluoro group to nucleophilic attack, thio compounds are readily substituted under mild conditions (*35, 36*). When $TPPF_{20}$ (1 equiv.) is stirred with 2,3,4,6-tetra-O-acetyl-glucosylthioacetate (1.4 equiv.), 2,3,4-tri-O-acetyl-xylosylthioacetate (1.4 equiv.), 4-mercaptopyridine (1.4 equiv.) and diethylamine (20 equiv.) at room temperature in DMF for 24 hours, a 21-membered library with acetyl-protected sugars was obtained (Scheme 1). ESI-MS spectra indicated all the peaks correspond with those predicted from the simulated spectrum (Figure 1). Deprotection of the sugars used an equal molar ratio of NaOMe to the acetate protecting groups and it

was quantitative. Since ESI-MS does not give high-quality spectra of the free sugar libraries, MALDI-MS is used. The peaks in MALDI spectra are also consistent with the peaks in simulated spectra (Figure 2). In both cases, there are satellite peaks 23 mass

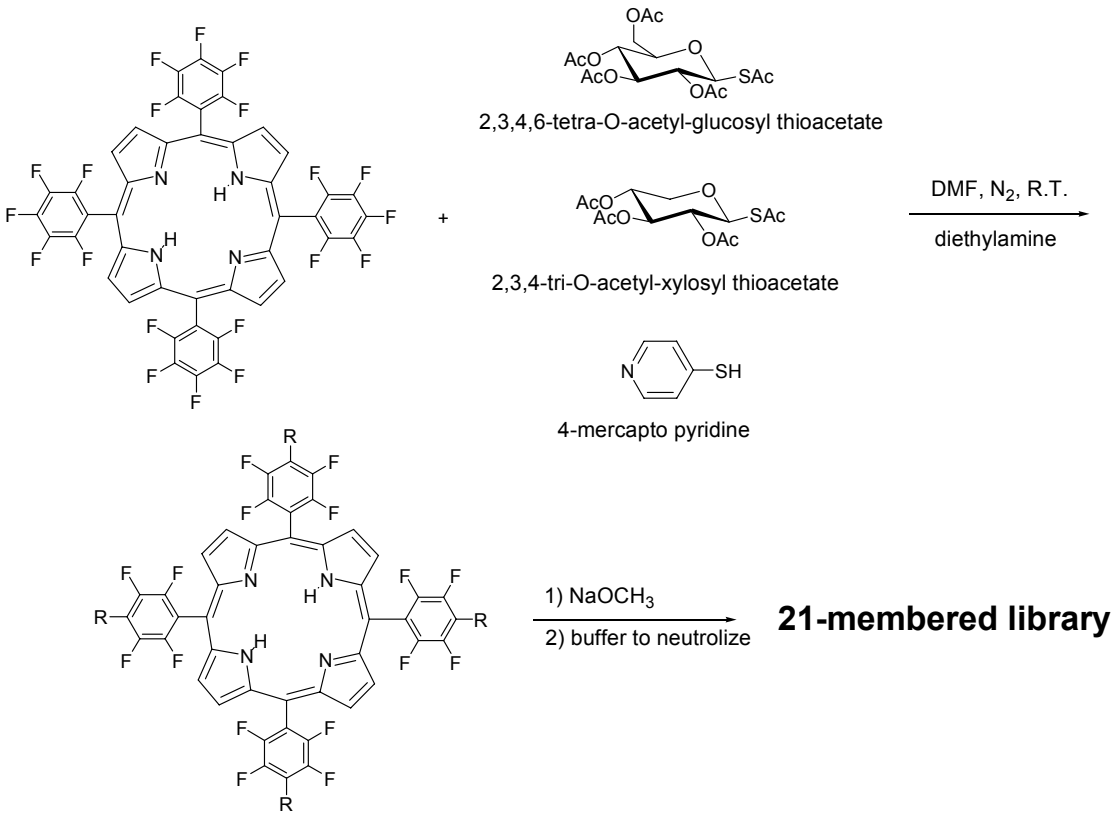

Scheme 1. Synthesis and deprotection of solution-phase 21-membered S-glycoporphyrin combinatorial library.

units greater than the parent peaks, and Na+ adducts are often formed for sugars in mass spectrometry. This accounts for the small differences between the simulated spectra and the experimental spectra. The reaction scheme is general to large number of sugars and molecules having a thiol or thioacetate. Using the same strategy, we have produced 406-membered library with 7 thio-substituted sugars and other thiols (supporting information).

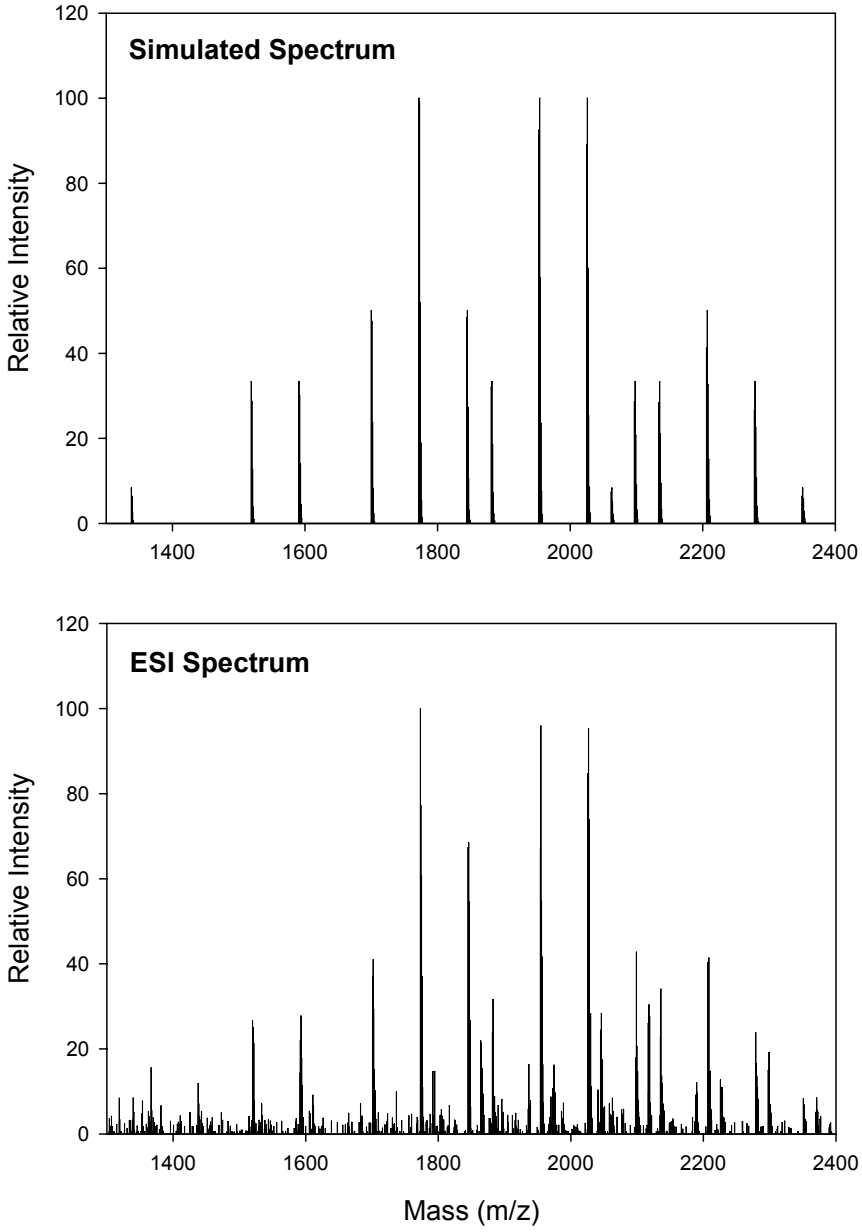

Figure 1. Simulated (top) and experimental ESI-MS (bottom) spectra of 21-membered library with acetyl protected sugar moieties. The actual ESI-MS spectrum is representative of more than 3 separate preparations.

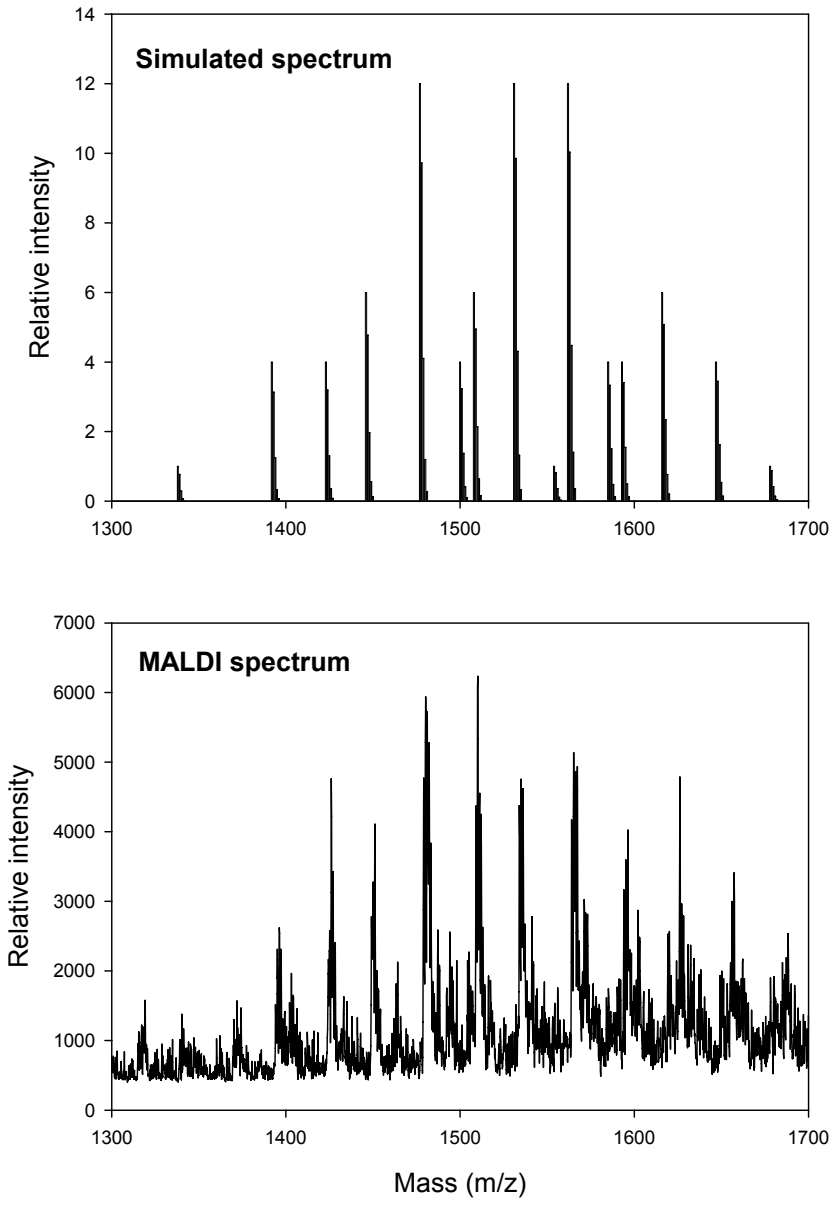

Figure 2. Simulated (top) and experimental MALDI-MS (bottom) spectra of 21-membered library with unprotected sugar moieties. The MALDI-MS spectrum is representative of more than 3 separate experiments.

Selection from human breast cancer (MDA-MB-231) cells.

Although there are many potential applications at present, the primary use of porphyrinoids in PDT is for macular degeneration and for cancer. For some applications, such as for the treatment of cancer, one goal is to kill or eliminate cells by any means that targets the diseased cells over healthy tissues. Thus, when elimination of the entire cell is the goal, there are a variety of cellular processes and components that can be targeted.

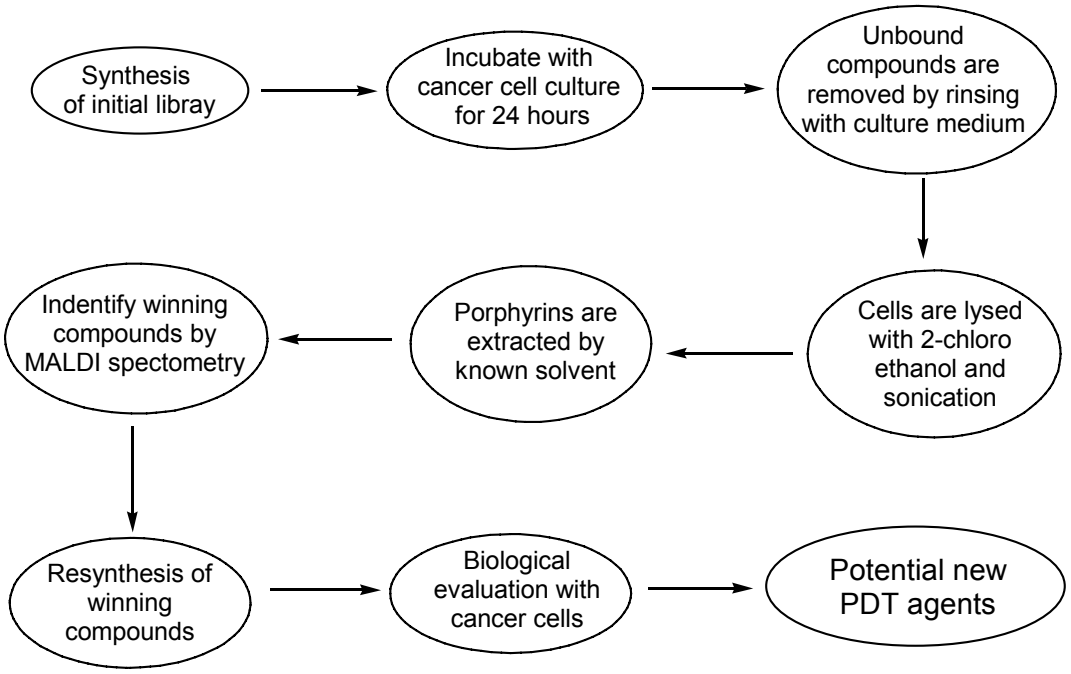

Scheme 2. Strategy of selection method from human breast cancer (MDA-MB-231) cells.

Since most crucial cellular processes have various repair mechanisms, it may be preferable to target more than one, or even many, parts of the cell to maximize the probability of killing it. Rather than specifically targeting a particular cellular component or process, designing a molecule or a class of molecules and testing them for PDT efficacy, we hypothesized that the cells themselves may indicate what bind(s) most efficiently. We have designed an assay where human breast cancer (MDA-MB-231) cells themselves select molecules with high affinities to the cells. The strategy is shown in

Scheme 2. After incubation of the library mixture with the cells, the cells were rinsed and collected. 2-Chloroethanol was added, followed by sonication and evaporation of the solvents. Porphyrins selected by the cancer cells were extracted back by methanol (in which the library was initially dissolved) and subjected to MALDI-MS. Eight winning compounds were identified by four peaks (each with 2 isomers) in MALDI spectrum (Figure 3). The low signal to noise ratio formed in the cell extract spectra is largely due to both instrumental noise and some small amount of compounds extracted with the porphyrins. No attempt was made to purify the porphyrins from the cell extract to avoid losing or missing some compounds from the already dilute and small volume of the mixture. The total amount of porphyrins extracted from the cancer cells, as estimated by ultraviolet-visible (UV-VIS) spectra is typically on the order of 10μg/0.2mL. At this stage of the research program, we do not know if there are any bio-conjugated porphyrins present which would manifest themselves as species with unknown molar mass. Two major peaks and two minor peaks were successfully identified. No attempt was made to identify the small peaks that are not from the initial library, since there are a number of possibilities from the cancer cell itself.

A

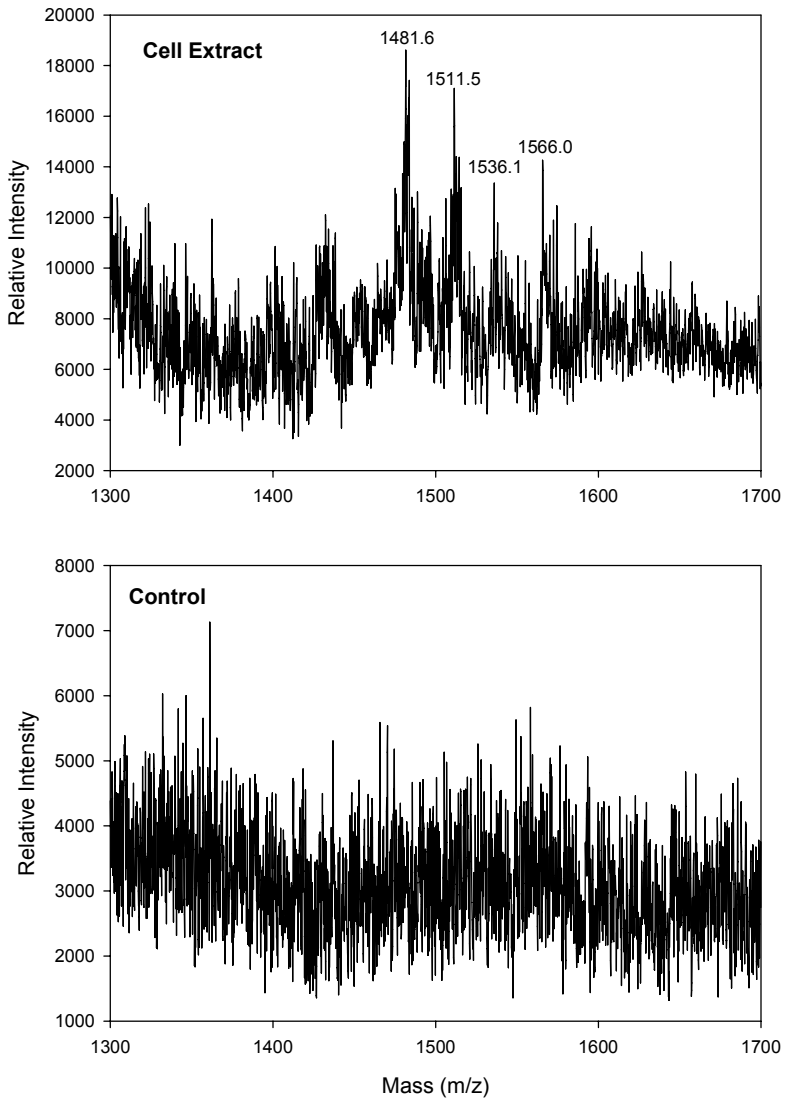

Figure 3A. Selection of winning compounds from human breast cancer (MDA-MB-231) cells. MALDI-MS spectra of cell extract with library and control. The spectra are representative for more than 3 separate experiments.

B

Winning Compounds

Major Peaks:

Mass	R	
1481.6	Glu / Xyl / Py / Py	2 isomers
1511.5	Glu / Glu / Py / Py	2 isomers

Minor Peaks:

Mass	R	
1536.1	Glu / Xyl / Xyl / Py	2 isomers
1566.0	Glu / Glu / Xyl / Py	2 isomers

Figure 3B. Winning compounds determined by molecular weights.

C

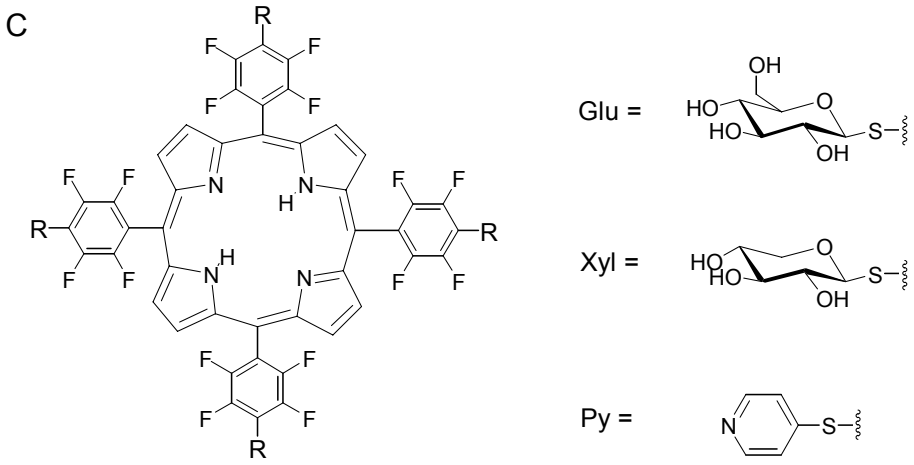

Figure 3C. The structures of winning compounds.

Resynthesis of winning compounds

Compounds Glu/Glu/Py/Py (2 isomers) was chosen to be the representatives as the winning compounds. As shown in Scheme 3, the synthesis of the 2 compounds is

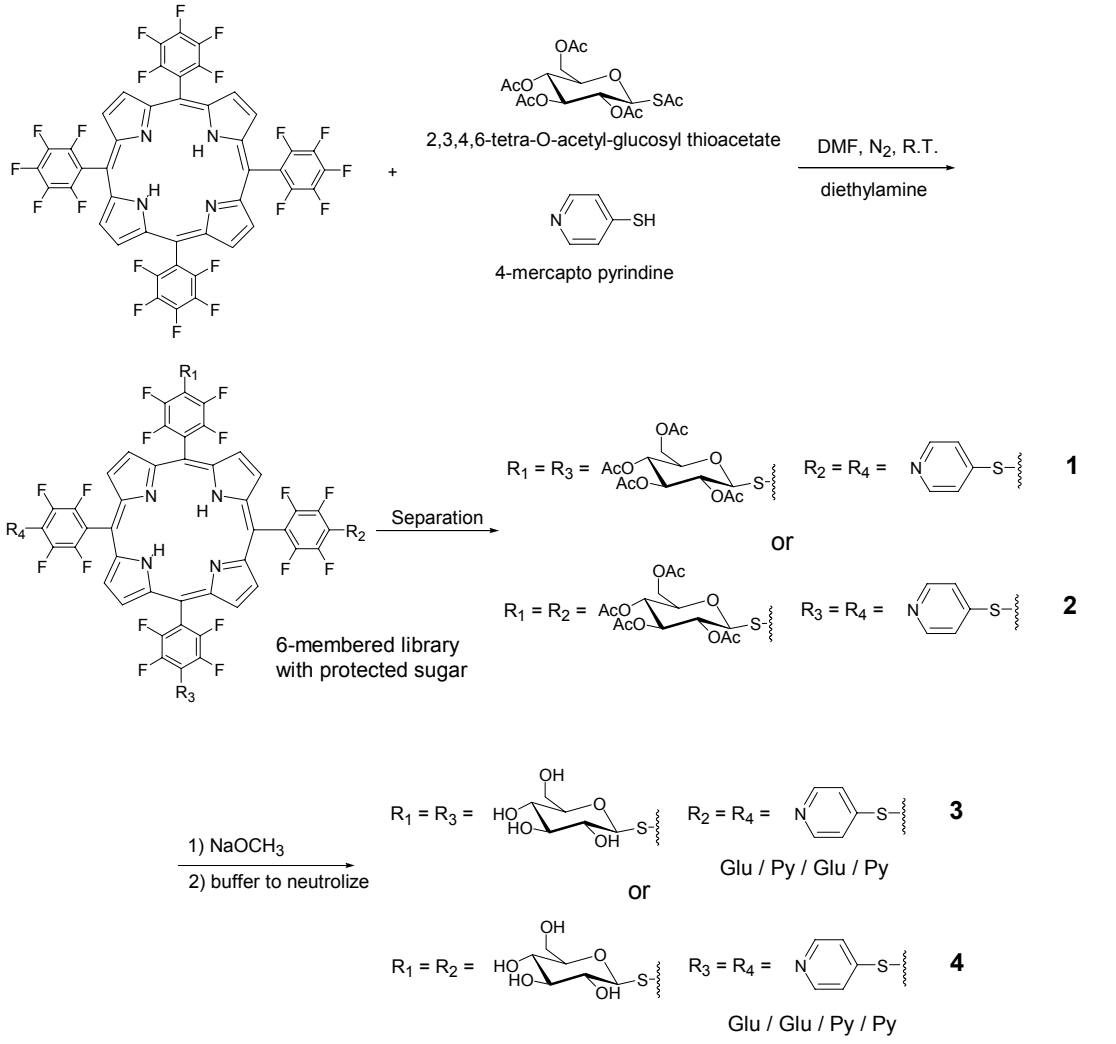

Scheme 3. Synthesis of winning compounds.

straightforward. $TPPF_{20}$ (1 equiv.) stirred with 2,3,4,6-tetra-O-acetyl-glucosylthioacetate (2 equiv.), 4-mercaptopyridine (2 equiv.) and diethylamine (20 equiv.) at room temperature in DMF for 24 hours, a 6-membered library with acetyl-protected sugars was obtained. The members of this small library are separated by silica gel column and preparative TLC to obtain the protected *trans*-isomer 5,15-di-(4-1'-thio-2',3',4',6'-O-

acetyl-glucosyl-2,3,5,6-tetrafluorophenyl)-10,20-di-(4-4'-thiopyridyl-2,3,5,6-tetrafluorophenyl)porphyrin (**1**) and the *cis*-isomer 5,10-di-(4-1'-thio-2',3',4',6'-O-acetyl-glucosyl-2,3,5,6-tetrafluorophenyl)-15,20-di-(4-4'-thiopyridyl-2,3,5,6-tetrafluorophenyl)porphyrin (**2**) (Scheme 3). Deprotection with 8 equivalents NaOMe yields the free sugars quantitatively to obtain the deprotected *trans*-isomer 5,15-di-(4-1'-thio-glucosyl-2,3,5,6-tetrafluorophenyl)-10,20-di-(4-4'-thiopyridyl-2,3,5,6-tetrafluorophenyl)porphyrin (**3**) and *cis*-isomer 5,10-di-(4-1'-thio-glucosyl-2,3,5,6-tetrafluorophenyl)-15,20-di-(4-4'-thiopyridyl-2,3,5,6-tetrafluorophenyl)porphyrin (**4**) (Scheme 3). The solutions were then neutralized by pH 7.2 ammonium acetate buffer.

Under the conditions used for the cell selection assay, the lowest concentration of a member of the library was ~1μM and the highest was ~10μM (see Table 1). There are six sets of isomeric compounds denoted as *cis* (5,10-meso substituted) and *trans* (5,15-meso substituted). Each isomer of course having the same molar mass, but present in the library in different amounts that are in principle dictated solely by the statistics of library formation. The MALDI spectra of the cell extracts cannot differentiate between *cis* and *tran*s isomers. The MALDI peaks are assigned as "major" and "minor" based on their intensity. The notable results include: (1) only 4 peaks are observed corresponding to 8 possible compounds; (2) the major peak is assigned to the cis and trans isomers of Glu Glu Py Py, which are of average amounts in the library (not the highest concentrations)

Table 1. Abundance of each compound in the 21-membered library.

R	% in library	% of cis-isomer	% of trans-isomer
Py / Py / Py / Py	1.23	/	/
Py / Py / Py / Xyl	4.94	/	/
Py / Py / Py / Glu	4.94	/	/

Py / Py / Xyl / Xyl	7.41	4.94	2.47
Py / Py / Glu / Xyl	14.81	9.88	4.94
Py / Py / Glu / Glu	7.41	4.94	2.47
Py / Xyl / Xyl / Xyl	4.94	/	/
Py / Glu / Xyl / Xyl	14.81	9.88	4. 94
Py / Glu / Glu / Xyl	14.81	9.88	4.94
Xyl / Xyl / Xyl / Xyl	1.23	/	/
Py / Glu / Glu / Glu	4.94	/	/
Glu / Xyl / Xyl / Xyl	4.94	/	/
Glu / Glu / Xyl / Xyl	7.41	4.94	2.47
Glu / Glu / Glu / Xyl	4.94	/	/
Glu / Glu / Glu / Glu	1.23	/	/

Affinities of cis- and trans-isomers toward human breast cancer MDA-MB-231 cells

Affinities of winning compounds as well as a tetra-glucose porphyrin control (synthesis as previous reported (*37*)) toward human breast cancer MDA-MB-231 cells were investigated by fluorescence microscopy. Cells cultured under the same conditions on glass cover slips were incubated with 10 μM of the porphyrin derivatives under identical conditions. After rinsing the unbound compounds from the cells on the cover slips and fixing the cells, fluorescence images of the cells were taken on the same day of fixing and one week later. The observed fluorescence intensity was taken to be proportional to the quantity of porphyrin bound to the cells, and was quantified by comparing the integrated RGB vectors for identical areas (see experimental procedures).

The images in Figure 4A clearly show that the affinity of *cis*-isomer (**4**, Glu/Glu/Py/Py) toward the cancer cells is at least 2-fold greater than the affinity of *trans*-isomer (**3**, Glu/Py/Glu/Py). The *cis*-isomer (**4**) has a structure with the two glucose groups on the adjacent *meso*-phenyl groups on the porphyrin, while the two glucosyl moieties are on the opposite sides of the porphyrin in the *trans*-isomer (**3**). Thus, the *cis*-compound is more likely to distribute into both the polar head group and the non-polar

tail of the cell membrane, due to its well-separated polar and non-polar groups. When cells are treated with the *cis* and *trans* isomer (**4** and **3**) for 24 hours, rinsed, and fixed, little fluorescence is observed by fluorescence microscopy just after fixing the cells (Figure 4B). Cells treated with P-Glu_4 under the same conditions brightly luminesce. However, when the same slides bearing the cells treated with **3** and **4** are re-examined one weak later, the fluorescence micrographs show a large increase in luminescence (Figure 4A). Since the cells were rinsed to remove unbound porphyrins, no further uptake of porphyrin is possible.

A. Fluorescence images taken one week after fixing the cells:

Cis-isomer (**4**) Trans-isomer (**3**) P-Glu_4

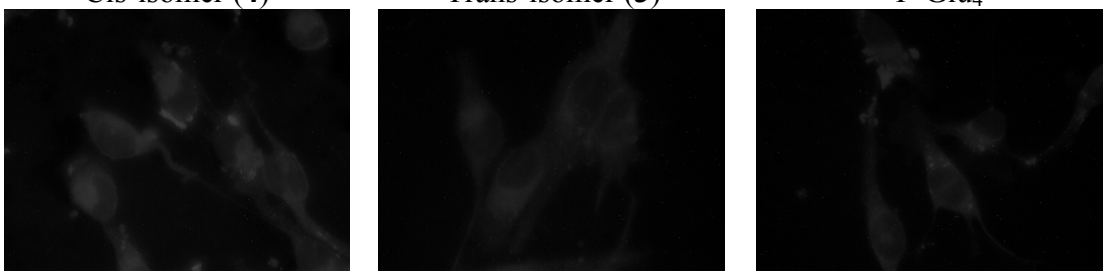

B. Fluorescence images taken the same day of fixing the cells:

Cis-isomer (**4**) Trans-isomer (**3**) P-Glu_4

Figure 4. Different affinities of winning Glu_2Py_2 compounds cis- (**4**) and trans- (**3**) isomers toward human breast cancer MDA-MB-231 cells assayed by fluorescence images and compared with the tetra-glucose porphyrin (10 μM incubated with cells followed by rinsing and fixing the cells). Images were taken a week after fixation (A) and the same day of fixation (B). (See supporting information for other concentrations tested.

These results suggest that the *cis*- and *trans*-isomers bind and/or enter the cells as aggregates which have quenched fluorescence. This hypothesis is supported by comparing the UV-VIS spectra of *cis*- and *trans*-isomers in CH_3OH/DME (1:1) and in DMEM (cell growth medium) without phenol red (Figure 5). The peak-width broadening and the splitting of the Soret band of both porphyrins in DMEM are clear indications that these porphyrins aggregate in aqueous solution. During a period of one week, the aggregates likely dissemble and the porphyrins diffuse into different parts of the cell and no longer quench each other, therefore much brighter fluorescence images are observed. The aggregates are 30 to 130 nm in diameter by dynamic light scattering in water. The absorbtion of nanoparticles by cells has been well documented (*38, 39*). Thus it is reasonable to hypothesize that nanoparticles/aggregates of compound **3** or **4** are formed in the cell culture medium wherein their fluorescence is quenched by well-understood mechanisms (*40, 41*). Once absorbed by the cells, the nanoparticles slowly de-aggregate due to interactions with various cellular components, which is manifested by the observed increase in fluorescence intensity. The cells may take up the smaller nanoparticles preferentially. Clinically, these results may indicate a delay between dosing and irradiation.

A

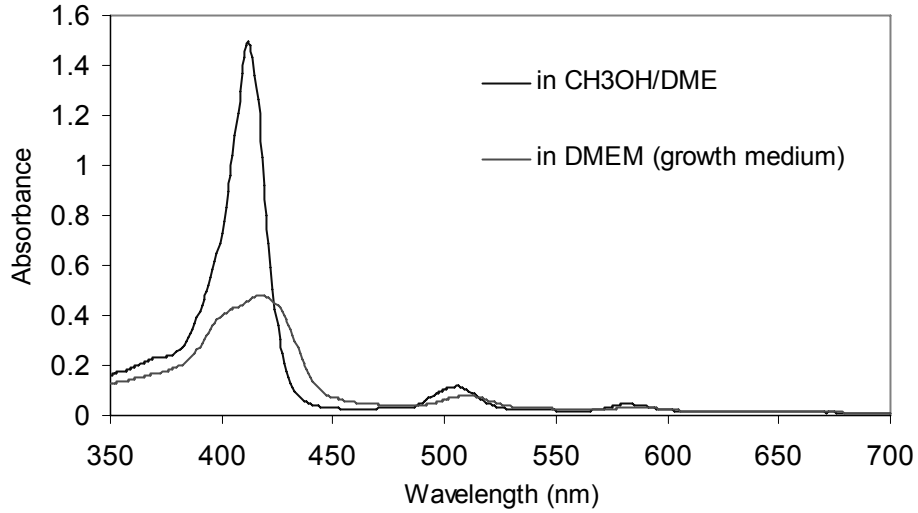

B

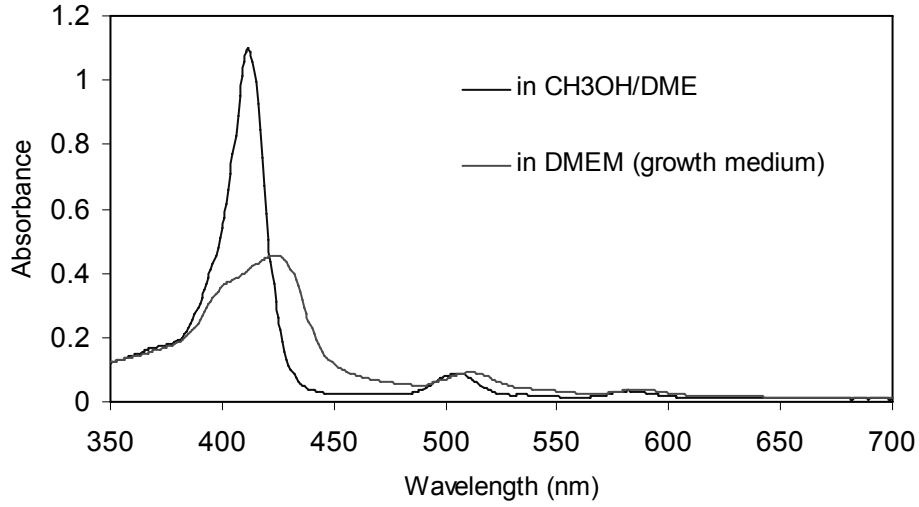

Figure 5. The UV-VIS spectra of 10 μM (A) cis-isomer (**4**) and (B) trans-isomer (**3**) in CH_3OH/DME (organic solvent) and growth medium DMEM (aqueous solution).

Conclusion

A proof-of-principle method using human breast cancer MDA-MB-231 cells to select winning compounds from a 21-membered porphyrin-cored solution-phase

combinatorial library is presented. The porphyrin library bearing carbohydrate moieties is synthesized in solution phase. After applying the library mixture in cultured cells, the winning compounds, selected by the cells, are identified by MALDI mass spectrometry and individual porphyrins showed high affinities toward human breast cancer cells.

Experimental Procedures

Synthesis of 21-membered porphyrin library

A mixture of $TPPF_{20}$ (30 mg, 30.8 μmol), 2,3,4,6-tetra-O-acetyl-glucosylthioacetate (17.1 mg, 42.1 μmol), 2,3,4-tri-O-acetyl-xylosylthioacetate (14.1 mg, 42.1 μmol), 4-mercaptopyridine (4.7 mg, 42.1 μmol) and diethylamine (63.6 μL, 616 μmol) were stirred in DMF in the dark under nitrogen at room temperature for 24 hours. Solvent was evaporated and the library was subjected to ESI-MS without purification. The library (5 mg, 2.87 μmol) was stirred with sodium methoxide (53.5 μL of 0.5 M in CH_3OH, 2.87 μmol) in dry 10 mL CH_3OH/CH_2Cl_2 (9:1) for 1 hour and followed by neutralization with a pH 7.2 ammonium acetate buffer. A large excess of $NaOCH_3$ should be avoided as it partially cleaves the porphyrin-saccharide conjugate. The solvents were evaporated and the library was subjected to MALDI-MS.

Extraction of 21-membered library from human breast cancer (MDA-MB-231) cells

The 21-membered library (6.74 mM) dissolved in 144 μL CH_3OH was added to 10 mL culture medium in a 100 mm cell culture dish to make a final concentration of 100 μM. 24 Hours later, the cells were rinsed with medium to wash off any unbound porphyrins and collected with a rubber policeman and 0.5 mL distilled water; a second collection is make using the same procedures. 1.5 mL 2-Chloroethanol was added to the

mixture. The vial was put in ice and sonicated for 1.5 minute. Solvents were evaporated and 300 μL of CH_3OH was added. The mixture was centrifuged and the supernatant was collected. The solvent was evaporated again and 100 μL of CH_3OH was added. The mixture was centrifuged again; the supernatant was collected and submitted to MALDI-MS.

Cell culture

Cells were maintained in Dulbecco's Modified Eagle Medium (DMEM), 10% bovine calf serum, 1% antimycotic at 37^0C and in 5% CO_2 atmosphere (*42*). For experiments, $2x10^5$ cells/mL were seeded in cell culture plates and then allowed to grow for 24 hours.

Synthesis and characterization of winning compounds

5,15-di-(4-1'-thio-glucosyl-2,3,5,6-tetrafluorophenyl)-10,20-di-(4-4'-thiopyridyl-2,3,5,6-tetrafluorophenyl)porphyrin (**3**) and 5,10-di-(4-1'-thio-glucosyl-2,3,5,6-tetrafluorophenyl)-15,20-di-(4-4'-thiopyridyl-2,3,5,6-tetrafluorophenyl)porphyrin (**4**). A mixture of $TPPF_{20}$ (30 mg, 30.8 μmol), 2,3,4,6-tetra-O-acetyl-glucosylthioacetate (25.0 mg, 61.6 μmol), 4-mercaptopyridine (6.8 mg, 61.6 μmol) and diethylamine (63.6 μL, 616 μmol) were stirred in DMF in the dark under nitrogen at room temperature for 24 hours. The resulting mixture was subjected to a 2 x 20 cm silica gel column using 0 – 3% gradient of methanol in methylene chloride as eluent, followed by preparatory thin layer chromatography using 5% methanol in methylene chloride as eluent to obtain the glucose protected *trans*- (**1**) and *cis*- isomer (**2**) with yields of 6.9 % and 10.0%, respectively. **1** or **2** (5mg, 2.7 μmol) was treated with 8 equivalents $NaOCH_3$ at room temperature in 9:1 v/v

solution of methanol/methylene chloride for 1 hour to afford **3** or **4** in quantitative yield (Scheme 3). The products were neutralized by pH 7.2 ammonium acetate buffer.

5,15-di-(4-1'-thio-2',3',4',6'-O-acetyl-glucosyl-2,3,5,6-tetrafluorophenyl)-10,20-di-(4-4'-thiopyridyl-2,3,5,6-tetrafluorophenyl)porphyrin (**1**)

^{1}H-NMR (300MHz, CD_2Cl_2): δ = 9.07 (s, β pyrrole, 8H), 8.63 (m, 2',6'-pyridyl, 4H), 7.40 (m, 3', 5'-pyridyl, 4H), 5.38 (d, J=7.69Hz, 1'-glucosyl, 2H), 5.24 (m, 2',3',4'-glucosyl, 6H), 4.31 (s, 6'-glucosyl, 4H), 3.93 (m, 5'-glucosyl, 2H), 2.22 (s, OAc×2, 6H), 2.07 (s, OAc×6, 18H), -2.88 (s, pyrrole NH, 2H).

ESI-MS (calcd. for $C_{82}H_{56}N_6O_{18}S_4F_{16}$: 1844) *m/z* found (rel. intensity): 1845 (100), 1846 (99), 1847 (64).

UV-VIS (CH_2CL_2) λmax, nm: 415, 508, 542, 584, 638.

5,10-di-(4-1'-thio-2',3',4',6'-O-acetyl-glucosyl-2,3,5,6-tetrafluorophenyl)-15,20-di-(4-4'-thiopyridyl-2,3,5,6-tetrafluorophenyl)porphyrin (**2**)

^{1}H-NMR (300MHz, CD_2Cl_2): δ = 9.07 (s, β pyrrole, 8H), 8.63 (m, 2',6'-pyridyl, 4H), 7.40 (m, 3',5'-pyridyl, 4H), 5.38 (d, J=7.32Hz, 1'-glucosyl, 2H), 5.24 (m, 2',3',4'-glucosyl, 6H), 4.31 (s, 6'-glucosyl, 4H), 3.93 (m, 5'-glucosyl, 2H), 2.22 (s, OAc×2, 6H), 2.07 (s, OAc×6, 18H), -2.88 (s, pyrrole NH, 2H).

ESI-MS (calcd. for $C_{82}H_{56}N_6O_{18}S_4F_{16}$: 1844) *m/z* found (rel. intensity): 1845 (100), 1846 (92), 1847 (68).

UV-VIS (CH_2CL_2) λmax, nm: 415, 508, 541, 584, 638.

5,15-di-(4-1'-thio-glucosyl-2,3,5,6-tetrafluorophenyl)-10,20-di-(4-4'-thiopyridyl-2,3,5,6-tetrafluorophenyl)porphyrin (**3**)

MALDI-MS (calcd. for $C_{66}H_{40}N_6O_{18}S_4F_{16}$: 1508) *m/z* found (rel. intensity): 1509.83 (78.0), 1510.82 (100.0), 1511.84 (90.8), 1512.85 (87.2), 1513.82 (31.9).

UV-VIS (CH_3OH:DME = 1:1) λmax, nm: 412, 505, 537, 582, 637.

5,10-di-(4-1'-thio-glucosyl-2,3,5,6-tetrafluorophenyl)-15,20-di-(4-4'-thiopyridyl-2,3,5,6-tetrafluorophenyl)porphyrin (**4**)

MALDI-MS (calcd. for $C_{66}H_{40}N_6O_{18}S_4F_{16}$: 1508) *m/z* found (rel. intensity): 1510.05 (83.8), 1511.08 (100.0), 1512.05 (89.9), 1513.06 (80.4), 1514.04 (55.4).

UV-VIS (CH_3OH:DME = 1:1) λmax, nm: 412, 505, 538, 582, 635.

Fluorescence imaging cells. Cells were plated onto cover slips in cell culture dishes. Porphyrins (dissolved in methanol) were added to the cultures to a final concentration of 2 to 20 μM. Twenty-four hours later cells were washed twice with PBS (136 mM NaCl, 2.6 mM KCl, 1.4 mM KH_2PO_4, 4.2 mM Na_2HPO_4) and fixed in 4% paraformaldehyde solution in PBS for 20 min at room temperature. The cells were then washed with PBS 5 times (*43, 44*). The cover slips were mounted in Dako fluorescent mounting medium, put onto slides, air dried, and then visualized using a Nikon Optiphot 2 fluorescence microscope where images were captured as high quality TIFF files. (Excitation: 505-565nm and Emission: 565-685nm). For comparison and to record cell morphology, images were also captured as JPEG images using a phase contrast light microscope. For each set of experiments, cells were cultured and the fluorescence images were taken under identical culture and microscopic conditions.

For quantitative studies, the image intensities of the cells in the fluorescence micrographs were calculated by Scientific Image software, developed by Advanced

Science & Technology (*45*). This program can analyze images in JPEG format as briefly outlined below.

1. The Red, Green, Blue (R, G, B) components of several selected cell regions in the first image were averaged to get (Rc, Gc, Bc).

2. For the same image several regions of background were selected and (R, G, B) for the background regions are averaged to get (Rb, Gb, Bb). The background intensity was considered as noise, which was subtracted from the intensity of the cell region. This gives the background adjusted (R1, G1, B1) for the first image.

3. For the second image (R2, G2 B2) was obtained in the same way.

4. For each image, the absolute intensity, expressed as a (R, G, B) vector, was obtained as the scalar value of the vector.

5. The relative fluorescent intensity between two images was taken as the ratio of the absolute intensity of two images.

6. Additionally, the ratios for the red, green, and blue components of two images can be separately calculated in a straightforward manner.

The data were calculated from the original RGB data of the unprocessed images. For publication purpose, the images were enhanced using Microsoft Photo Editor® using the same parameters for each set of images.

Abbreviations:

DCC	dynamic combinatorial chemistry
DME	ethylene glycol dimethyl ether
DMEM	dulbecco's Modified Eagle Medium
ESI	electrospray ionization
MALDI	matrix-assisted laser desorption/ionization
MS	mass spectrometry
PDT	photodynamic therapy
SER	sequestration enabling reagent
$TPPF_{20}$	*meso*-tetrakis(pentafluorophenyl)porphyrin
UV-VIS	ultraviolet-visible
VCLs	virtual combinatorial libraries

References:

1. Merrifield, R. B. (1963) Solid Phase Peptide Synthesis. I. The Synthesis of a Tetrapeptide, *J. Am. Chem. Soc. 85*, 2149-2154.
2. Merrifield, R. B. (1964) Solid phase peptide synthesis. II. the synthesis of bradykinin, *J. Am. Chem. Soc. 86*, 304-305.
3. Merrifield, R. B. (1964) Solid-Phase Peptide Synthesis. III. An Improved Synthesis of Bradykinin, *Biochem. 3*, 1385-1390.
4. An, H., and Cook, P. D. (2000) Methodologies for generating solution-phase combinatorial libraries, *Chem. Rev. 100*, 3311-3340.
5. Carell, T., Winter, E. A., Bashir-Hashemi, A., and J. Rebek, J. (1994) A Novel Procedure for the Synthesis of Lisbraries Containing Small Organic Molecules, *Angew. Chem. Int. Edit. Engl. 33*, 2059-2061.
6. Perrier, H., and Labelle, M. (1999) Liquid-phase synthesis with solid-phase workup: application to multistep and combinatorial syntheses, *J. Org. Chem. 64*, 2110-2113.
7. Curran, D. P., and Hadida, S. (1996) Tris(2-(perfluorohexyl)ethyl)tin hydride: a new Fluorous reagent for use in traditional organic synthesis and liquid phase combinatorial synthesis, *J. Am. Chem. Soc. 118*, 2531-2532.
8. Siegel, M. G., Hahn, P. J., Dressman, B. A., Fritz, J. E., Grunwell, J. R., and Kaldor, S. W. (1997) Rapid purification of small molecule libraries by ion exchange chromatography, *Tet. Lett. 38*, 3357-3360.

9. Griffey, R. H., An, H., Cummins, L. L., Gaus, H. J., Haly, B., Herrmann, R., and Cook, P. D. (1998) Rapid deconvolution of combinatorial libraries using HPLC Fractionation, *Tetrahedron 54*, 4067-4076.

10. Warmus, J. S., and da Silva, M. I. (2000) Polyaromatic Scavenger Reagents (PAHSR): A New Methodology for Rapid Purification in Solution-Phase Combinatorial Synthesis, *Org. Lett. 2*, 1807-1809.

11. Parlow, J. J., Naing, W., South, M. S., and Flynn, D. L. (1997) In Situ chemical tagging: Tetrafluorophthalic anhydride as a "Sequestration Enabling Reagent" (SER) in the purification of solution-phase combinatorial libraries, *Tetrahedron Lett. 38*, 7959-7962.

12. Barrett, A. G. M., Smith, M. L., and Zecri, F. J. (1998) Impurity annihilation: a trategy for solution phase combinatorial chemistry with niminal purification, *Chem. Commun.*, 2317-2318.

13. Drain, C. M., Gong, X., Ruta, V., Soll, C. E., and Chicoineau, P. F. (1999) Combinatorial Synthesis and Modification of Functional Porphyrin Libraries: Identification of New, Amphipathic Motifs for Biomolecule Binding, *J. Comb. Chem. 1*, 286-290.

14. Berlin, K., Jain, R. K., Tetzlaff, C., Steinbeck, C., and Richert, C. (1997) Spectrometrically monitored selection experiments: quantitative laser desorption mass spectrometry of small chemical libraries, *Chemistry & Biology 4*, 63-77.

15. Boger, D. L., and Chai, W. (1998) Solution-phase combinatorial synthesis: Convergent multiplication of diversity via the olefin metathesis reaction, *Tetrahedron 54*, 3955-3970.

16. An, H., Cummins, L. L., Griffey, R. H., Bharadwaj, R., Haly, B. D., Fraser, A. S., Wilson-Lingardo, L., Risen, L. M., Wyatt, J. R., and Cook, P. D. (1997) Solution phase combinatorial chemistry. Discovery of novel polyazapyridinophanes with potent antibacterial activity by a solutionphase simultaneous addition of functionalities approach, *J. Am. Chem. Soc. 119*, 3696-3708.

17. Takahashi, M., Ueno, A., and Mihara, H. (2000) Peptide design based on an antibody complementarity-determining region (CDR): construction of porphyrin-binding peptides and their affinity maturation by a combinatorial method, *Chem. Eur. J. 6*, 3196-3203.

18. Goldberg, J., Jin, Q., Ambroise, Y., Satoh, S., Desharnais, J., Capps, K., and Boger, D. L. (2002) Erythropoietin Mimetics Derived from Solution Phase Combinatorial Libraries, *J. Am. Chem. Soc. 124*, 544-555.

19. Boger, D. L., and Lee, J. K. (2000) Development of a Solution-Phase Synthesis of Minor Groove Binding Bis-Intercalators Based on Triostin A Suitable for Combinatorial Synthesis, *J. Org. Chem. 65*, 5996-6000.

20. Lehn, J.-M. (1999) Dynamic Combinatorial Chemistry and Virtual Combinatorial Libraries, *Chem. Eur. J. 5*, 2455-2463.

21. Huc, I., and Lehn, J.-M. (1997) Virtual combinatorial libraries: Dynamic generation of molecular and supramolecular diversity by self-assembly, *Proc. Natl. Acad. Sci. USA 94*, 2106-2110.

22. Otto, S., Furlan, R. L. E., and Sanders, J. K. M. (2002) Selection and amplification of hosts from dynamic combinatorial libraries of macrocyclic disulfides, *Science 297*, 590-593.

23. Brown, M. (2003) PDT: light at the end of the tunnel?, *Drug Discovery Today 8*, 767-768.

24. Jori, G. (1996) Tumor photosensitizers: approaches to enhance the selectivity and efficiency of photodynamic therapy, *J. Photochem. Photobiol. B 36*, 87-93.

25. Mody, T. D. (2000) Pharmaceutical developement and medical applications of porphyrin-type macrocycles, *J. Porphyrins Phthalocyanines 4*, 362-367.

26. Pandey, R. K. (2000) Recent advances in photodynamic therapy, *J. Porphyrins Phthalocyanines 4*, 368-373.

27. MacDonald, I. J., and Dougherty, T. J. (2001) Basic principles of photodynamic therapy, *J. Porphyrins Phthalocyanines 5*, 105-129.

28. Sternberg, E. D., Bruckner, C., and Dolphin, D. (1998) Porphyrin-based photosensitizers for use in photodynamic therapy, *Tetrahedron 54*, 4151-4202.

29. Stojiljkovic, I., Evavold, B. D., and Kumar, V. (2001) Antimicrobial properties of porphyrins, *Exp. Opin. Invest. Drugs 10*, 309-320.

30. Neurath, A. R., Strick, N., and Debnath, A. K. (1995) Structural requirements for and consequences of an antiviral porphyrin binding to the V3 loop of the human immunodeficiency virus (HIV-1) envelope glycoprotein gp120, *J. Mol. Recog. 8*, 345-357.

31. Vzorov, A. N., Dixon, D. W., Trommel, J. S., Marzilli, L. G., and Compans, R. W. (2002) Inactivation of human immunodeficiency virus type 1 by porphyrins, *Antimicrob. Agents Chemother. 46*, 3917-3925.

32. Chen, X., and Drain, C. M. (2004) Photodynamic therapy using carbohydrate conjugated porphyrins, *Drug Design Reviews - Online 1*, 215-234.

33. Sylvain, I., Benhaddou, R., Carre, V., Cottaz, S., Driguez, H., Granet, R., Guilloton, M., and Krausz, P. (1999) Synthesis and biological evaluation of thioglycosylated meso- arylporphyrins, *J. Porphyrins Phthalocyanines 3*, 1 - 4.

34. Sylvain, I., Zerrouki, R., Granet, R., Huang, Y. M., Lagorce, J.-F., Guilloton, M., Blais, J.-C., and Krausz, P. (2002) Synthesis and Biological Evaluation of Thioglycosylated Porphyrins for an Application in Photodynamic Therapy, *Bioorg. Med. Chem. 10*, 57-69.

35. Shaw, S. J., Edwards, C., and Boyle, R. W. (1999) Regioselective Synthesis of Multifunctionalised Porphyrins - Coupling of Mono-(pentafluorophenyl)porphyrins to Electrophiles, *Tetrahedron Lett. 40*, 7585-7586.

36. Shaw, S. J., Elgie, K. J., Edwards, C., and Boyle, R. W. (1999) Mono-(pentafluorophenyl)porphyrins - Useful Intermediates in the Regioselective Synthesis of Multifunctionalised Porphyrins, *Tetrahedron Lett. 40*, 1595-1596.

37. Chen, X., Hui, L., Foster, D. A., and Drain, C. M. (2004) Efficient Synthesis and Photodynamic Activity of Porphyrin-Saccharide Conjugates: Targeting and Incapacitating Cancer Cells, *Biochem. accepted*.

38. Davda, J., and Labhasetwar, V. (2002) Characterization of nanoparticle uptake by endothelial cells, *Int. J. Pharm. 233*, 51-59.

39. Gao, X., Cui, Y., Levenson, R. M., Chung, L. W. K., and Nie, S. (2004) In vivo cancer targeting and imaging with semiconductor quantum dots, *Nature Biotechnology 22*, 969-976.

40. Akins, D. L., Ozcelik, S., Zhu, H. R., and Guo, C. (1996) Fluorescence decay kinetics and structure of aggregated tetrakis (p - Sulfonatophenyl) porphyrin, *J. Phys. Chem. 100*, 14390 - 14396.

41. Harriman, A., and Hosie, R. J. (1981) Fluorescence quenching effect of substituted tetraphenylporphyrins, *J. Photochem. 15*, 163-167.

42. Hornia, A., Lu, Z., Sukezane, T., Zhong, M., Joseph, R., Frankel, P., and Foster, D. A. (1999) Antogonistic effects of protein kinase C alpha and gama on both transformation and phospholipase D activity mediated by the epidermal growth factor receptor, *Molecular and Celluar Biology 19*, 7672-7680.

43. Shen, Y., Xu, L., and Foster, D. A. (2001) Role for phospholiase D in receptor-mediated endocytosis, *Molecular and Celluar Biology 21*, 595-602.

44. Willingham, M. C., and Pastan, I. (1985) *An Atlas of Immunofluorescence in Cultured Cells*, Academic Press, Orlando.

45. Qian, G. (2003), Advanced Science & Technology, http://www.howardast.com, New York.

Appendices:

A. Fluorescence images taken a week after fixation:

Cis-isomer (**4**) Trans-isomer (**3**) P-Glu_4

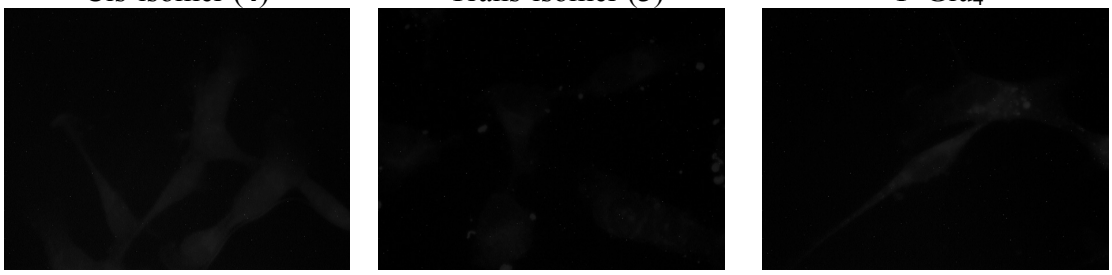

B. Fluorescence images taken the same day of fixation:

Cis-isomer (**4**) Trans-isomer (**3**) P-Glu_4

Appendix I. Different affinities of winning compounds (2 μM) cis- (**4**) and trans- (**3**) isomer toward human breast cancer MDA-MB-231 cells by fluorescence images, compared with tetra-glucose porphyrin. Images were taken a week after fixation (A) and the same day of fixation (B).

A. Fluorescence images taken a week after fixation:

Cis-isomer (**4**) Trans-isomer (**3**) P-Glu_4

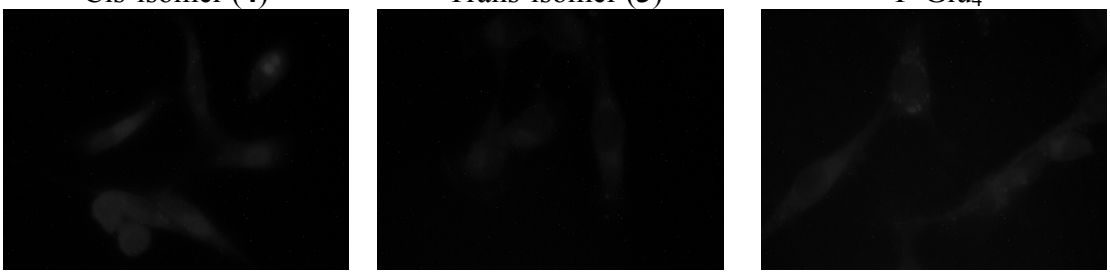

B. Fluorescence images taken the same day of fixation:

Cis-isomer (**4**) Trans-isomer (**3**) P-Glu_4

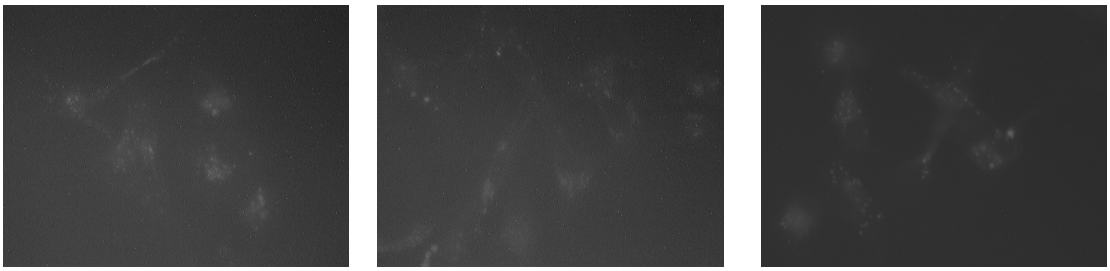

Appendix II. Different affinities of winning compounds (4 μM) cis- (**4**) and trans- (**3**) isomer toward human breast cancer MDA-MB-231 cells by fluorescence images, compared with tetra-glucose porphyrin. Images were taken a week after fixation (A) and the same day of fixation (B).

A. Fluorescence images taken a week after fixation:

Cis-isomer (**4**) Trans-isomer (**3**) P-Glu_4

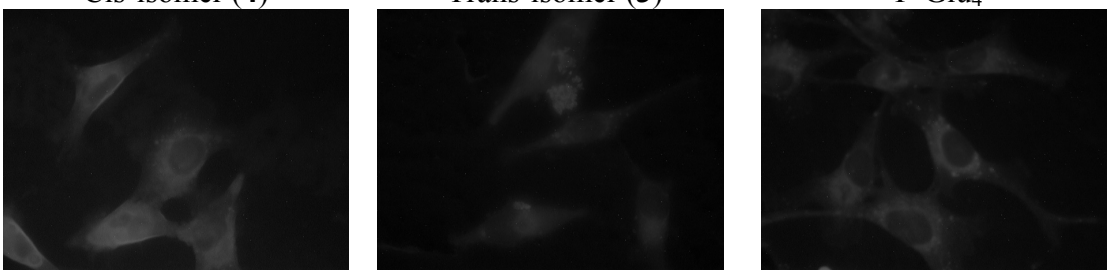

B. Fluorescence images taken the same day of fixation:

Cis-isomer (**4**) Trans-isomer (**3**) P-Glu_4

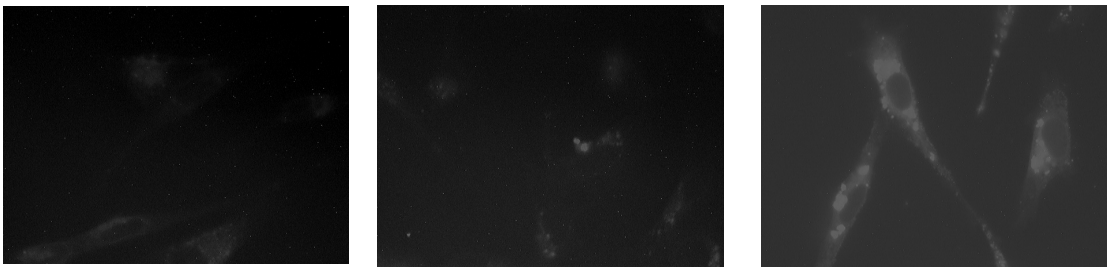

Appendix III. Different affinities of winning compounds (20 μM) cis- (**4**) and trans- (**3**) isomer toward human breast cancer MDA-MB-231 cells by fluorescence images, compared with tetra-glucose porphyrin. Images were taken a week after fixation (A) and the same day of fixation (B).

Appendix IV. MALDI mass spectra of trans-isomer **3** (Glu/Py/Glu/Py) and cis-isomer **4** (Glu/Glu/Py/Py).

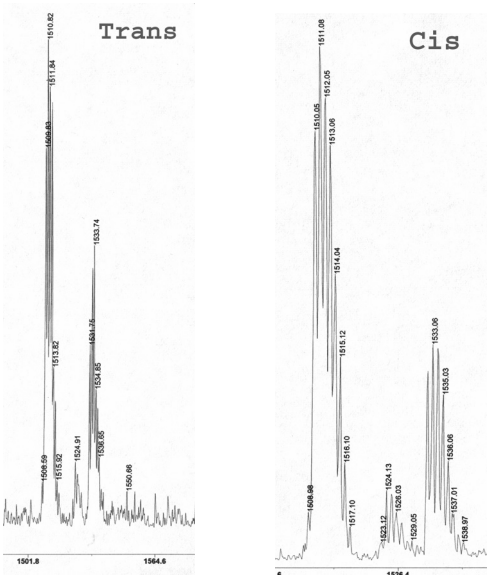

Appedix V. Synthesis of 55-membered solution-phase combinatorial porphyrin library.

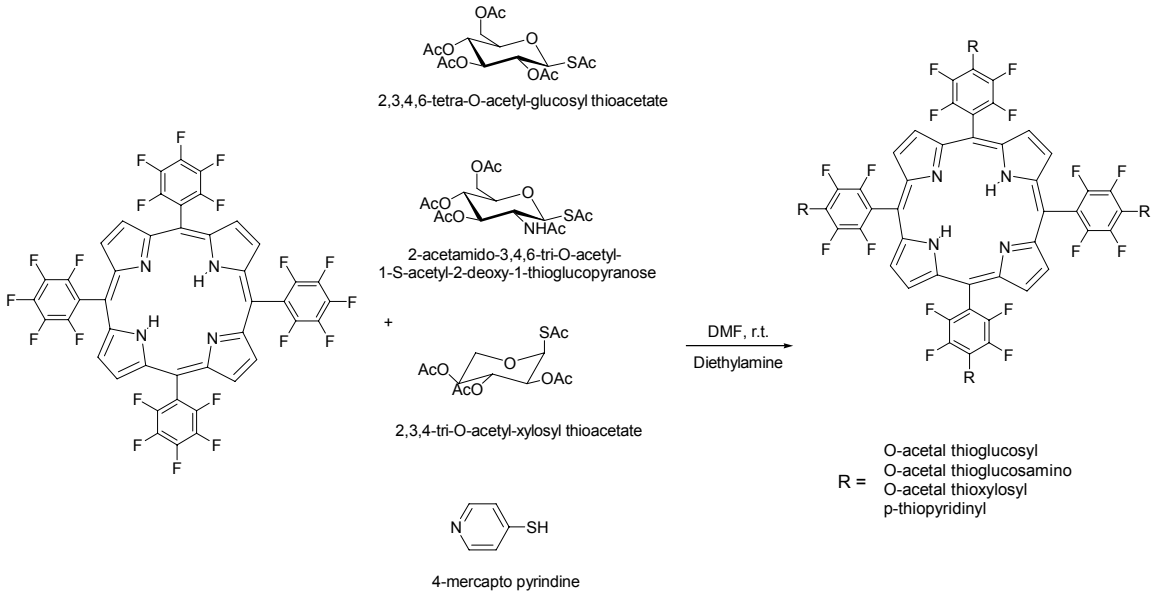

Appendix VI. Simulated mass spectrum (top) and ESI mass spectrum (bottom) of 55-membered solution-phase combinatorial porphyrin library.

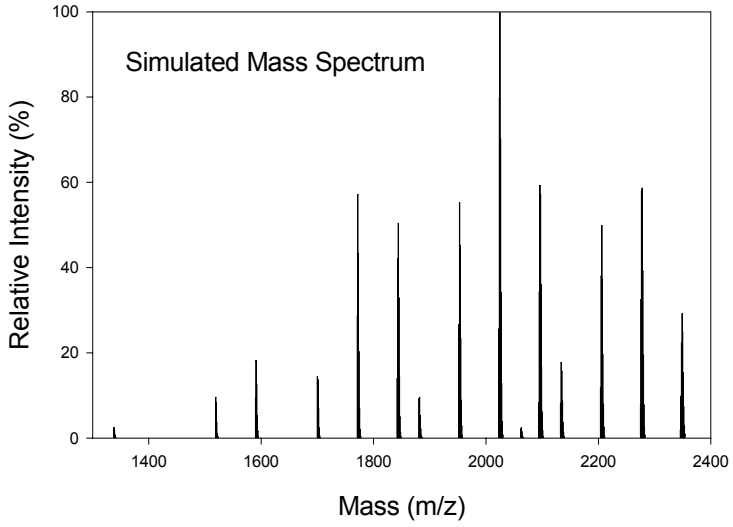

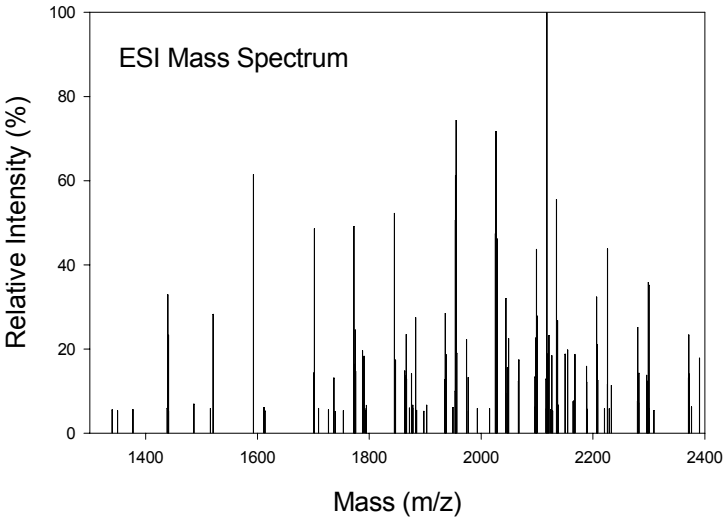

Appendix VII. Synthesis of 406-membered solution-phase combinatorial porphyrin library.

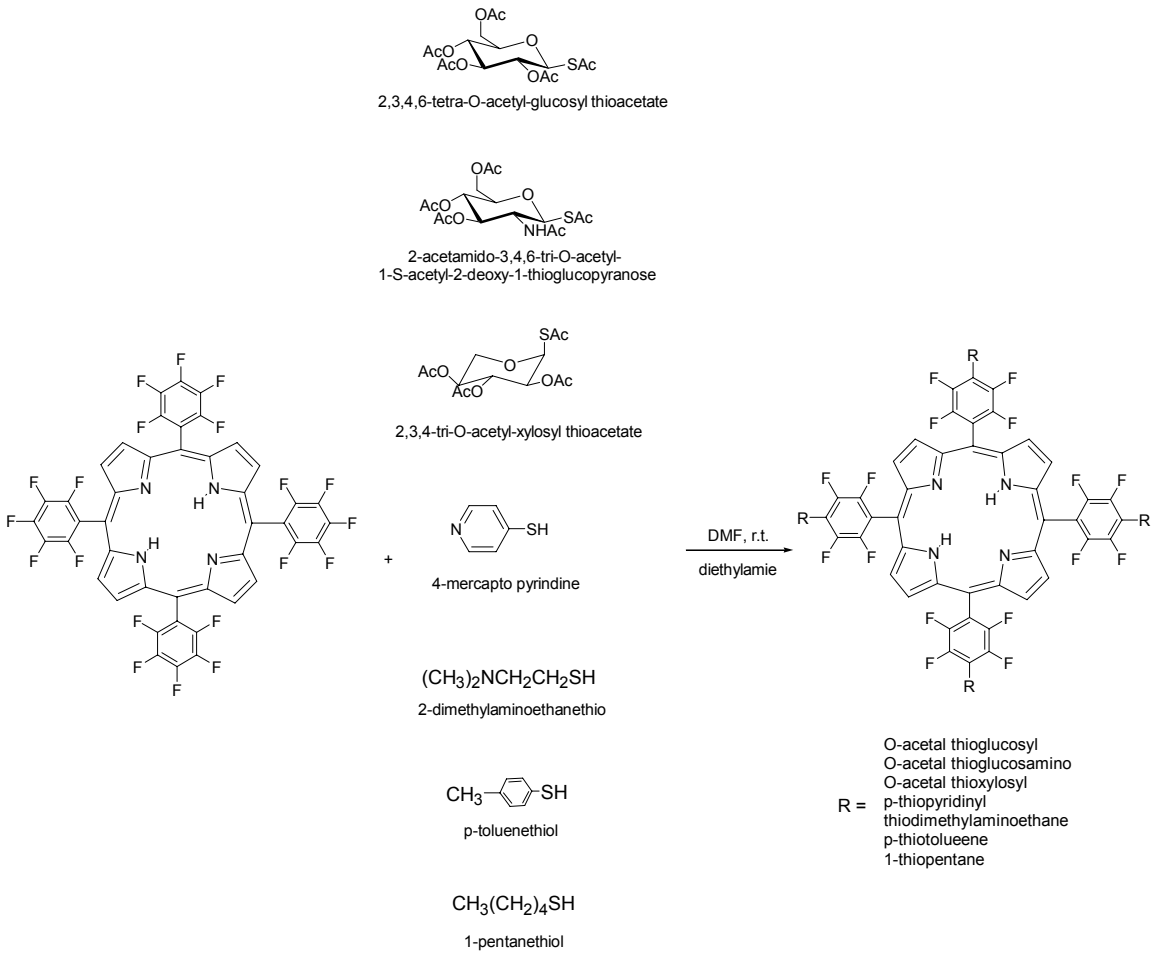

Appendix VIII. Simulated mass spectrum (top) and ESI mass spectrum (bottom) of 406-membered solution-phase combinatorial porphyrin library.

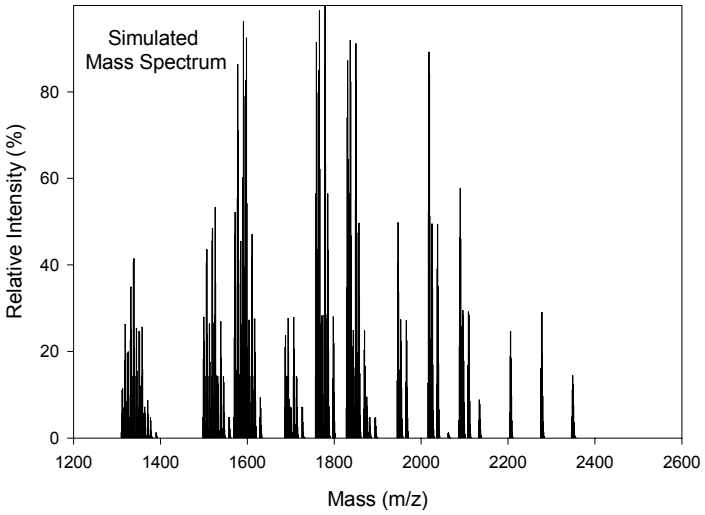

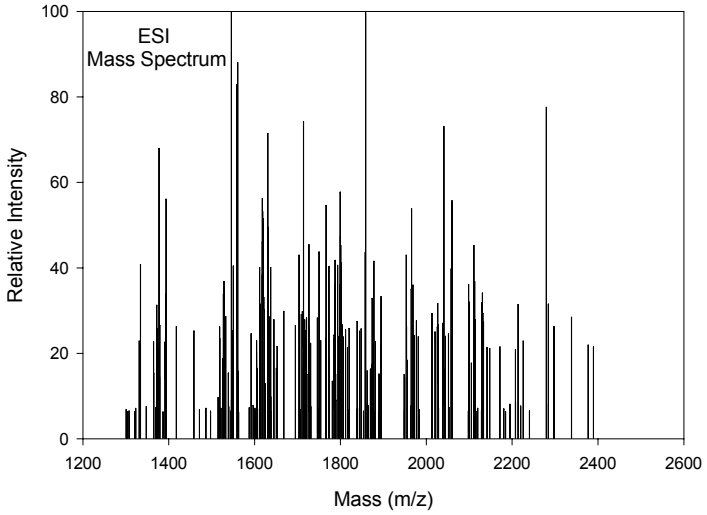

References

Chapter 1

1. Mauzerall, D. C. *Clin. Dermat.*, **1998**, *16*, 195.

2. Chen, X.; Drain, C. M. In *Encyclopedia of Nanoscience and Nanotechnology*, Nalwa, H. S., Ed.; American Scientific Publishers: **2004**; Vol. *9*, pp. 593-616.

3. Perutz, M. F.; Fermi, G.; Luisi, B.; Shaanan, B.; Liddington, R. C. *Acc. Chem. Res.*, **1987**, *20*, 309.

4. Ungashe, S. B.; Groves, J. T. *Adv. Inorg. Biochem.*, **1994**, *9*, 317.

5. Boxer, S. G. *Biophys. Biochim.*, **1983**, *726*, 265.

6. Drain, C. M.; Sable, D. B.; Corden, B. B. *Inorg. Chem.*, **1988**, *27 (14)*, 2396.

7. Lane, N. *Sci. Am.*, **2003**, *288 (1)*, 38.

8. Drain, C. M.; Nifiatis, F.; Vasenko, A.; Batteas, J. D. *Angew. Chem. Int. Edit. Engl.*, **1998**, *37*, 2344.

9. Milic, T. N.; Chi, N.; Yablon, D. G.; Flynn, G. W.; Batteas, J. D.; Drain, C. M. *Angew. Chem. Int. Edit. Engl.*, **2002**, *41*, 2117.

10. Drain, C. M.; Russel, K. C.; Lehn, J.-M. *Chem. Commun.*, **1996**, 337.

11. Drain, C. M. *Proc. Natl. Acad. Sci. USA*, **2002**, *99 (8)*, 5178.

12. Gong, X.; Milic, T.; Xu, C.; Batteas, J. D.; Drain, C. M. *J. Am. Chem. Soc.*, **2002**, *124 (48)*, 14290.

13. Diskin-Posner, Y.; Dahal, S.; Goldberg, I. *Angew. Chem. Int. Edit. Engl.*, **2000**, *39 (7)*, 1288.

14. Drain, C. M.; Hupp, J. T.; Suslick, K. S.; Wasielewski, M. R.; Chen, X. *J. Porphyrins Phthalocyanines*, **2002**, *6*, 243.

15. Rakow, N. A.; Suslick, K. S. *Nature*, **2000**, *406 (6797)*, 710.

16. Kral, V.; Sessler, J. L.; Furuta, H. *J. Am. Chem. Soc.*, **1992**, *114*, 8704.

17. Wall, R. K.; Shelton, A. H.; Bonaccorsi, L. C.; Bejune, S. A.; Dube, D.; McMillin, D. R. *J. Am. Chem. Soc*, **2001**, *123*, 11480.

18. Guliaev, A. B.; Leontis, N. B. *Biochemistry*, **1999**, *38 (47)*, 15425.

19. Drain, C. M.; Gong, X.; Ruta, V.; Soll, C. E.; Chicoineau, P. F. *J. Comb. Chem.*, **1999**, *1*, 286.

20. Brown, M. *Drug Discovery Today*, **2003**, *8 (17)*, 767.

21. Oleinick, N. L.; Morris, R. L.; Belichenko, I. *Photochem. Photobiol. Sci.*, **2002**, *1 (1)*, 1.

22. Jori, G. *J. Photochem. Photobiol. B*, **1996**, *36*, 87.

23. Mody, T. D. *J. Porphyrins Phthalocyanines*, **2000**, *4*, 362.

24. Thacker, P. D. *Drug Discovery Today*, **2003**, *8 (5)*, 190.

25. Pandey, R. K. *J. Porphyrins Phthalocyanines*, **2000**, *4 (4)*, 368.

26. MacDonald, I. J.; Dougherty, T. J. *J. Porphyrins Phthalocyanines*, **2001**, *5 (2)*, 105.

27. Neurath, A. R.; Strick, N.; Debnath, A. K. *J. Mol. Recog.*, **1995**, *8*, 345.

28. Vzorov, A. N.; Dixon, D. W.; Trommel, J. S.; Marzilli, L. G.; Compans, R. W. *Antimicrob. Agents Chemother.*, **2002**, *46 (12)*, 3917.

29. Sternberg, E. D.; Dolphin, D.; Bruckner, C. *Tetrahedron*, **1998**, *54*, 4151.

30. Osterloh, J.; Vicente, M. G. H. *J. Porphyrins Phthalocyanines*, **2002**, *6*, 305.

31. Bonnett, R. *Chem. Soc. Rev.*, **1995**, 19.

32. Moan, J.; Christensen, T. *Tumor Res.*, **1980**, *15*, 1.

33. Piette, J.; Volanti, C.; Vantieghem, A.; Matroule, J.-Y.; Habraken, Y.; Agostinis, P. *Biochem. Pharmacol.*, **2003**, *66*, 1651.

34. Granville, D. J.; Hunt, D. W. C. *Curr. Opin. Drug Discovery Develop.*, **2000**, *3 (2)*, 232.

35. Moor, A. C. E. *J. Photochem. Photobiol. B*, **2000**, *57*, 1.

36. Nyman, E. S.; Hynninen, P. H. *J. Photochem. Photobiol. B*, **2004**, *73*, 1.

37. Pandey, R. K.; Zheng, G. In *The Porphyrin Handbook*, Kadish, K. M., Smith, K. M. and Guilard, R., Ed.; Academic Press: New York. **2000**; Vol. *6*, pp. 157-230.

38. Dougherty, T. J. *Photochem. Photobiol.*, **1993**, *58 (6)*, 895.

39. Salva, K. A. *Clin. Dermat.*, **2002**, *20*, 571.

40. Rouhi, A. M. *Chem. Eng. News*, **1998**, *Nov. 2*, 22.

41. Prinsep, M. R.; Caplan, F. R.; Moore, R. E.; Patterson, G. M. L.; Smith, C. D. *J. Am. Chem. Soc.*, **1992**, *114*, 385.

42. Drain, C. M.; Mauzerall, D. C. *Biophys. J.*, **1992**, *63*, 1544.

43. Momenteau, M.; Oulmi, D.; Maillard, P.; Croisy, A. *SPIE*, **1994**, *2325 Photodynamic Therapy of Cancer II*, 13.

44. Baláž, S. *Perspect. Drug Discov. Des.*, **2000**, *19 (1)*, 157.

45. Testa, B.; Crivori, P.; Reist, M.; Carrupt, P.-A. *Perspect. Drug Discov. Des.*, **2000**, *19 (1)*, 179.

46. Drain, C. M.; Mauzerall, D. C. *Biophys. J.*, **1992**, *63*, 1556.

47. Konan, Y. N.; Gurny, R.; Allemann, E. *J. Photochem. Photobiol. B*, **2002**, *66*, 89.

48. Boyle, R. W.; Dolphin, D. *Photochem. Photobiol.*, **1996**, *64 (3)*, 469.

49. Valenzeno, D. P. *Photochem. Photobiol.*, **1987**, *46 (1)*, 147.

50. Drain, C. M.; Mauzerall, D. C. *Proc. Natl. Acad. Sci. USA*, **1989**, *86*, 6959.

51. Ricchelli, F. *J. Photochem. Photobiol. B*, **1995**, *29*, 109.

52. Maillard, P.; Guerquin-Kern, J.-L.; Huel, C.; Momenteau, M. *J. Org. Chem.*, **1993**, *58*, 2774.

53. Lindsey, J. S.; Schreiman, I. C.; Hsu, H. C.; Kearney, P. C.; Marguerettaz, A. M. *J. Org. Chem.*, **1987**, *52 (5)*, 827.

54. Wagner, R. W.; Lawrence, D. S.; Lindsey, J. S. *Tetrahedron Lett.*, **1987**, *28*, 3069.

55. Oulmi, D.; Maillard, P.; Guerquin-Kern, J.-L.; Huel, C.; Momenteau, M. *J. Org. Chem.*, **1995**, *60 (6)*, 1554.

56. Csik, G.; Balog, E.; Voszka, I.; Tolgyesi, F.; Oulmi, D.; Maillard, P.; Momenteau, M. *J. Photochem. Photobiol. B*, **1998**, *44*, 216.

57. Voszka, I.; Galantai, R.; Maillard, P.; Csik, G. *J. Photochem. Photobiol. B*, **1999**, *52*, 92.

58. Gaud, O.; Granet, R.; Kaouadji, M.; Krausz, P.; Blais, J.-C.; Bolbach, G. *Can. J. Chem.*, **1996**, *74*, 481.

59. Bourhim, A.; Gaud, O.; Granet, R.; Krausz, P.; Spiro, M. *Synlett*, **1993**, 563.

60. Carre, V.; Gaud, O.; Sylvain, I.; Bourdon, O.; Spiro, M.; Blais, J.; Granet, R.; Krausz, P.; Guilloton, M. *J. Photochem. Photobiol. B*, **1999**, *48*, 57.

61. Sol, V.; Branland, P.; Granet, R.; Kaldapa, C.; Verneuil, B.; Krausz, P. *Bioorg. Med. Chem. Lett.*, **1998**, *8*, 3007.

62. Malik, Z.; Ladan, H.; Nitzan, Y. *J. Photochem. Photobiol. B*, **1992**, *14 (3)*, 262.

63. Driaf, K.; Krausz, P.; Verneuil, B.; Spiro, M.; Blais, J. C.; Bolbach, G. *Tetrahedron Lett.*, **1993**, *34 (6)*, 1027.

64. Driaf, K.; Granet, R.; Krausz, P.; Kaouadji, M.; Thomasson, F.; Chulia, A. J.; Verneuil, B.; Spiro, M.; Blais, J.-C.; Bolbach, G. *Can. J. Chem.*, **1996**, *74*, 1550.

65. Kaldapa, C.; Blais, J. C.; Carre, V.; Granet, R.; Sol, V.; Guilloton, M.; Spiro, M.; Krausz, P. *Tetrahedron Lett.*, **2000**, *41*, 331.

66. Mikata, Y.; Onchi, Y.; Tabata, K.; Ogura, S.-i.; Okura, I.; Ono, H.; Yano, S. *Tetrahedron Lett.*, **1998**, *39*, 4505.

67. Kohata, K.; Higashio, H.; Yamaguchi, Y.; Koketsu, M.; Odashima, T. *Bull. Chem. Soc. Jpn.*, **1994**, *67*, 668.

68. Hombrecher, H. K.; Schell, C. *Bioorg. Med. Chem. Lett.*, **1996**, *6 (11)*, 1199.

69. Schell, C.; Hombrecher, H. K. *Bioorg. Med. Chem.*, **1999**, *7*, 1857.

70. Schell, C.; Hombrecher, H. K. *Chem.-Eur. J.*, **1999**, *5 (2)*, 587.

71. Sol, V.; Blais, J. C.; Carre, V.; Granet, R.; Guilloton, M.; Spiro, M.; Krausz, P. *J. Org. Chem.*, **1999**, *64 (12)*, 4431.

72. Sol, V.; Blais, J. C.; Bolbach, G.; Carre, V.; Granet, R.; Guilloton, M.; Spiro, M.; Krausz, P. *Tetrahedron Lett.*, **1997**, *38 (36)*, 6391.

73. Chaleix, V.; Sol, V.; Huang, Y.-M.; Guilloton, M.; Granet, R.; Blais, J. C.; Krausz, P. *Eur. J. Org. Chem.*, **2003**, 1486.

74. Little, R. G.; Anton, J. A.; Loach, P. A.; Ibers, J. A. *J. Heterocycl. Chem.*, **1975**, *12*, 345.

75. Adler, A. D.; Longo, F. R.; Finarelli, J. D.; Goldmacher, J.; Assour, J.; Korsakoff, L. *J. Org. Chem.*, **1967**, *32*, 476.

76. Perree-Fauvet, M.; Verchere-Beaur, C.; Tarnaud, E.; Anneheim-Herbelin, G.; Bone, N.; Gaudemer, A. *Tetrahedron*, **1996**, *52 (43)*, 13569.

77. Verchere-Beaur, C.; Perree-Fauvet, M.; Tarnaud, E.; Anneheim-Herbelin, G.; Bone, N.; Gaudemer, A. *Tetrahedron*, **1996**, *52 (43)*, 13589.

78. Zoladek, T.; Nhi, N. B.; Jagletto, I.; Graczyk, A.; Rytka, J. *Photochem. Photobiol.*, **1997**, *66 (2)*, 253.

79. Hamazawa, A.; Kinoshita, I.; Breedlove, B.; Isobe, K.; Shibata, M.; Baba, Y.; Kakuchi, T.; Hirohara, S.; Obata, M.; Mikata, Y.; Yano, S. *Chem. Lett.*, **2002**, *31 (3)*, 388.

80. Maillard, P.; Vilain, S.; Huel, C.; Momenteau, M. *J. Org. Chem.*, **1994**, *59*, 2887.

81. Maillard, P.; Guerquin-Kern, J. L.; Momenteau, M. *Tetrahedron Lett.*, **1991**, *32 (37)*, 4901.

82. Kohata, K.; Yamaguchi, Y.; Higashio, H.; Odashima, T.; Ishii, H. *Chem. Lett.*, **1992**, 477.

83. Maillard, P.; Guerquin-Kern, J.-L.; Momenteau, M.; Gaspard, S. *J. Am. Chem. Soc.*, **1989**, *111*, 9125.

84. Fulling, G.; Schroder, D.; Franck, B. *Angew. Chem. Int. Edit. Engl.*, **1989**, *28 (11)*, 1519.

85. Hombrecher, H. K.; Schell, C. *Carbohydr. Polymers*, **1997**, *34 (4)*, 422.

86. Bourhim, A.; Czernecki, S.; Krausz, P.; Viari, A.; Vigny, P. *J. Carbohydr. Chem.*, **1990**, *9 (5)*, 761.

87. Belica, P. S.; Franck, R. W. *Tetrahedron Lett.*, **1998**, *39*, 8225.

88. Yang, G.; Franck, R. W.; Byun, H.-S.; Bittman, R.; Samadder, P.; Arthur, G. *Org. Lett.*, **1999**, *1*, 2149.

89. Li, F.; Yang, K.; Tyhonas, J. S.; MacCrum, K. A.; Lindsey, J. S. *Tetrahedron*, **1997**, *53*, 12339.

90. Pasetto, P.; Chen, X.; Drain, C. M.; Franck, R. W. *Chem. Commun.*, **2001**, 81.

91. Arsenault, G. P.; Bullock, E.; MacDonald, S. F. *J. Am Chem. Soc.*, **1960**, *82*, 4384.

92. Littler, B. J.; Ciringh, Y.; Lindsey, J. S. *J. Org. Chem.*, **1999**, *64*, 2864.

93. Cornia, M.; Menozzi, M.; Ragg, E.; Mazzini, S.; Scarafoni, A.; Zanardi, F.; Casiraghi, G. *Tetrahedron*, **2000**, *56*, 3977.

94. Ono, N.; Bougauchi, M.; Maruyama, K. *Tetrahedron Lett.*, **1992**, *33 (12)*, 1629.

95. Maillard, P.; Huel, C.; Momenteau, M. *Tetrahedron Lett.*, **1992**, *33 (52)*, 8081.

96. Cornia, M.; Valenti, C.; Capacchi, S.; Cozzini, P. *Tetrahedron*, **1998**, *54*, 8091.

97. Casiraghi, G.; Cornia, M.; Zanardi, F.; Rassu, G.; Ragg, E.; Bortolini, R. *J. Org. Chem.*, **1994**, *59*, 1801.

98. Cornia, M.; Casiraghi, G.; Binacchi, S.; Zanardi, F.; Rassu, G. *J. Org. Chem.*, **1994**, *59*, 1226.

99. Casiraghi, G.; Cornia, M.; Rassu, G.; Sante, C. D.; Spanu, P. *Tetrahedron*, **1992**, *48 (27)*, 5619.

100. Defaye, J.; Gelas, J. In *Studies in Natural Products Chemistry*, Atta-ur-Rahman, Ed.; Elsevier Science Publishers B. V.: Amsterdam. **1991**; Vol. *8*, pp. 315-357.

101. Sylvain, I.; Benhaddou, R.; Carre, V.; Cottaz, S.; Driguez, H.; Granet, R.; Guilloton, M.; Krausz, P. *J. Porphyrins Phthalocyanines*, **1999**, *3*, 1.

102. Sylvain, I.; Zerrouki, R.; Granet, R.; Huang, Y. M.; Lagorce, J.-F.; Guilloton, M.; Blais, J.-C.; Krausz, P. *Bioorg. Med. Chem.*, **2002**, *10*, 57.

103. Davoust, E.; Granet, R.; Krausz, P.; Carre, V.; Guilloton, M. *Tetrahedron Lett.*, **1999**, *40*, 2513.

104. Bardos-Nagy, I.; Galantai, R.; Fidy, J. *Biochimica et Biophysica Acta*, **2001**, *1512*, 125.

105. Hombrecher, H. K.; Ohm, S.; Koll, D. *Tetrahedron*, **1996**, *52 (15)*, 5441.

106. Li, H.; Czuchajowski, L. *Tetrahedron Lett.*, **1994**, *35 (11)*, 1629.

107. Czuchajowski, L.; Habdas, J.; Niedbala, H.; Wandrekar, V. *Tetrahedron Lett.*, **1991**, *32 (51)*, 7511.

108. Czuchajowski, L.; Niedbala, H. *Bioorg. Med. Chem. Lett.*, **1992**, *2 (12)*, 1645.

109. Czuchajowski, L.; Palka, A.; Morra, M.; Wandrekar, V. *Tetrahedron Lett.*, **1993**, *34 (34)*, 5409.

110. Czuchajowski, L.; Habdas, J.; Niedbala, H.; Wandrekar, V. *J. Heterocycl. Chem.*, **1992**, *29*, 479.

111. Li, H.; Czuchajowski, L. *Trends Heterocyc. Chem.*, **1999**, *6*, 57.

112. Fujimoto, K.; Miyata, T.; Aoyama, Y. *J. Am. Chem. Soc.*, **2000**, *122*, 3558.

113. Fuhrhop, J.-H.; Demoulin, C.; Boettcher, C.; Koning, J.; Siggel, U. *J. Am. Chem. Soc.*, **1992**, *114*, 4159.

Chapter 2

1. Drain, C. M., Christensen, B., and Mauzerall, D. C. (1989) Photogating of ionic currents across a lipid bilayer, *Proc. Natl. Acad. Sci. USA 86*, 6959-6962.
2. Drain, C. M., and Mauzerall, D. C. (1992) Photogating of ionic currents across lipid bilayers: Hydrophobic ion conductance by an ion chain mechanism, *Biophys. J. 63*, 1556-1563.
3. MacDonald, I. J., and Dougherty, T. J. (2001) Basic principles of photodynamic therapy, *J. Porphyrins Phthalocyanines 5*, 105-129.
4. Neurath, A. R., Strick, N., and Debnath, A. K. (1995) Structural requirements for and consequences of an antiviral porphyrin binding to the V3 loop of the human immunodeficiency virus (HIV-1) envelope glycoprotein gp120, *J. Mol. Recog. 8*, 345-357.
5. Vzorov, A. N., Dixon, D. W., Trommel, J. S., Marzilli, L. G., and Compans, R. W. (2002) Inactivation of human immunodeficiency virus type 1 by porphyrins, *Antimicrob. Agents Chemother. 46*, 3917-3925.
6. Pandey, R. K. (2000) Recent advances in photodynamic therapy, *J. Porphyrins Phthalocyanines 4*, 368-373.
7. Sternberg, E. D., Dolphin, D., and Bruckner, C. (1998) Porphyrin-based photosensitizers for use in photodynamic therapy, *Tetrahedron 54*, 4151-4202.
8. Bonnett, R. (1995) Photosensitizers of the porphyrin and phthalocyanine series for photodynamic therapy, *Chem. Soc. Rev.*, 19-33.
9. Moor, A. C. E. (2000) Signaling pathways in cell death and survival after photodynamic therapy, *J. Photochem. Photobiol. B: Biol. 57*, 1-13.

10. Mody, T. D. (2000) Pharmaceutical development and medical applications of porphyrin-type macrocycles, *J. Porphyrins Phthalocyanines 4*, 362-367.
11. Jori, G. (1996) Tumor photosensitizers: approaches to enhance the selectivity and efficiency of photodynamic therapy, *J. Photochem. Photobiol. B: Biol. 36*, 87-93.
12. Yang, S. I., Seth, J., Strachan, J.-P., Gentlemann, S., Kim, D., Holten, D., Lindsey, J. S., and Bocian, D. F. (1999) Ground and excited state electronic properties of halogenated tetraarylporphyrins. Tuning the building blocks for porphyrin-based photonic devices., *J. Porphyrins Phthalocyanines. 3*, 117-147
13. Dougherty, T. J. (1993) Yearly review Photodynamic therapy, *Photochem. Photobiol. 58*, 895-900.
14. Granville, D. J., and Hunt, D. W. C. (2000) Porphyrin-mediated photosensitization - Taking the apoptosis fast lane, *Curr. Opin. Drug Discovery Develop. 3*, 232-243.
15. Salva, K. A. (2002) Photodynamic therapy; Unapproved uses, dosages, or indications, *Clin. Dermat. 20*, 571-581.
16. Mauzerall, D. C., and Drain, C. M. (1992) Photogating of ionic currents across lipid bilayers: Electrostatics of ions and dipoles inside the membrane, *Biophys. J. 63*, 1544-1555.
17. Gong, X., Milic, T., Xu, C., Batteas, J. D., and Drain, C. M. (2002) Preparation and characterization of porphyrin nanoparticles, *J. Am. Chem. Soc. 124*, 14290-14291.
18. Hombrecher, H. K., and Schell, C. (1997) Carbohydrate substituted porphyrins. Synthesis, characterization and lipoprotein binding properties, *Carbohydr. Polymers 34*, 422-423.

19. Sol, V., Blais, J. C., Carre, V., Granet, R., Guilloton, M., Spiro, M., and Krausz, P. (1999) Synthesis, spectroscopy, and photocytotoxicity of glycosylated amino acid porphyrin derivatives as promising molecules for cancer phototherapy, *J. Org. Chem. 64*, 4431-4444.
20. Schell, C., and Hombrecher, H. K. (1999) Synthesis and investigation of glycosylated mono- and diarylporphyrins for photodynamic therapy, *Bioorg. Med. Chem. 7*, 1857-1865.
21. Mikata, Y., Onchi, Y., Tabata, K., Ogura, S.-i., Okura, I., Ono, H., and Yano, S. (1998) Sugar-dependent photocytotoxic property of tetra- and octa-glycoconjugated tetraphenylporphyrins, *Tetrahedron Lett. 39*, 4505-4508.
22. Maillard, P., Vilain, S., Huel, C., and Momenteau, M. (1994) Efficient preparation of the alpha, alpha, alpha, alpha-atropoisomer of meso-tetrakis[2-(2,3,4,6-tetraacetyl-O-beta-glucosyl)phenyl]porphyrin, *J. Org. Chem. 59*, 2887-2890.
23. Chen, X., and Drain, C. M. (2004) Photodynamic therapy using carbohydrate conjugated porphyrins, *Drug Design Review - Online 1*, 215-234, http://www.bentham.org/ddro/.
24. Pasetto, P., Chen, X., Drain, C. M., and Franck, R. W. (2001) Synthesis of hydrolytically stable porphyrin C- and S-glycoconjugates in high yields, *Chem. Commun.*, 81-82.
25. Brown, R. S., and Wahl, R. L. (1993) Overexpression of Glut-1 glucose transporter in human breast cancer. An immunohistochemical study, *Cancer 72*, 2979-2985.
26. Sharon, M., and Lis, H. (1989) Lectins as cell recognition molecules, *Science 246*, 227-234.

27. Cornia, M., Valenti, C., Capacchi, S., and Cozzini, P. (1998) Synthesis, characterisation and conformational studies of lipophilic, amphiphilic and water-soluble C-glyco-conjugated porphyrins, *Tetrahedron 54*, 8091-8106.

28. Cornia, M., Menozzi, M., Ragg, E., Mazzini, S., Scarafoni, A., Zanardi, F., and Casiraghi, G. (2000) Synthesis and utility of novel C-*meso*-glycosylated metalloporphyrins, *Tetrahedron 56*, 3977-3983.

29. Sylvain, I., Benhaddou, R., Carre, V., Cottaz, S., Driguez, H., Granet, R., Guilloton, M., and Krausz, P. (1999) Synthesis and biological evaluation of thioglycosylated meso- arylporphyrins, *J. Porphyrins Phthalocyanines 3*, 1 - 4.

30. Sylvain, I., Zerrouki, R., Granet, R., Huang, Y. M., Lagorce, J.-F., Guilloton, M., Blais, J.-C., and Krausz, P. (2002) Synthesis and biological evaluation of thioglycosylated porphyrins for an application in photodynamic therapy, *Bioorg. Med. Chem. 10*, 57-69.

31. Hornia, A., Lu, Z., Sukezane, T., Zhong, M., Joseph, T., Frankel, P., and Foster, D. A. (1999) Antagonistic effects of protein kinase C alpha and delta on both transformation and phospholipase D activity mediated by the epidermal growth factor receptor, *Mol. Cell Biol. 19*, 7672-7680.

32. Shen, Y., Xu, L., and Foster, D. A. (2001) Role for phospholipase D in receptor-mediated endocytosis, *Mol. Cell Biol. 21*, 595-602.

33. Willingham, M. C., and Pastan, I. (1985) *An Atlas of Immunofluorescence in Cultured Cells*, Academic Press, Orlando.

34. Qian, G. (2003), Advanced Science & Technology, http://www.howardast.com, New York.

35. Lu, Z., Hornia, A., Joseph, T., Sukezane, T., Frankel, P., Zhong, M., Bychenok, S., Xu, L., Feig, L. A., and Foster, D. A. (2000) Phospholipase D and RalA cooperate with the epidermal growth factor receptor to transform 3Y1 rat fibroblasts, *Mol. Cell Biol. 20*, 462-467.

36. Shen, Y., Zheng, Y., and Foster, D. A. (2002) Phospholipase D2 stimulates cell protrusion in v-Src-transformed cells, *Biochem. Biophys. Res. Commun. 293*, 201-206.

37. Adler, A. D., Sklar, L., Longo, F. R., Finarelli, J. D., and Finarelli, M. G. (1968) A mechanistic study of the synthesis of meso-tetraphenylporphin, *5*, 669-677.

38. Lindsey, J. S., Schreiman, I. C., Hsu, H. C., Kearney, P. C., and Marguerettaz, A. M. (1987) Rothemund and Adler-Longo reactions revisited: synthesis of tetraphenylporphyrins under equilibrium conditions, *J. Org. Chem. 52*, 827-836.

39. Defaye, J., and Gelas, J. (1991) Thio-oligosaccharides: Their Synthesis and Reactions with Enzymes, in *Studies in Natural Products Chemistry* (Atta-ur-Rahman, Ed.) pp 315-357, Elsevier Science Publishers B. V., Amsterdam.

40. Shaw, S. J., Edwards, C., and Boyle, R. W. (1999) Regioselective synthesis of multifunctionalised porphyrins - coupling of mono-(pentafluorophenyl)porphyrins to electrophiles, *Tet. Lett. 40*, 7585-7586.

41. Shaw, S. J., Elgie, K. J., Edwards, C., and Boyle, R. W. (1999) Mono-(pentafluorophenyl)porphyyrins - Useful intermediates in the regioselective synthesis of multifunctionalised porphyrins, *Tet. Lett. 40*, 1595-1596.

42. Momenteau, M., Oulmi, D., Maillard, P., and Croisy, A. F. (1994) In vitro photobiological activity of a new series of photosensitizers: the glycoconjugated porphyrins, *Proc. SPIE 2325 Photodynamic Therapy of Cancer II*, 13-23.

43. Adams, K. R., Berenbaum, M. C., Bonnett, R., Nizhnik, A. N., Salgado, A., and Valles, M. A. (1992) Second generation tumour photosensitisers: the synthesis and biological activity of octaalkyl chlorins and bacteriochlorins with graded amphiphilic character, *J. Chem. Soc., Perkin Trans. 1*, 1465-1470.

44. Oulmi, D., Maillard, P., Guerquin-Kern, J.-L., Huel, C., and Momenteau, M. (1995) Glycoconjugated porphyrins. 3. synthesis of flat amphiphilic mixed meso-(glycosylated aryl)arylporphyrins and mixed meso-(glycosylated aryl)alkylporphyrins bearing some mono- and disaccharide groups, *J. Org. Chem. 60*, 1554-1564.

45. Drain, C. M., Gong, X., Ruta, V., Soll, C. E., and Chicoineau, P. F. (1999) Combinatorial synthesis and modification of functional porphyrin libraries: identification of new, amphipathic motifs for biomolecule binding, *J. Comb. Chem. 1*, 286-290.

46. Maziere, J. C., Santus, R., Morliere, P., Reyftmann, J. P., Candide, C., Mora, L., Salmon, S., Maziere, C., Gatt, S., and Dubertret, L. (1990) Cellular uptake and photosensitizing properties of anticancer porphyrins in cell membranes and low and high density lipoproteins, *J. Photochem. Photobiol. B: Biol. 6*, 61-68.

47. Bourhim, A., Gaud, O., Granet, R., Krausz, P., and Spiro, M. (1993) Synthesis of new glycosylated porphyrin derivatives with a hydrocarbon spacer arm, *Synlett*, 563-564.

48. Gaud, O., Granet, R., Kaouadji, M., Krausz, P., Blais, J.-C., and Bolbach, G. (1996) Synthese et analyse structurale de nouvelles meso-arylporphyrines glycosylees en vue de l'application en phototherapie des cancers, *Can. J. Chem. 74*, 481-499.

49. Carre, V., Gaud, O., Sylvain, I., Bourdon, O., Spiro, M., Blais, J., Granet, R., Krausz, P., and Guilloton, M. (1999) Fungicidal properties of meso-arylglycosylporphyrins: influence of sugar substituents on photoinduced damage in the yeast Saccharomyces cerevisia, *J. Photochem. Photobiol. B: Biol. 48*, 57-62.

50. Grover-McKay, M., Walsh, S. A., Seftor, E. A., Thomas, P. A., and Hendrix, M. J. (1998) Role for glucose transporter 1 protein in human breast cancer, *Pathol. Oncol. Res. 4*, 115-120.

51. Younes, M., Brown, R. W., Mody, D. R., Fernandez, L., and Laucirica, R. (1995) GLUT1 expression in human breast carcinoma: correlation with known prognostic markers, *Anticancer Res. 15*, 2895-2898.

52. Brault, D. (1990) Physical chemistry of porphyrins and their interactions with membranes: the importance of pH, *J. Photochem. Photobiol. B: Biol. 6*, 79-86.

53. Bohmer, R. M., and Morstyn, G. (1985) Uptake of hematoporphyrin derivative by normal and malignant cells: effect of serum, pH, temperature, and cell size, *Cancer Res. 45*, 5328-5334.

54. Friberg, E. G., Cunderlikova, B., Pettersen, E. O., and Moan, J. (2003) pH effects on the cellular uptake of four photosensitizing drugs evaluated for use in photodynamic therapy of cancer, *Cancer Lett. 195*, 73-80.

55. Pandey, R. K., and Zheng, G. (2000) Porphyrins as photosensitizers in photodynamic therapy, in *The Porphyrin Handbook* (Kadish, K. M., Smith, K. M., and Guilard, R., Eds.) pp 157-230, Academic Press, New York.

56. Fujimoto, K., Miyata, T., and Aoyama, Y. (2000) Saccharide-directed cell recognition and molecular delivery using macrocyclic saccharide clusters: masking of hydrophobicity to enhance the saccharide specificity, *J. Am. Chem. Soc. 122*, 3558-3559.

57. Kroemer, G., Dallaporta, B., and Resche-Rigon, M. (1998) The mitochondrial death/life regulator in apoptosis and necrosis, *Annu. Rev. Physiol. 60*, 619-642.

58. Yu, S.-W., Wang, H., Poitras, M. F., Coombs, C., Bowers, W. J., Federoff, H. J., Poirier, G. G., Dawson, T. M., and Dawson, V. L. (2002) Mediation of poly(ADP-ribose) polymerase-1–dependent cell death by apoptosis-inducing factor, *Science 297*, 259-263.

59. de Murcia, G., and Menissier de Murcia, J. (1994) Poly(ADP-ribose) polymerase: a molecular nick-sensor, *Trends Biochem. Sci. 19*, 172-176.

60. Oleinick, N. L., Morris, R. L., and Belichenko, I. (2002) The role of apoptosis in response to photodynamic therapy: what, where, why, and how, *Photochem. Photobiol. Sci. 1*, 1-21.

61. Ridley, A. J., Schwartz, M. A., Burridge, K., Firtel, R. A., Ginsberg, M. H., Borisy, G., Parsons, J. T., and Horwitz, A. R. (2003) Cell migration: integrating signals from front to back, *Science 302*, 1704-1709.

62. Zhong, M., Joseph, T., Jackson, D., Beychenok, S., and Foster, D. A. (2002) Elevated phospholipase D activity induces apoptosis in normal rat fibroblasts, *Biochem. Biophys. Res. Commun. 298*, 474-477.

63. Zhong, M., Lu, Z., and Foster, D. A. (2002) Downregulating PKC delta provides a PI3K/Akt-indepentdent survival signal that overcomes apoptotic signals generated by c-Src overexpression, *Oncogene 21*, 1071-1078.

64. Zhong, M., Shen, Y., Zheng, Y., Joseph, T., Jackson, D., and Foster, D. A. (2003) Phospholipase D prevents apoptosis in v-Src-tranformed rat fibroblasts and MDA-MB-231 breast cancer cells, *Biochem. Biophys. Res. Commun. 302*, 615-619.

65. Pandey, R. K., and Zheng, G. (2000) Porphyrins as photosensitizers in photodynamic therapy, in *The porphyrin handbook* (Guilard, R., Ed.) pp 157-, Academic Press.

66. Lipscomb, L. A., Zhou, F. X., Presnell, S. R., Woo, R. J., Peek, M. E., Plaskon, R. R., and Williams, L. D. (1996) Structure of DNA-porphyrin complex, *Biochem. 35*, 2818-2823.

Chapter 3

1. Kroemer, G., Dallaporta, B., and Resche-Rigon, M. (1998) The mitochondrial death/life regulator in apoptosis and necrosis, *Annu. Rev. Physiol. 60*, 619-642.
2. Lawen, A. (2003) Apoptosis-an introduction, *BioEssays 25*, 888-896.
3. MacDonald, I. J., and Dougherty, T. J. (2001) Basic principles of photodynamic therapy, *J. Porphyrins Phthalocyanines 5*, 105-129.
4. Sternberg, E. D., Dolphin, D., and Bruckner, C. (1998) Porphyrin-based photosensitizers for use in photodynamic therapy, *Tetrahedron 54*, 4151-4202.
5. Osterloh, J., and Vicente, M. G. H. (2002) Mechanisms of porphyrinoid localization in tumors, *J. Porphyrins Phthalocyanines 6*, 305-324.
6. Bonnett, R. (1995) Photosensitizers of the porphyrin and phthalocyanine series for photodynamic therapy, *Chem. Soc. Rev.*, 19-33.
7. Oleinick, N. L., Morris, R. L., and Belichenko, I. (2002) The role of apoptosis in response to photodynamic therapy: what, where, why, and how, *Photochem. Photobiol. Sci. 1*, 1-21.
8. Granville, D. J., and Hunt, D. W. C. (2000) Porphyrin-mediated photosensitization---- Taking the apoptosis fast lane, *Curr. Opin. Drug Discovery Develop. 3*, 232-243.
9. Moor, A. C. E. (2000) Signaling pathways in cell death and survival after photodynamic therapy, *J. Photochem. Photobiol. B: Biol. 57*, 1-13.
10. Reed, J. C. (1997) Cytochrome c: Can't Live with It-Can't Live without It, *Cell 91*, 559-562.

11. Adler, A. D., Longo, F. R., Finarelli, J. D., Goldmacher, J., Assour, J., and Korsakoff, L. (1967) A simplified synthesis for meso-tetraphenylporphine, *J. Org. Chem. 32*, 476-476.

12. Lindsey, J. S., Schreiman, I. C., Hsu, H. C., Kearney, P. C., and Marguerettaz, A. M. (1987) Rothemund and Adler-Longo reactions revisited: synthesis of tetraphenylporphyrins under equilibrium conditions, *J. Org. Chem. 52*, 827-836.

13. Chen, X., and Drain, C. M. (2004) Photodynamic therapy using carbohydrate conjugated porphyrins, *Drug Design Review - Online 3*, in press, http://www.bentham.org/ddro/.

14. Pasetto, P., Chen, X., Drain, C. M., and Franck, R. W. (2001) Synthesis of hydrolytically stable porphyrin C- and S-glycoconjugates in high yields, *Chem. Commun.*, 81-82.

15. Chen, X., Hui, L., Foster, D., and Drain, C. M. (2004) Efficient synthesis and photodynamic activity of porphyrin-saccharide conjugates: targeting and incapacitating cancer cells, *Biochem. in press*.

16. Johnson, P. R., Dolman, N. J., Pope, M., Vaillant, C., Petersen, O. H., Tepikin, A. V., and Erdemli, G. (2003) Non-uniform distribution of mitochondria in pancreatic acinar cells, *Cell Tissue Res. 313*, 37-45.

17. Takahashi, A. (1999) Caspase: executioner and undertaker of apoptosis, *Int. J. Hematol. 70*, 226-232.

18. Kohler, C., Orrenius, S., and Zhivotovsky, B. (2002) Evaluation of caspase activity in apoptotic cells, *J. Immunological Methods 265*, 97-110.

19. Reddy, B. S. P., Sondhi, S. M., and Lown, J. W. (1999) Synthetic DNA minor groove-binding drugs, *Pharmacology & Therapeutics 84*, 1-111.

20. Yu, S.-W., Wang, H., Poitras, M. F., Coombs, C., Bowers, W. J., Federoff, H. J., Poirier, G. G., Dawson, T. M., and Dawson, V. L. (2002) Mediation of Poly(ADP-Ribose) Polymerase-1–Dependent Cell Death by Apoptosis-Inducing Factor, *Science 297*, 259-263.

21. de Murcia, G., and Menissier de Murcia, J. (1994) Poly(ADP-ribose) polymerase: a molecular nick-sensor, *Trends Biochem. Sci. 19*, 172-176.

Chapter 4

1. Merrifield, R. B. (1963) Solid Phase Peptide Synthesis. I. The Synthesis of a Tetrapeptide, *J. Am. Chem. Soc. 85*, 2149-2154.
2. Merrifield, R. B. (1964) Solid phase peptide synthesis. II. the synthesis of bradykinin, *J. Am. Chem. Soc. 86*, 304-305.
3. Merrifield, R. B. (1964) Solid-Phase Peptide Synthesis. III. An Improved Synthesis of Bradykinin, *Biochem. 3*, 1385-1390.
4. An, H., and Cook, P. D. (2000) Methodologies for generating solution-phase combinatorial libraries, *Chem. Rev. 100*, 3311-3340.
5. Carell, T., Winter, E. A., Bashir-Hashemi, A., and J. Rebek, J. (1994) A Novel Procedure for the Synthesis of Lisbraries Containing Small Organic Molecules, *Angew. Chem. Int. Edit. Engl. 33*, 2059-2061.
6. Perrier, H., and Labelle, M. (1999) Liquid-phase synthesis with solid-phase workup: application to multistep and combinatorial syntheses, *J. Org. Chem. 64*, 2110-2113.
7. Curran, D. P., and Hadida, S. (1996) Tris(2-(perfluorohexyl)ethyl)tin hydride: a new Fluorous reagent for use in traditional organic synthesis and liquid phase combinatorial synthesis, *J. Am. Chem. Soc. 118*, 2531-2532.
8. Siegel, M. G., Hahn, P. J., Dressman, B. A., Fritz, J. E., Grunwell, J. R., and Kaldor, S. W. (1997) Rapid purification of small molecule libraries by ion exchange chromatography, *Tet. Lett. 38*, 3357-3360.
9. Griffey, R. H., An, H., Cummins, L. L., Gaus, H. J., Haly, B., Herrmann, R., and Cook, P. D. (1998) Rapid deconvolution of combinatorial libraries using HPLC Fractionation, *Tetrahedron 54*, 4067-4076.

10. Warmus, J. S., and da Silva, M. I. (2000) Polyaromatic Scavenger Reagents (PAHSR): A New Methodology for Rapid Purification in Solution-Phase Combinatorial Synthesis, *Org. Lett. 2*, 1807-1809.
11. Parlow, J. J., Naing, W., South, M. S., and Flynn, D. L. (1997) In Situ chemical tagging: Tetrafluorophthalic anhydride as a "Sequestration Enabling Reagent" (SER) in the purification of solution-phase combinatorial libraries, *Tetrahedron Lett. 38*, 7959-7962.
12. Barrett, A. G. M., Smith, M. L., and Zecri, F. J. (1998) Impurity annihilation: a trategy for solution phase combinatorial chemistry with niminal purification, *Chem. Commun.*, 2317-2318.
13. Drain, C. M., Gong, X., Ruta, V., Soll, C. E., and Chicoineau, P. F. (1999) Combinatorial Synthesis and Modification of Functional Porphyrin Libraries: Identification of New, Amphipathic Motifs for Biomolecule Binding, *J. Comb. Chem. 1*, 286-290.
14. Berlin, K., Jain, R. K., Tetzlaff, C., Steinbeck, C., and Richert, C. (1997) Spectrometrically monitored selection experiments: quantitative laser desorption mass spectrometry of small chemical libraries, *Chemistry & Biology 4*, 63-77.
15. Boger, D. L., and Chai, W. (1998) Solution-phase combinatorial synthesis: Convergent multiplication of diversity via the olefin metathesis reaction, *Tetrahedron 54*, 3955-3970.
16. An, H., Cummins, L. L., Griffey, R. H., Bharadwaj, R., Haly, B. D., Fraser, A. S., Wilson-Lingardo, L., Risen, L. M., Wyatt, J. R., and Cook, P. D. (1997) Solution phase combinatorial chemistry. Discovery of novel polyazapyridinophanes with

potent antibacterial activity by a solutionphase simultaneous addition of functionalities approach, *J. Am. Chem. Soc. 119*, 3696-3708.

17. Takahashi, M., Ueno, A., and Mihara, H. (2000) Peptide design based on an antibody complementarity-determining region (CDR): construction of porphyrin-binding peptides and their affinity maturation by a combinatorial method, *Chem. Eur. J. 6*, 3196-3203.
18. Goldberg, J., Jin, Q., Ambroise, Y., Satoh, S., Desharnais, J., Capps, K., and Boger, D. L. (2002) Erythropoietin Mimetics Derived from Solution Phase Combinatorial Libraries, *J. Am. Chem. Soc. 124*, 544-555.
19. Boger, D. L., and Lee, J. K. (2000) Development of a Solution-Phase Synthesis of Minor Groove Binding Bis-Intercalators Based on Triostin A Suitable for Combinatorial Synthesis, *J. Org. Chem. 65*, 5996-6000.
20. Lehn, J.-M. (1999) Dynamic Combinatorial Chemistry and Virtual Combinatorial Libraries, *Chem. Eur. J. 5*, 2455-2463.
21. Huc, I., and Lehn, J.-M. (1997) Virtual combinatorial libraries: Dynamic generation of molecular and supramolecular diversity by self-assembly, *Proc. Natl. Acad. Sci. USA 94*, 2106-2110.
22. Otto, S., Furlan, R. L. E., and Sanders, J. K. M. (2002) Selection and amplification of hosts from dynamic combinatorial libraries of macrocyclic disulfides, *Science 297*, 590-593.
23. Brown, M. (2003) PDT: light at the end of the tunnel?, *Drug Discovery Today 8*, 767-768.

24. Jori, G. (1996) Tumor photosensitizers: approaches to enhance the selectivity and efficiency of photodynamic therapy, *J. Photochem. Photobiol. B 36*, 87-93.

25. Mody, T. D. (2000) Pharmaceutical developement and medical applications of porphyrin-type macrocycles, *J. Porphyrins Phthalocyanines 4*, 362-367.

26. Pandey, R. K. (2000) Recent advances in photodynamic therapy, *J. Porphyrins Phthalocyanines 4*, 368-373.

27. MacDonald, I. J., and Dougherty, T. J. (2001) Basic principles of photodynamic therapy, *J. Porphyrins Phthalocyanines 5*, 105-129.

28. Sternberg, E. D., Bruckner, C., and Dolphin, D. (1998) Porphyrin-based photosensitizers for use in photodynamic therapy, *Tetrahedron 54*, 4151-4202.

29. Stojiljkovic, I., Evavold, B. D., and Kumar, V. (2001) Antimicrobial properties of porphyrins, *Exp. Opin. Invest. Drugs 10*, 309-320.

30. Neurath, A. R., Strick, N., and Debnath, A. K. (1995) Structural requirements for and consequences of an antiviral porphyrin binding to the V3 loop of the human immunodeficiency virus (HIV-1) envelope glycoprotein gp120, *J. Mol. Recog. 8*, 345-357.

31. Vzorov, A. N., Dixon, D. W., Trommel, J. S., Marzilli, L. G., and Compans, R. W. (2002) Inactivation of human immunodeficiency virus type 1 by porphyrins, *Antimicrob. Agents Chemother. 46*, 3917-3925.

32. Chen, X., and Drain, C. M. (2004) Photodynamic therapy using carbohydrate conjugated porphyrins, *Drug Design Reviews - Online 1*, 215-234.

33. Sylvain, I., Benhaddou, R., Carre, V., Cottaz, S., Driguez, H., Granet, R., Guilloton, M., and Krausz, P. (1999) Synthesis and biological evaluation of thioglycosylated meso- arylporphyrins, *J. Porphyrins Phthalocyanines 3*, 1 - 4.

34. Sylvain, I., Zerrouki, R., Granet, R., Huang, Y. M., Lagorce, J.-F., Guilloton, M., Blais, J.-C., and Krausz, P. (2002) Synthesis and Biological Evaluation of Thioglycosylated Porphyrins for an Application in Photodynamic Therapy, *Bioorg. Med. Chem. 10*, 57-69.

35. Shaw, S. J., Edwards, C., and Boyle, R. W. (1999) Regioselective Synthesis of Multifunctionalised Porphyrins - Coupling of Mono-(pentafluorophenyl)porphyrins to Electrophiles, *Tetrahedron Lett. 40*, 7585-7586.

36. Shaw, S. J., Elgie, K. J., Edwards, C., and Boyle, R. W. (1999) Mono-(pentafluorophenyl)porphyrins - Useful Intermediates in the Regioselective Synthesis of Multifunctionalised Porphyrins, *Tetrahedron Lett. 40*, 1595-1596.

37. Chen, X., Hui, L., Foster, D. A., and Drain, C. M. (2004) Efficient Synthesis and Photodynamic Activity of Porphyrin-Saccharide Conjugates: Targeting and Incapacitating Cancer Cells, *Biochem. accepted*.

38. Davda, J., and Labhasetwar, V. (2002) Characterization of nanoparticle uptake by endothelial cells, *Int. J. Pharm. 233*, 51-59.

39. Gao, X., Cui, Y., Levenson, R. M., Chung, L. W. K., and Nie, S. (2004) In vivo cancer targeting and imaging with semiconductor quantum dots, *Nature Biotechnology 22*, 969-976.

40. Akins, D. L., Ozcelik, S., Zhu, H. R., and Guo, C. (1996) Fluorescence decay kinetics and structure of aggregated tetrakis (p - Sulfonatophenyl) porphyrin, *J. Phys. Chem. 100*, 14390 - 14396.

41. Harriman, A., and Hosie, R. J. (1981) Fluorescence quenching effect of substituted tetraphenylporphyrins, *J. Photochem. 15*, 163-167.

42. Hornia, A., Lu, Z., Sukezane, T., Zhong, M., Joseph, R., Frankel, P., and Foster, D. A. (1999) Antogonistic effects of protein kinase C alpha and gama on both transformation and phospholipase D activity mediated by the epidermal growth factor receptor, *Molecular and Celluar Biology 19*, 7672-7680.

43. Shen, Y., Xu, L., and Foster, D. A. (2001) Role for phospholiase D in receptor-mediated endocytosis, *Molecular and Celluar Biology 21*, 595-602.

44. Willingham, M. C., and Pastan, I. (1985) *An Atlas of Immunofluorescence in Cultured Cells*, Academic Press, Orlando.

45. Qian, G. (2003), Advanced Science & Technology, http://www.howardast.com, New York.